12 The MOS model, level 1101

12.1 Introduction

General Remarks

MOS Model 11 (MM11) is a new compact MOSFET model, intended for digital, analogue and RF circuit simulation in modern and future CMOS technologies. MM11 is the successor of MOS Model 9, it was especially developed to give not only an accurate description of currents and charges and their first-order derivatives (i.e. transconductance, conductance, capacitances), but also of the higher-order derivatives, resulting in an accurate description of electrical distortion behaviour [1]. The latter is especially important for analog and RF circuit design. The model furthermore gives an accurate description of the noise behaviour of MOSFETs.
MOS Model 11 gives a complete description of all transistor-action related quantities: nodal currents, nodal charges and noise-power spectral densities. The equations describing these quantities are based on surface-potential formulations, resulting in equations valid over all operation regions (i.e. accumulation, depletion and inversion). Although in general the surface potential is implicitly related to the terminal voltages and has to be calculated iteratively, in MM11 it has been approximated by an explicit expression [2]. Additionally, in order for the model to be valid for modern and future MOS devices, several important physical effects have been included in the model: mobility reduction, bias-dependent series-resistance, velocity saturation, drain-induced barrier lowering, static feedback, channel length modulation, self-heating, weak-avalanche (or impact ionization), gate current due to tunnelling, poly-depletion, quantum-mechanical effects on charges and bias-dependent overlap capacitances.

MOS Model 11 only provides a model for the intrinsic transistor and the gate/source- and gate/drain overlap regions. Junction charges, junction leakage currents and interconnect capacitances are not included. They are covered by separate models, which are not part of this documentation.

MOS Model 11, Level 1101, is an updated version of Level 1100, see Chapter 11. It uses the same basic equations as Level 1100, but uses different geometry scaling rules. It includes two types of geometrical scaling rules: physical rules and binning rules. It should be noted that using the source code of the Modelkit on the Philips' website (which can be found at http://www.semiconductors.philips.com/Philips_Models)

1. the physical geometry scaling rules can be selected by using Level11010, while
2. the binning geometry scaling rules can be selected by using Level 11011.

Moreover, in Level 1101 the temperature scaling has been implemented on the “miniset” level instead of the “maxiset” level (see below) as was the case for Level 1100.

Structural Elements of MOS Model 11

The structure of MOS Model 11 is the same as the structure of MOS Model 9. The model is separable into a number of relatively independent parts, namely:

- **Model embedding**

It is convenient to use one single model for both *n*- and *p*-channel devices. For this reason, any *p*-channel device and its bias conditions are mapped onto those of an equivalent *n*-channel transistor. This mapping comprises a number of sign changes. Also, the model describes a symmetrical device, i.e. the source and drain nodes can be interchanged without changing the electrical properties. The assignment of source and drain to the channel nodes is based on the voltages of these nodes: for an *n*-channel transistor the node at the highest potential is called drain. In a circuit simulator the nodes are denoted by their network numbers, based on the circuit configuration. Again, a transformation is necessary involving a number of sign changes, including the directional noise-current sources.

- **Preprocessing**

The complete set of all the parameters, as they occur in the equationsfor the various electrical quantities, is denoted as the set of actual parameters, usually called the "miniset". In MM11, Level 1101, the temperature scaling parameters are included in the “miniset”. Each of these actual parameters can be determined by purely electrical measurements. Since most of these parameters scale with geometry the process as a whole is characterized by an enlarged set of parameters, which is denoted as the set of scaling parameters, usually called the "maxiset". This set of parameters contains most of the actual parameters for an infinitely long and broad device and a large set of sensitivity coefficients. From this, the actual parameters for an arbitrary transistor are obtained by applying a set of transformation rules. The transformation rules describe the dependencies of the actual parameters on the length, width, and temperature. This procedure is called preprocessing, as it is normally done only once, prior to the actual electrical simulation.

In MM11, Level 1101, parameter binning has been facilitated by adding a second, separate set of geometry scaling rules. Consequently, besides the *physical* geometrical scaling rules there is also a set of *binning* geometrical scaling rules. The physical geometry scaling rules of Level 1101 have been developed to give a good description over the whole geometry range of CMOS technologies. For processes under development, however, it is sometimes useful to have more flexible scaling relations. In

this case one could opt for a binning strategy, where the accuracy with geometry is mostly determined by the number of bins used. The physical scaling rules of Level 1101 are not straightforwardly applicable to binning strategies, since they may result in discontinuities in parameter values at the bin boundaries. Consequently, special geometrical binning scaling relations have been developed, which guarantee continuity in the model parameters at the bin boundaries.

- **Clipping**

For very uncommon geometries or temperatures, the preprocessing rules may generate parameters that are outside a physically realistic range or that may create difficulties in the numerical evaluation of the model, for example division by zero. In order to prevent this, all parameters are limited to a pre-specified range directly after the preprocessing. This procedure is called clipping.

- **Current equations**

These are all expressions needed to obtain the DC nodal currents as a function of the bias conditions. They are segmentable in equations for the channel current, the gate tunnelling current and the avalanche current.

Charge equations

These are all the equations that are used to calculate both the intrinsic and extrinsic charge quantities, which are assigned to the nodes.

- **Noise equations**

The total noise output of a transistor consists of a thermal- and a flicker noise part. which create fluctuations in the channel current. Owing to the capacitive coupling between gate and channel region, current fluctuations in the gate current are induced as well, which is referred to as induced gate noise.

Structure of the Documentation

After this introductory section, the physical background of the current, the charge and the noise equations is discussed to elucidate the model. Next the temperature dependence and the basic equations are presented. To facilitate an unambiguous discussion of these equations, the nomenclature of the parameter set for an individual transistor (“miniset”) and the model constants is given right at the beginning of this documentation. Next all the information, which is needed for the implementation of the model in a circuit simulator, is present. After the full nomenclature of all different model parameters (both for the physical and the binning scaling rules), quantities and variables, the different structural elements of the model are discussed in

detail. The extended model equations contain all the numerical adaptations necessary to facilitate unproblematic evaluation in a circuit simulator. Next the methodology to extract the model parameters is presented. Finally the default values and clipping limits of all parameters are presented, in addition the operating point output (OPO) parameters are described.

12.2 Nomenclature

The symbolic representation and the recommended programming names of the quantities listed in the following sections, have been chosen in such a way to express their purpose and relations to other quantities and to preclude ambiguity and inconsistency.

12.2.1 Glossary of used symbols

All parameters which refer to the reference transistor and / or the reference temperature have a symbol with the subscript R and a programming name ending with R. All characters 0 (zero) in subscripts of parameters are represented by the capital letter O in the programming name, because often they are distinguishable with great difficulty! Scaling parameters are indicated by *S* with a subscript where the variables on which the parameter depends, preceed a semicolon whereas the parameter succeeds it, e.g. $S_{T;\theta sr}$.

List of numerical constants

No.	Constant	Prog. Name	Value
1	A	LN_MINDOUBLE	-1600

List of circuit simulator variables

No.	Symbol	Prog. Name	Units	Description
1	L	L	m	Drawn channel length in the lay-out of the actual transistor
2	W	W	m	Drawn channel width in the lay-out of the actual transistor
3	T_A	TA	°C	Ambient circuit temperature
4	f	F	s^{-1}	Operation frequency

External Electrical Variables

The definitions of the external electrical variables are illustrated in Fig. 72.

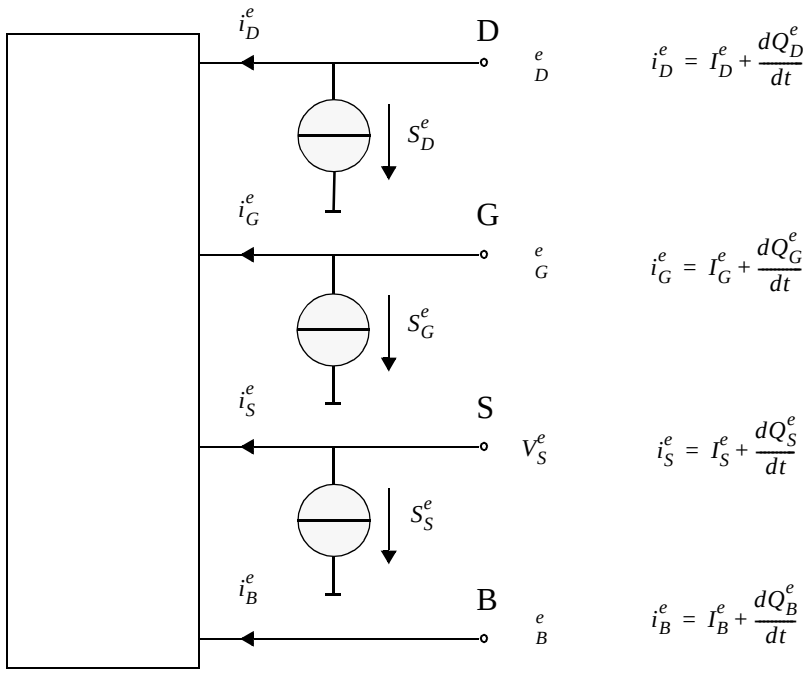

Figure 72: Definition of the external electrical quantities and variables

No.	Variable	Prog. Name	Units	Description
1	V_D^e	VDE	V	Potential applied to the drain node
2	V_G^e	VGE	V	Potential applied to the gate node
3	V_S^e	VSE	V	Potential applied to the source node
4	V_B^e	VBE	V	Potential applied to the bulk node
5	I_D^e	IDE	A	DC current into the drain
6	I_G^e	IGE	A	DC current into the gate
7	I_S^e	ISE	A	DC current into the source
8	I_B^e	IBE	A	DC current into the bulk
9	Q_D^e	QDE	C	Charge in the device attributed to the drain node
10	Q_G^e	QGE	C	Charge in the device attributed to the gate node
11	Q_S^e	QSE	C	Charge in the device attributed to the source node
12	Q_B^e	QBE	C	Charge in the device attributed to the bulk node
13	S_D^e	SDE	A^2s	Spectral density of the noise current into the drain
14	S_G^e	SGE	A^2s	Spectral density of the noise current into the gate
15	S_S^e	SSE	A^2s	Spectral density of the noise current into the source

No.	Variable	Prog. Name	Units	Description
16	S^e_{DG}	SDGE	A^2s	Cross spectral density between the drain and the gate noise currents
17	S^e_{GS}	SGSE	A^2s	Cross spectral density between the gate and the source noise currents
18	S^e_{SD}	SSDE	A^2s	Cross spectral density between the source and the drain noise currents

Internal Electrical Variables

No.	Variable	Progr. Name	Units	Description
1	V_{DS}	VDS	V	Drain-to-source voltage applied to the equivalent n-MOST
2	V_{GS}	VGS	V	Gate-to-source voltage applied to the equivalent n-MOST
3	V_{SB}	VSB	V	Source-to-bulk voltage applied to the equivalent n-MOST
4	I_{DS}	IDS	A	DC current through the channel flowing from drain to source
5	I_{AVL}	IAVL	A	DC current flowing from drain to bulk due to the weak-avalanche effect
6	I_{GS}	IGS	A	DC current flowing from gate to source due to the direct tunnelling effect
7	I_{GD}	IGD	A	DC current flowing from gate to drain due to the direct tunnelling effect
8	I_{GB}	IGB	A	DC current flowing from gate to bulk due to the direct tunnelling effect
9	Q_D	QD	C	Charge in the equivalent n-MOST attributed to the drain node
10	Q_G	QG	C	Charge in the equivalent n-MOST attributed to the gate node
11	Q_S	QS	C	Charge in the equivalent n-MOST attributed to the source node
12	Q_B	QB	C	Charge in the equivalent n-MOST attributed to the bulk node
13	Q_{ov0}	QOVO	C	Extrinsic charge in the equivalent n-MOST attributed to the gate-source overlap
14	Q_{ovL}	QOVL	C	Extrinsic charge in the equivalent n-MOST attributed to the gate-drain overlap
15	S_{th}	STH	A^2s	Spectral density of the thermal-noise current of the channel

16	S_{fl}	SFL	A^2s	Spectral density of the flicker-noise current of the channel
17	S_{ig}	SIG	A^2s	Spectral density of the noise current induced in the gate
18	S_{igth}	SIGTH	A^2s	Cross spectral density of the noise current induced in the gate and the thermal-noise current of the channel

12.2.2 Parameters

In MOS Model 11, level 1101, parameter binning has been facilitated by adding a second, separate set of geometry scaling rules. Consequently, besides the physical geometrical scaling rules there is also a set of binning geometrical scaling rules. The physical geometry scaling rules of Level 1101 have been developed to give a good description over the whole geometry range of CMOS technologies. For processes under development, however, it is sometimes useful to have more flexible scaling relations. In this case one could opt for a binning strategy, where the accuracy with geometry is mostly determined by the number of bins used. The physical scaling rules of Level 1101 are not straightforwardly applicable to binning strategies, since they may result in discontinuities in parameter values at the bin boundaries. Consequently, special binning geometrical scaling relations have been developed which guarantee continuity in the model parameters at the bin boundaries. It should be noted that using the source code of the Modelkit on the Philips' website (which can be found at http://www.semiconductors.philips.com/Philips_Models)

1) the physical geometry scaling rules can be selected by using Level 11010, while

2) the binning geometry scaling rules can be selected by using Level 11011.

Parameters for physical geometry scaling

- These parameters correspond to the geometrical model (MN, MP)**.**

No.	Symbol	Progr. Name	Units	Description
0		LEVEL	-	Must be 11010
1	ΔL_{PS}	LVAR	m	Difference between the actual and the programmed poly-silicon gate length
2	$\Delta L_{overlap}$	LAP	m	Effective channel length reduction per side due to the lateral diffusion of the source/drain dopant ions
3	ΔW_{OD}	WVAR	m	Difference between the actual and the programmed field-oxide opening
4	ΔW_{narrow}	WOT	m	Effective reduction of the channel width per side due to the lateral diffusion of the channel-stop dopant ions
5	T_R	TR	°C	Reference temperature

No.	Symbol	Progr. Name	Units	Description
6	V_{FBR}	VFBR	V	Flat-band voltage at the reference temperature
7	$S_{T;V_{FB}}$	STVFB	VK^{-1}	Coefficient of the temperature dependence of V_{FB}
8	k_{0R}	KOR	$V^{1/2}$	Body-effect factor for an infinite square transistor
9	$S_{L;k_0}$	SLKO	m	Coefficient of the length dependence of k_0
10	$S_{L2;k_0}$	SL2KO	m^2	Second coefficient of the length dependence of k_0
11	$S_{W;k_0}$	SWKO	m	Coefficient of the width dependence of k_0
12	$1/k_p$	KPINV	$V^{-1/2}$	Inverse of body-effect factor of the polysilicon gate
13	ϕ_{BR}	PHIBR	V	Surface potential at the onset of strong inversion at the reference temperature
14	$S_{T;\phi_B}$	STPHIB	VK^{-1}	Coefficient of the temperature dependence of ϕ_B
15	$S_{L;\phi_B}$	SLPHIB	m	Coefficient of the length dependence of ϕ_B
16	$S_{L2;\phi_B}$	SL2PHIB	m^2	Second coefficient of the length dependence of ϕ_B
17	$S_{W;\phi_B}$	SWPHIB	m	Coefficient of the width dependence of ϕ_B
18	β_{sq}	BETSQ	AV^{-2}	Gain factor for an infinite square transistor at the reference temperature
19	$\eta_{\beta R}$	ETABETR	-	Exponent of the temperature dependence of the gain factor of an infinite square transistor
20	$S_{L;\eta_\beta}$	SLETABET	-	Coefficient of the length dependence of $\eta_{\beta R}$
21	$f_{\beta,1}$	FBET1	-	Relative mobility decrease due to first lateral profile
22	$L_{P,1}$	LP1	m	Characteristic length of first lateral profile

No.	Symbol	Progr. Name	Units	Description
23	$f_{\beta,2}$	FBET2	-	Relative mobility decrease due to second lateral profile
24	$L_{P,2}$	LP2	m	Characteristic length of second lateral profile
25	θ_{srR}	THESRR	V^{-1}	Coefficient of the mobility reduction due to surface roughness scattering for an infinite square transistor at the reference temperature
26	η_{sr}	ETASR	-	Exponent of the temperature dependence of θ_{sr}
27	$S_{W;\theta_{sr}}$	SWTHESR	m	Coefficient of the width dependence of θ_{sr}
28	θ_{phR}	THEPHR	V^{-1}	Coefficient of the mobility reduction due to phonon scattering for an infinite square transistor at the reference temperature
29	η_{ph}	ETAPH	-	Exponent of the temperature dependence of θ_{ph} for the reference transistor
30	$S_{W;\theta_{ph}}$	SWTHEPH	m	Coefficient of the width dependence of θ_{ph}
31	η_{mobR}	ETAMOBR	-	Effective field parameter for dependence on depletion/ inversion charge for an infinite square transistor
32	$S_{T;\eta_{mob}}$	STETAMOB	K^{-1}	Coefficient of the temperature dependence of η_{mob}
33	$S_{W;\eta_{mob}}$	SWETAMOB	m	Coefficient of the width dependence of η_{mob}
34	υ	NU	-	Exponent of the field dependence of the mobility model at the reference temperature
35	υ_{EXP}	NUEXP	-	Exponent of the temperature dependence of parameter ν
36	θ_{RR}	THERR	V^{-1}	Coefficient of the series resistance per unit length for an infinitely wide transistor at the reference temperature

No.	Symbol	Progr. Name	Units	Description
37	η_R	ETAR	-	Exponent of the temperature dependence of θ_R
38	$S_{W;\theta_R}$	SWTHER	m	Coefficient of the width dependence of θ_R
39	θ_{R1}	THER1	V	Numerator of the gate voltage dependent part of series resistance
40	θ_{R2}	THER2	V	Denominator of the gate voltage dependent part of series resistance
41	θ_{satR}	THESATR	V^{-1}	Velocity saturation parameter due to optical/acoustic phonon scattering for an infinite square transistor at the reference temper-ature
42	η_{sat}	ETASAT	-	Exponent of the temperature dependence of θ_{sat}
43	$S_{L;\theta_{sat}}$	SLTHESAT	-	Coefficient of the length dependence of θ_{sat}
44	θ_{satEXP}	THESATEXP	-	Exponent of the length dependence of θ_{sat}
45	$S_{W;\theta_{sat}}$	SWTHESAT	m	Coefficient of the width dependence of θ_{sat}
46	θ_{ThR}	THETHR	V^{-3}	Coefficient of self-heating per unit length for an infinitely wide transistor at the reference temperature
47	θ_{ThEXP}	THETHEXP	-	Exponent of the length dependence of θ_{Th}
48	$S_{W;\theta_{Th}}$	SWTHETH	m	Coefficient of the width dependence of θ_{Th}
49	σ_{dibl0}	SDIBLO	$V^{-1/2}$	Drain-induced barrier-lowering parameter per unit length
50	$\sigma_{diblEXP}$	SDIBLEXP	-	Exponent of the length dependence of σ_{dibl}
51	m_{00}	MOO	-	Parameter for short-channel subthreshold slope
52	m_{0R}	MOR	-	Parameter for short-channel subthreshold slope per unit length
53	m_{0EXP}	MOEXP	-	Exponent of the length dependence of m_0

No.	Symbol	Progr. Name	Units	Description
54	σ_{sfR}	SSFR	$V^{-1/2}$	Static feedback parameter for an infinite square transistor
55	$S_{L;\sigma_{sf}}$	SLSSF	m	Coefficient of the length dependence of σ_{sf}
56	$S_{W;\sigma_{sf}}$	SWSSF	m	Coefficient of the width dependence of σ_{sf}
57	α_R	ALPR	-	Factor of the channel length modulation for an infinite square transistor
58	$S_{L;\alpha}$	SLALP	-	Coefficient of the length dependence of α
59	α_{EXP}	ALPEXP	-	Exponent of the length dependence of α
60	$S_{W;\alpha}$	SWALP	m	Coefficient of the width dependence of α
61	V_P	VP	V	Characteristic voltage of the channel length modulation
62	L_{min}	LMIN	m	Minimum effective channel length in technology, used for calculation of smoothing factor *m*
63	a_{1R}	A1R	-	Factor of the weak-avalanche current for an infinite square transistor at the reference temperature
64	$S_{T;a_1}$	STA1	K^{-1}	Coefficient of the temperature dependence of a_1
65	$S_{L;a_1}$	SLA1	m	Coefficient of the length dependence of a_1
66	$S_{W;a_1}$	SWA1	m	Coefficient of the width dependence of a_1
67	a_{2R}	A2R	V	Exponent of the weak-avalanche current for an infinite square transistor
68	$S_{L;a_2}$	SLA2	Vm	Coefficient of the length dependence of a_2
69	$S_{W;a_2}$	SWA2	Vm	Coefficient of the width dependence of a_2
70	a_{3R}	A3R	-	Factor of the drain-source voltage above which weak-avalanche occurs, for an infinite square transistor

No.	Symbol	Progr. Name	Units	Description
71	$S_{L;a_3}$	SLA3	m	Coefficient of the length dependence of a_3
72	$S_{W;a_3}$	SWA3	m	Coefficient of the width dependence of a_3
73	I_{GINVR}	IGINVR	AV^{-2}	Gain factor for intrinsic gate tunnelling current in inversion for a channel area of $1\mu m^2$
74	B_{inv}	BINV	V	Probability factor for intrinsic gate tunnelling current in inversion
75	I_{GACCR}	IGACCR	AV^{-2}	Gain factor for intrinsic gate tunnelling current in accumulation for a channel area of $1\mu m^2$
76	B_{acc}	BACC	V	Probability factor for intrinsic gate tunnelling current in accumulation
77	V_{FBov}	VFBOV	V	Flat-band voltage for the source/drain overlap extensions
78	k_{ov}	KOV	$V^{1/2}$	Body-effect factor for the source/drain overlap extensions
79	I_{GOVR}	IGOVR	AV^{-2}	Gain factor for source/drain overlap gate tunnelling current for a channel width of $1\mu m$
80		AGIDLR	AV^{-3}	Gain factor for gate-induced drain leakage current for a channel width of 1 µm
81		BGIDL	V	Probability factor for gate-induced drain leakage current at the reference temperature
82		STBGIDL	VK^{-1}	Coefficient of the temperature dependence of BGIDL
83		CGIDL	-	Factor for the lateral field dependence of the gate-induced drain leakage current
84	t_{ox}	TOX	m	Thickness of the gate-oxide layer.
85	C_{ol}	COL	Fm^{-1}	Gate overlap capacitance for a channel width of $1\mu m$

No.	Symbol	Progr. Name	Units	Description
86	-	GATENOISE	-	Flag for in/exclusion of induced gate thermal noise
87	N_T	NT	J	Coefficient of the thermal noise at the reference temperature
88	N_{FAR}	NFAR	$V^{-1}m^{-4}$	First coefficient of the flicker noise for a channel area of $1\mu m^2$
89	N_{FBR}	NFBR	$V^{-1}m^{-2}$	Second coefficient of the flicker noise for a channel area of $1\mu m^2$
90	N_{FCR}	NFCR	V^{-1}	Third coefficient of the flicker noise for a channel area of $1\mu m^2$
91	L	L	m	Drawn channel length in the lay-out of the actual transistor
92	W	W	m	Drawn channel width in the lay-out of the actual transistor
93	ΔT_A	DTA	°C	Temperature offset of the device with respect to T_A
94	N_{MULT}	MULT	-	Number of devices in parallel

Remark: The parameters *L*, *W*, and *DTA* are used to calculate the electrical parameters of the actual transistor, as specified in the section on parameter preprocessing.

Default and clipping values (physical geometrical model)

The default values and clipping values as used for the parameters of the physical geometrical MOS model, level 1101 (n-channel) are listed below.

No.	Parameter	Units	Default	Clip low	Clip high
0	*LEVEL*	-	11010	-	-
1	*LVAR*	m	0.000	-	-
2	*LAP*	m	4.0×10^{-8}	-	-
3	*WVAR*	m	0.000	-	-
4	*WOT*	m	0.000	-	-
5	*TR*	°C	21.0	-273.15	-
6	*VFB*	V	-1.050	-	-
7	*STVFB*	VK^{-1}	0.5×10^{-3}	-	-
8	*KOR*	$V^{1/2}$	0.500	-	-
9	*SLKO*	-	0.000	-	-
10	*SL2KO*	-	0.000	-	-
11	*SWKO*	-	0.000	-	-
12	*KPINV*	$V^{-1/2}$	0.000	-	-
13	*PHIBR*	V	0.950	-	-
14	*STPHIB*	VK^{-1}	-8.5×10^{-4}	-	-
15	*SLPHIB*	-	0.000	-	-
16	*SL2PHIB*	-	0.000	-	-
17	*SWPHIB*	-	0.000	-	-
18	*BETSQ*	AV^{-2}	3.709×10^{-4}	-	-
19	*ETABETR*	-	1.300	-	-
20	*SLETABET*	-	0.000	-	-
21	*FBET1*	-	0.000	-	-

No.	Parameter	Units	Default	Clip low	Clip high
22	*LP1*	m	0.8×10^{-6}	1.0×10^{-10}	-
23	*FBET2*	-	0.000	-	-
24	*LP2*	m	0.8×10^{-6}	1.0×10^{-10}	-
25	*THESRR*	V^{-1}	0.400	-	-
26	*ETASR*	-	0.650	-	-
27	*SWTHESR*	-	0.000	-	-
28	*THEPHR*	V^{-1}	1.29×10^{-2}	-	-
29	*ETAPH*	-	1.350	-	-
30	*SWTHEPH*	-	0.000	-	-
31	*ETAMOBR*	-	1.40	-	-
32	*STETAMOB*	K^{-1}	0.000	-	-
33	*SWETAMOB*	-	0.000	-	-
34	*NU*	-	2.000	1.000	-
35	*NUEXP*	-	5.250	-	-
36	*THERR*	V^{-1}	0.155	1.0×10^{-10}	-
37	*ETAR*	-	0.950	-	-
38	*SWTHER*	-	0.000	-	-
39	*THER1*	V	0.000	-	-
40	*THER2*	V	1.000	-	-
41	*THESATR*	V^{-1}	0.500	-	-
42	*ETASAT*	-	1.040	-	-
43	*SLTHESAT*	-	1.000	-	-
44	*THESATEXP*	-	1.000	0.000	-
45	*SWTHESAT*	-	0.000	-	-
46	*THETHR*	V^{-3}	1.0×10^{-3}	-	-
47	*THETHEXP*	-	1.000	0.000	-

No.	Parameter	Units	Default	Clip low	Clip high
48	*SWTHETH*	-	0.000	-	-
49	*SDIBLO*	$V^{-1/2}$	1.0×10^{-4}	-	-
50	*SDIBLEXP*	-	1.350	-	-
51	*MOO*	-	0.000	-	-
52	*MOR*	-	0.000	-	-
53	*MOEXP*	-	1.340	-	-
54	*SSSFR*	$V^{-1/2}$	6.25×10^{-3}	-	-
55	*SLSSF*	-	1.000	-	-
56	*SWSSF*	-	0.000	-	-
57	*ALPR*	-	1.0×10^{-2}	-	-
58	*SLALP*	-	1.000	-	-
59	*ALPEXP*	-	1.000	0.000	-
60	*SWALP*	-	0.000	-	-
61	*VP*	V	5.0×10^{-2}	-	-
62	*LMIN*	m	1.5×10^{-7}	1.0×10^{-10}	2.5×10^{-6}
63	*A1R*	-	6.000	-	-
64	*STA1*	K^{-1}	0.000	-	-
65	*SLA1*	-	0.000	-	-
66	*SWA1*	-	0.000	-	-
67	*A2R*	V	38.00	-	-
68	*SLA2*	-	0.000	-	-
69	*SWA2*	-	0.000	-	-
70	*A3R*	-	1.000	-	-
71	*SLA3*	-	0.000	-	-
72	*SWA3*	-	0.000	-	-
73	*IGINVR*	AV^{-2}	0.000	0.000	-

No.	Parameter	Units	Default	Clip low	Clip high
74	*BINV*	V	48.00	0.000	-
75	*IGACCR*	AV^{-2}	0.000	0.000	-
76	*BACC*	V	48.00	0.000	-
77	*VFBOV*	V	0.000	-	-
78	*KOV*	$V^{1/2}$	2.500	1.0×10^{-12}	-
79	*IGOVR*	AV^{-2}	0.000	0.000	-
80	*AGIDLR*	AV^{-3}	0.000	0.000	-
81	*BGIDL*	V	41.00	0.000	-
82	*STBGIDL*	VK^{-1}	$-3.638X10^{-4}$	-	-
83	*CGIDL*	-	0.000	0.000	-
84	*TOX*	m	3.2×10^{-9}	1.0×10^{-12}	-
85	*COL*	F	3.2×10^{-16}	-	-
86	*GATENOISE*	-	0.000	0.000	1.000
87	*NT*	J	1.656×10^{-20}	0.000	-
88	*NFAR*	$V^{-1}m^{-4}$	1.573×10^{23}	-	-
89	*NFBR*	$V^{-1}m^{-2}$	4.752×10^{9}	-	-
90	*NFCR*	V^{-1}	0.000	-	-
91	*L*	m	2.000×10^{-6}	-	-
92	*W*	m	1.000×10^{-5}	-	-
93	*DTA*	K	0.000	-	-
94	*MULT*	-	1.000	0.000	-

The default values and clipping values as used for the parameters of the physical geometrical MOS model, level 1101 (p-channel) are listed below.

No.	Parameter	Units	Default	Clip low	Clip high
0	*LEVEL*	-	11010	-	-
1	*LVAR*	m	0.000	-	-
2	*LAP*	m	4.0×10^{-8}	-	-
3	*WVAR*	m	0.000	-	-
4	*WOT*	m	0.000	-	-
5	*TR*	°C	21.0	-273.15	-
6	*VFB*	V	-1.050	-	-
7	*STVFB*	VK^{-1}	0.5×10^{-3}	-	-
8	*KOR*	$V^{1/2}$	0.500	-	-
9	*SLKO*	-	0.000	-	-
10	*SL2KO*	-	0.000	-	-
11	*SWKO*	-	0.000	-	-
12	*KPINV*	$V^{-1/2}$	0.000	-	-
13	*PHIBR*	V	0.950	-	-
14	*STPHIB*	VK^{-1}	-8.5×10^{-4}	-	-
15	*SLPHIB*	-	0.000	-	-
16	*SL2PHIB*	-	0.000	-	-
17	*SWPHIB*	-	0.000	-	-
18	*BETSQ*	AV^{-2}	1.150×10^{-4}	-	-
19	*ETABETR*	-	0.500	-	-
20	*SLETABET*	-	0.000	-	-
21	*FBET1*	-	0.000	-	-
22	*LP1*	m	0.8×10^{-6}	1.0×10^{-10}	-

No.	Parameter	Units	Default	Clip low	Clip high
23	*FBET2*	-	0.000	-	-
24	*LP2*	m	0.8×10^{-6}	1.0×10^{-10}	-
25	*THESRR*	V^{-1}	0.730	-	-
26	*ETASR*	-	0500	-	-
27	*SWTHESR*	-	0.000	-	-
28	*THEPHR*	V^{-1}	1.0×10^{-3}	-	-
29	*ETAPH*	-	3.750	-	-
30	*SWTHEPH*	-	0.000	-	-
31	*ETAMOBR*	-	3.000	-	-
32	*STETAMOB*	K^{-1}	0.000	-	-
33	*SWETAMOB*	-	0.000	-	-
34	*NU*	-	2.000	1.000	-
35	*NUEXP*	-	3.230	-	-
36	*THERR*	V^{-1}	0.080	1.0×10^{-10}	-
37	*ETAR*	-	0.400	-	-
38	*SWTHER*	-	0.000	-	-
39	*THER1*	V	0.000	-	-
40	*THER2*	V	1.000	-	-
41	*THESATR*	V^{-1}	0.200	-	-
42	*ETASAT*	-	0.860	-	-
43	*SLTHESAT*	-	1.000	-	-
44	*THESATEXP*	-	1.000	0.000	-
45	*SWTHESAT*	-	0.000	-	-
46	*THETHR*	V^{-3}	0.5×10^{-3}	-	-
47	*THETHEXP*	-	1.000	0.000	-
48	*SWTHETH*	-	0.000	-	-

No.	Parameter	Units	Default	Clip low	Clip high
49	*SDIBLO*	$V^{-1/2}$	1.0×10^{-4}	-	-
50	*SDIBLEXP*	-	1.350	-	-
51	*MOO*	-	0.000	-	-
52	*MOR*	-	0.000	-	-
53	*MOEXP*	-	1.340	-	-
54	*SSSFR*	$V^{-1/2}$	6.25×10^{-3}	-	-
55	*SLSSF*	-	1.000	-	-
56	*SWSSF*	-	0.000	-	-
57	*ALPR*	-	1.0×10^{-2}	-	-
58	*SLALP*	-	1.000	-	-
59	*ALPEXP*	-	1.000	0.000	-
60	*SWALP*	-	0.000	-	-
61	*VP*	V	5.0×10^{-2}	-	-
62	*LMIN*	m	1.5×10^{-7}	1.0×10^{-10}	2.5×10^{-6}
63	*A1R*	-	6.000	-	-
64	*STA1*	K^{-1}	0.000	-	-
65	*SLA1*	-	0.000	-	-
66	*SWA1*	-	0.000	-	-
67	*A2R*	V	38.00	-	-
68	*SLA2*	-	0.000	-	-
69	*SWA2*	-	0.000	-	-
70	*A3R*	-	1.000	-	-
71	*SLA3*	-	0.000	-	-
72	*SWA3*	-	0.000	-	-
73	*IGINVR*	AV^{-2}	0.000	0.000	-
74	*BINV*	V	87.50	0.000	-

No.	Parameter	Units	Default	Clip low	Clip high
75	*IGACCR*	AV^{-2}	0.000	0.000	-
76	*BACC*	V	48.00	0.000	-
77	*VFBOV*	V	0.000	-	-
78	*KOV*	$V^{1/2}$	2.500	1.0×10^{-12}	-
79	*IGOVR*	AV^{-2}	0.000	0.000	-
80	*AGIDLR*	AV^{-3}	0.000	0.000	-
81	*BGIDL*	V	41.00	0.000	-
82	*STBGIDL*	VK^{-1}	$-3.638X10^{-4}$	-	-
83	*CGIDL*	-	0.000	0.000	-
84	*TOX*	m	3.2×10^{-9}	1.0×10^{-12}	-
85	*COL*	F	3.2×10^{-16}	-	-
86	*GATENOISE*	-	0.000	0.000	1.000
87	*NT*	J	1.656×10^{-20}	0.000	-
88	*NFAR*	$V^{-1}m^{-4}$	3.825×10^{24}	-	-
89	*NFBR*	$V^{-1}m^{-2}$	1.015×10^{9}	-	-
90	*NFCR*	V^{-1}	7.300×10^{-8}	-	-
91	*L*	m	2.000×10^{-6}	-	-
92	*W*	m	1.000×10^{-5}	-	-
93	*DTA*	K	0.000	-	-
94	*MULT*	-	1.000	0.000	-

Parameters for Binning Geometrical Scaling

These parameters correspond to the geometrical model (MN, MP) for binning geometrical scaling in the model.

Note that for each bin (W_{min},W_{max},L_{min},L_{max}) there is a separate parameter set, which is valid for (W,L) values with $W_{min} \le W \le W_{max}$ and $L_{min} \le L \le L_{max}$.

No.	Symbol	Progr. Name	Units	Description
0		LEVEL	-	Must be 11011
1	ΔL_{PS}	LVAR	m	Difference between the actual and the programmed poly-silicon gate length
2	$\Delta L_{overlap}$	LAP	m	Effective channel length reduction per side due to the lateral diffusion of the source/drain dopant ions
3	ΔW_{OD}	WVAR	m	Difference between the actual and the programmed field-oxide opening
4	ΔW_{narrow}	WOT	m	Effective reduction of the channel width per side due to the lateral diffusion of the channel-stop dopant ions
5	T_R	TR	°C	Reference temperature
6	V_{FB}	VFB	V	Flat-band voltage for all the transistors in the bin at the reference temperature
7	$P_{0;k_0}$	POKO	$V^{1/2}$	Coefficient for the geometry independent part of k_0
8	$P_{L;k_0}$	PLKO	$V^{1/2}$	Coefficient for the length dependence of k_0
9	$P_{W;k_0}$	PWKO	$V^{1/2}$	Coefficient for the width dependence of k_0
10	$P_{LW;k_0}$	PLWKO	$V^{1/2}$	Coefficient for the length times width dependence of k_0
11	$1/k_P$	KPINV	$V^{-1/2}$	Inverse of the body-effect factor of the poly-silicon gate

No.	Symbol	Progr. Name	Units	Description
12	$P_{0;\phi_B}$	POPHIB	V	Coefficient for the geometry independent part of ϕ_B
13	$P_{L;\phi_B}$	PLPHIB	V	Coefficient for the length dependence of ϕ_B
14	$P_{W;\phi_B}$	PWPHIB	V	Coefficient for the width dependence of ϕ_B
15	$P_{LW;\phi_B}$	PLWPHIB	V	Coefficient for the length times width dependence of ϕ_B
16	$P_{0;\beta}$	POBET	AV^{-2}	Coefficient for the geometry independent part of β
17	$P_{L;\beta}$	PLBET	AV^{-2}	Coefficient for the length dependence of β
18	$P_{W;\beta}$	PWBET	AV^{-2}	Coefficient for the width dependence of β
19	$P_{LW;\beta}$	PLWBET	AV^{-2}	Coefficient for the width over length dependence of β
20	$P_{0;\theta_{sr}}$	POTHESR	V^{-1}	Coefficient for the geometry independent part of θ_{sr}
21	$P_{L;\theta_{sr}}$	PLTHESR	V^{-1}	Coefficient for the length dependence of θ_{sr}
22	$P_{W;\theta_{sr}}$	PWTHESR	V^{-1}	Coefficient for the width dependence of θ_{sr}
23	$P_{LW;\theta_{sr}}$	PLWTHESR	V^{-1}	Coefficient for the length times width dependence of θ_{sr}
24	$P_{0;\theta_{ph}}$	POTHEPH	V^{-1}	Coefficient for the geometry independent part of θ_{ph}
25	$P_{L;\theta_{ph}}$	PLTHEPH	V^{-1}	Coefficient for the length dependence of θ_{ph}

No.	Symbol	Progr. Name	Units	Description
26	$P_{W;\theta_{ph}}$	PWTHEPH	V^{-1}	Coefficient for the width dependence of θ_{ph}
27	$P_{LW;\theta_{ph}}$	PLWTHEPH	V^{-1}	Coefficient for the length times width dependence of θ_{ph}
28	$P_{0;\eta_{mob}}$	POETAMOB	-	Coefficient for the geometry independent part of η_{mob}
29	$P_{L;\eta_{mob}}$	PLETAMOB	-	Coefficient for the length dependence of η_{mob}
30	$P_{W;\eta_{mob}}$	PWETAMOB	-	Coefficient for the width dependence of η_{mob}
31	$P_{LW;\eta_{mob}}$	PLWETAMOB	-	Coefficient for the length times width dependence of η_{mob}
32	$P_{0;\theta_R}$	POTHER	V^{-1}	Coefficient for the geometry independent part of θ_R
33	$P_{L;\theta_R}$	PLTHER	V^{-1}	Coefficient for the length dependence of θ_R
34	$P_{W;\theta_R}$	PWTHER	V^{-1}	Coefficient for the width dependence of θ_R
35	$P_{LW;\theta_R}$	PLWTHER	V^{-1}	Coefficient for the length times width dependence of θ_R
36	θ_{R1}	THER1	V	Numerator of the gate voltage dependent part of series resistance for all the transistors in the bin
37	θ_{R2}	THER2	V	Denominator of the gate voltage dependent part of series resistance for all the transistors in the bin
38	$P_{0;\theta_{sat}}$	POTHESAT	V^{-1}	Coefficient for the geometry independent part of θ_{sat}
39	$P_{L;\theta_{sat}}$	PLTHESAT	V^{-1}	Coefficient for the length dependence of θ_{sat}

No.	Symbol	Progr. Name	Units	Description
40	$P_{W;\theta_{sat}}$	PWTHESAT	V^{-1}	Coefficient for the width dependence of θ_{sat}
41	$P_{LW;\theta_{sat}}$	PLWTHESAT	V^{-1}	Coefficient for the length times width dependence of θ_{sat}
42	$P_{0;\theta_{Th}}$	POTHETH	V^{-3}	Coefficient for the geometry independent part of θ_{Th}
43	$P_{L;\theta_{Th}}$	PLTHETH	V^{-3}	Coefficient for the length dependence of θ_{Th}
44	$P_{W;\theta_{Th}}$	PWTHETH	V^{-3}	Coefficient for the width dependence of θ_{Th}
45	$P_{LW;\theta_{Th}}$	PLWTHETH	V^{-3}	Coefficient for the length times width dependence of θ_{Th}
46	$P_{0;\sigma_{dibl}}$	POSDIBL	$V^{-1/2}$	Coefficient for the geometry independent part of σ_{dibl}
47	$P_{L;\sigma_{dibl}}$	PLSDIBL	$V^{-1/2}$	Coefficient for the length dependence of σ_{dibl}
48	$P_{W;\sigma_{dibl}}$	PWSDIBL	$V^{-1/2}$	Coefficient for the width dependence of σ_{dibl}
49	$P_{LW;\sigma_{dibl}}$	PLWSDIBL	$V^{-1/2}$	Coefficient for the length times width dependence of σ_{dibl}
50	$P_{0;m_0}$	POMO	-	Coefficient for the geometry independent part of m_0
51	$P_{L;m_0}$	PLMO	-	Coefficient for the length dependence of m_0
52	$P_{W;m_0}$	PWMO	-	Coefficient for the width dependence of m_0
53	$P_{LW;m_0}$	PLWMO	-	Coefficient for the length times width dependence of m_0

No.	Symbol	Progr. Name	Units	Description
54	$P_{0;\sigma_{sf}}$	POSSF	$V^{-1/2}$	Coefficient for the geometry independent part of σ_{sf}
55	$P_{L;\sigma_{sf}}$	PLSSF	$V^{-1/2}$	Coefficient for the length dependence of σ_{sf}
56	$P_{W;\sigma_{sf}}$	PWSSF	$V^{-1/2}$	Coefficient for the width dependence of σ_{sf}
57	$P_{LW;\sigma_{sf}}$	PLWSSF	$V^{-1/2}$	Coefficient for the length times width dependence of σ_{sf}
58	$P_{0;\alpha}$	POALP	-	Coefficient for the geometry independent part of α
59	$P_{L;\alpha}$	PLALP	-	Coefficient for the length dependence of α
60	$P_{W;\alpha}$	PWALP	-	Coefficient for the width dependence of α
61	$P_{LW;\alpha}$	PLWALP	-	Coefficient for the length times width dependence of α
62	V_P	VP	V	Characteristic voltage of the channel length modulation
63	$P_{0;m}$	POMEXP	-	Coefficient for the geometry independent part of $1/m$
64	$P_{L;m}$	PLMEXP	-	Coefficient for the length dependence of $1/m$
65	$P_{W;m}$	PWMEXP	-	Coefficient for the width dependence of $1/m$
66	$P_{LW;m}$	PLWMEXP	-	Coefficient for the length times width dependence of $1/m$
67	$P_{0;a_1}$	POA1	-	Coefficient for the geometry independent part of a_1
68	$P_{L;a_1}$	PLA1	-	Coefficient for the length dependence of a_1

No.	Symbol	Progr. Name	Units	Description
69	$P_{W;a_1}$	PWA1	-	Coefficient for the width dependence of a_1
70	$P_{LW;a_1}$	PLWA1	-	Coefficient for the length times width dependence of a_1
71	$P_{0;a_2}$	POA2	V	Coefficient for the geometry independent part of a_2
72	$P_{L;a_2}$	PLA2	V	Coefficient for the length dependence of a_2
73	$P_{W;a_2}$	PWA2	V	Coefficient for the width dependence of a_2
74	$P_{LW;a_2}$	PLWA2	V	Coefficient for the length times width dependence of a_2
75	$P_{0;a_3}$	POA3	-	Coefficient for the geometry independent part of a_3
76	$P_{L;a_3}$	PLA3	-	Coefficient for the length dependence of a_3
77	$P_{W;a_3}$	PWA3	-	Coefficient for the width dependence of a_3
78	$P_{LW;a_3}$	PLWA3	-	Coefficient for the length times width dependence of a_3
79	$P_{0;I_{GINV}}$	POIGINV	AV^{-2}	Coefficient for the geometry independent part of I_{GINV}
80	$P_{L;I_{GINV}}$	PLIGINV	AV^{-2}	Coefficient for the length dependence of I_{GINV}
81	$P_{W;I_{GINV}}$	PWIGINV	AV^{-2}	Coefficient for the width dependence of I_{GINV}
82	$P_{LW;I_{GINV}}$	PLWIGINV	AV^{-2}	Coefficient for the length times width dependence of I_{GINV}

No.	Symbol	Progr. Name	Units	Description
83	$P_{0;B_{inv}}$	POBINV	V	Coefficient for the geometry independent part of B_{inv}
84	$P_{L;B_{inv}}$	PLBINV	V	Coefficient for the length dependence of B_{inv}
85	$P_{W;B_{inv}}$	PWBINV	V	Coefficient for the width dependence of B_{inv}
86	$P_{LW;B_{inv}}$	PLWBINV	V	Coefficient for the length times width dependence of B_{inv}
87	$P_{0;I_{GACC}}$	POIGACC	AV^{-2}	Coefficient for the geometry independent part of I_{GACC}
88	$P_{L;I_{GACC}}$	PLIGACC	AV^{-2}	Coefficient for the length dependence of I_{GACC}
89	$P_{W;I_{GACC}}$	PWIGACC	AV^{-2}	Coefficient for the width dependence of I_{GACC}
90	$P_{LW;I_{GACC}}$	PLWIGACC	AV^{-2}	Coefficient for the length times width dependence of I_{GACC}
91	$P_{0;B_{acc}}$	POBACC	V	Coefficient for the geometry independent part of B_{acc}
92	$P_{L;B_{acc}}$	PLBACC	V	Coefficient for the length dependence of B_{acc}
93	$P_{W;B_{acc}}$	PWBACC	V	Coefficient for the width dependence of B_{acc}
94	$P_{LW;B_{acc}}$	PLWBACC	V	Coefficient for the length times width dependence of B_{acc}
95	V_{FBov}	VFBOV	V	Flat-band voltage for the source/drain overlap extensions
96	k_{ov}	KOV	$V^{1/2}$	Bodu-effect factor for the source/drain overlap extensions

No.	Symbol	Progr. Name	Units	Description
97	$P_{0;I_{GOV}}$	POIGOV	AV^{-2}	Coefficient for the geometry independent part of I_{GOV}
98	$P_{L;I_{GOV}}$	PLIGOV	AV^{-2}	Coefficient for the length dependence of I_{GOV}
99	$P_{W;I_{GOV}}$	PWIGOV	AV^{-2}	Coefficient for the width dependence of I_{GOV}
100	$P_{LW;I_{GOV}}$	PLWIGOV	AV^{-2}	Coefficient for the length times width dependence of I_{GOV}
101	$P_{0;A_{GIDL}}$	POAGIDL	AV^{-3}	Coefficient for the geometry independent part of A_{GIDL}
102	$P_{L;A_{GIDL}}$	PLAGIDL	AV^{-3}	Coefficient for the length dependence of A_{GIDL}
103	$P_{W;A_{GIDL}}$	PWAGIDL	AV^{-3}	Coefficient for the width dependence of A_{GIDL}
104	$P_{LW;A_{GIDL}}$	PLWAGIDL	AV^{-3}	Coefficient for the width over length dependence of A_{GIDL}
105	$P_{0;B_{GIDL}}$	POBGIDL	V	Coefficient for the geometry independent part of B_{GIDL}
106	$P_{L;B_{GIDL}}$	PLBGIDL	V	Coefficient for the length dependence of B_{GIDL}
107	$P_{W;B_{GIDL}}$	PWBGIDL	V	Coefficient for the width dependence of B_{GIDL}
108	$P_{LW;B_{GIDL}}$	PLWBGIDL	V	Coefficient for the length times width dependence of B_{GIDL}
109	$P_{0;C_{GIDL}}$	POCGIDL	-	Coefficient for the geometry independent part of C_{GIDL}
110	$P_{L;C_{GIDL}}$	PLCGIDL	-	Coefficient for the length dependence of C_{GIDL}

No.	Symbol	Progr. Name	Units	Description
111	$P_{W;C_{GIDL}}$	PWCGIDL	-	Coefficient for the width dependence of C_{GIDL}
112	$P_{LW;C_{GIDL}}$	PLWCGIDL	-	Coefficient for the length times width dependence of C_{GIDL}
113	t_{ox}	TOX	m	Thickness of the gate oxide layer
114	$P_{0;C_{ox}}$	POCOX	F	Coefficient for the geometry independent part of C_{ox}
115	$P_{L;C_{ox}}$	PLCOX	F	Coefficient for the length dependence of C_{ox}
116	$P_{W;C_{ox}}$	PWCOX	F	Coefficient for the width dependence of C_{ox}
117	$P_{LW;C_{ox}}$	PLWCOX	F	Coefficient for the length times width dependence of C_{ox}
118	$P_{0;C_{GDO}}$	POCGDO	F	Coefficient for the geometry independent part of C_{GDO}
119	$P_{L;C_{GDO}}$	PLCGDO	F	Coefficient for the length dependence of C_{GDO}
120	$P_{W;C_{GDO}}$	PWCGDO	F	Coefficient for the width dependence of C_{GDO}
121	$P_{LW;C_{GDO}}$	PLWCGDO	F	Coefficient for the width over length dependence of C_{GDO}
122	$P_{0;C_{GSO}}$	POCGSO	F	Coefficient for the geometry independent part of C_{GSO}
123	$P_{L;C_{GSO}}$	PLCGSO	F	Coefficient for the length dependence of C_{GSO}
124	$P_{W;C_{GSO}}$	PWCGSO	F	Coefficient for the width dependence of C_{GSO}
125	$P_{LW;C_{GSO}}$	PLWCGSO	F	Coefficient for the width over length dependence of C_{GSO}

No.	Symbol	Progr. Name	Units	Description
126	-	GATENOISE		Flag for in/exclusion of induced gate thermal noise
127	N_T	NT	J	Coefficient of the thermal noise at the reference temperature
128	$P_{0;N_{FA}}$	PONFA	$V^{-1}m^{-4}$	Coefficient for the geometry independent part of N_{FA}
129	$P_{L;N_{FA}}$	PLNFA	$V^{-1}m^{-4}$	Coefficient for the length dependence of N_{FA}
130	$P_{W;N_{FA}}$	PWNFA	$V^{-1}m^{-4}$	Coefficient for the width dependence of N_{FA}
131	$P_{LW;N_{FA}}$	PLWNFA	$V^{-1}m^{-4}$	Coefficient for the length times width dependence of N_{FA}
132	$P_{0;N_{FB}}$	PONFB	$V^{-1}m^{-2}$	Coefficient for the geometry independent part of N_{FB}
133	$P_{L;N_{FB}}$	PLNFB	$V^{-1}m^{-2}$	Coefficient for the length dependence of N_{FB}
134	$P_{W;N_{FB}}$	PWNFB	$V^{-1}m^{-2}$	Coefficient for the width dependence of N_{FB}
135	$P_{LW;N_{FB}}$	PLWNFB	$V^{-1}m^{-2}$	Coefficient for the length times width dependence of N_{FB}
136	$P_{0;N_{FC}}$	PONFC	V^{-1}	Coefficient for the geometry independent part of N_{FC}
137	$P_{L;N_{FC}}$	PLNFC	V^{-1}	Coefficient for the length dependence of N_{FC}
138	$P_{W;N_{FC}}$	PWNFC	V^{-1}	Coefficient for the width dependence of N_{FC}
139	$P_{LW;N_{FC}}$	PLWNFC	V^{-1}	Coefficient for the length times width dependence of N_{FC}

No.	Symbol	Progr. Name	Units	Description
140	$P_{0;T;V_{FB}}$	POTVFB	VK^{-1}	Coefficient for the geometry independent part of $S_{T;V_{FB}}$
141	$P_{L;T;V_{FB}}$	PLTVFB	VK^{-1}	Coefficient for the length dependence of $S_{T;V_{FB}}$
142	$P_{W;T;V_{FB}}$	PWTVFB	VK^{-1}	Coefficient for the width dependence of $S_{T;V_{FB}}$
143	$P_{LW;T;V_{FB}}$	PLWTVFB	VK^{-1}	Coefficient for the length times width dependence of $S_{T;V_{FB}}$
144	$P_{0;T;\phi_B}$	POTPHIB	VK^{-1}	Coefficient for the geometry independent part of $S_{T;\phi_B}$
145	$P_{L;T;\phi_B}$	PLTPHIB	VK^{-1}	Coefficient for the length dependence of $S_{T;\phi_B}$
146	$P_{W;T;\phi_B}$	PWTPHIB	VK^{-1}	Coefficient for the width dependence of $S_{T;\phi_B}$
147	$P_{LW;T;\phi_B}$	PLWTPHIB	VK^{-1}	Coefficient for the length times width dependence of $S_{T;\phi_B}$
148	$P_{0;T;\eta_\beta}$	POTETABET	-	Coefficient for the geometry independent part of η_β
149	$P_{L;T;\eta_\beta}$	PLTETABET	-	Coefficient for the length dependence of η_β
150	$P_{W;T;\eta_\beta}$	PWTETABET	-	Coefficient for the width dependence of η_β
151	$P_{LW;T;\eta_\beta}$	PLWTETABET	-	Coefficient for the length times width dependence of η_β
152	$P_{0;T;\eta_{sr}}$	POTETASR	-	Coefficient for the geometry independent part of η_{sr}
153	$P_{L;T;\eta_{sr}}$	PLTETASR	-	Coefficient for the length dependence of η_{sr}

No.	Symbol	Progr. Name	Units	Description
154	$P_{W;T;\eta_{sr}}$	PWTETASR	-	Coefficient for the width dependence of η_{sr}
155	$P_{LW;T;\eta_{sr}}$	PLWTETASR	-	Coefficient for the length times width dependence of η_{sr}
156	$P_{0;T;\eta_{ph}}$	POTETAPH	-	Coefficient for the geometry independent part of η_{ph}
157	$P_{L;T;\eta_{ph}}$	PLTETAPH	-	Coefficient for the length dependence of η_{ph}
158	$P_{W;T;\eta_{ph}}$	PWTETAPH	-	Coefficient for the width dependence of η_{ph}
159	$P_{LW;T;\eta_{ph}}$	PLWTETAPH	-	Coefficient for the length times width dependence of η_{ph}
160	$P_{0;T;\eta_{mob}}$	POTETAMOB	K^{-1}	Coefficient for the geometry independent part of $S_{T;\eta_{mob}}$
161	$P_{L;T;\eta_{mob}}$	PLTETAMOB	K^{-1}	Coefficient for the length dependence of $S_{T;\eta_{mob}}$
162	$P_{W;T;\eta_{mob}}$	PWTETAMOB	K^{-1}	Coefficient for the width dependence of $S_{T;\eta_{mob}}$
163	$P_{LW;T;\eta_{mob}}$	PLWTETAMOB	K^{-1}	Coefficient for the length times width dependence of $S_{T;\eta_{mob}}$
164	υ	NU	-	Exponent of the field dependence of the mobility model at the reference temperature
165	$P_{0;T;\upsilon_{exp}}$	POTNUEXP	-	Coefficient for the geometry independent part of υ_{exp}
166	$P_{L;T;\upsilon_{exp}}$	PLTNUEXP	-	Coefficient for the length dependence of υ_{exp}
167	$P_{W;T;\upsilon_{exp}}$	PWTNUEXP	-	Coefficient for the width dependence of υ_{exp}

No.	Symbol	Progr. Name	Units	Description
168	$P_{LW;T;\upsilon_{exp}}$	PLWTNUEXP	-	Coefficient for the length times width dependence of υ_{exp}
169	$P_{0;T;\eta_R}$	POTETAR	-	Coefficient for the geometry independent part of η_R
170	$P_{L;T;\eta_R}$	PLTETAR	-	Coefficient for the length dependence of η_R
171	$P_{W;T;\eta_R}$	PWTETAR	-	Coefficient for the width dependence of η_R
172	$P_{LW;T;\eta_R}$	PLWTETAR	-	Coefficient for the length times width dependence of η_R
173	$P_{0;T;\eta_{sat}}$	POTETASAT	-	Coefficient for the geometry independent part of η_{sat}
174	$P_{L;T;\eta_{sat}}$	PLTETASAT	-	Coefficient for the length dependence of η_{sat}
175	$P_{W;T;\eta_{sat}}$	PWTETASAT	-	Coefficient for the width dependence of η_{sat}
176	$P_{LW;T;\eta_{sat}}$	PLWTETASAT	-	Coefficient for the length times width dependence of η_{sat}
177	$P_{0;T;a_1}$	POTA1	K^{-1}	Coefficient for the geometry independent part of $S_{T;a_1}$
178	$P_{L;T;a_1}$	PLTA1	K^{-1}	Coefficient for the length dependence of $S_{T;a_1}$
179	$P_{W;T;a_1}$	PWTA1	K^{-1}	Coefficient for the width dependence of $S_{T;a_1}$
180	$P_{LW;T;a_1}$	PLWTA1	K^{-1}	Coefficient for the length times width dependence of $S_{T;a_1}$
181	$P_{0;T;B_{GIDL}}$	POTBGIDL	VK^{-1}	Coefficient for the geometry independent part of $S_{T;B_{GIDL}}$

No.	Symbol	Progr. Name	Units	Description
182	$P_{L;T;B_{GIDL}}$	PLTBGIDL	VK^{-1}	Coefficient for the length dependence of $S_{T;B_{GIDL}}$
183	$P_{W;T;B_{GIDL}}$	PWTBGIDL	VK^{-1}	Coefficient for the width dependence of $S_{T;B_{GIDL}}$
184	$P_{LW;T;B_{GIDL}}$	PLWTBGIDL	VK^{-1}	Coefficient for the length times width dependence of $S_{T;B_{GIDL}}$
185	L	L	m	Drawn channel length in the lay-out of the actual transistor
186	W	W	m	Drawn channel width in the lay-out of the actual transistor
187	ΔT_A	DTA	°C	Temperature offset of the device with respect to T_A
188	N_{MULT}	MULT	-	Number of devices in parallel

Remark: The parameters *L*, *W*, and *DTA* are used to calculate the electrical parameters of the actual transistor, as specified in the section on parameter preprocessing.

Default and clipping values (binning geometrical model)

The default values and clipping values for the parameters of the binning geometrical scaling rules of MOS model, level 1101 (n-channel) are listed below.

No.	Parameter	Units	Default	Clip low	Clip high
0	*LEVEL*	-	11011	-	-
1	*LVAR*	m	0.000	-	-
2	*LAP*	m	4.0×10^{-8}	-	-
3	*WVAR*	m	0.000	-	-
4	*WOT*	m	0.000	-	-
5	*TR*	°C	21.0	-273.15	-
6	*VFB*	V	-1.050	-	-
7	*POKO*	$V^{1/2}$	0.500	-	-
8	*PLKO*	$V^{1/2}$	0.000	-	-
9	*PWKO*	$V^{1/2}$	0.000	-	-
10	*PLWKO*	$V^{1/2}$	0.000	-	-
11	*KPINV*	$V^{-1/2}$	0.000	-	-
12	*POPHIB*	V	0.950	-	-
13	*PLPHIB*	V	0.000	-	-
14	*PWPHIB*	V	0.000	-	-
15	*PLWPHIB*	V	0.000	-	-
16	*POBET*	AV^{-2}	1.922×10^{-3}	-	-
17	*PLBET*	AV^{-2}	0.000	-	-
18	*PWBET*	AV^{-2}	0.000	-	-
19	*PLWBET*	AV^{-2}	0.000	-	-
20	*POTHESR*	V^{-1}	3.562×10^{-1}	-	-

No.	Parameter	Units	Default	Clip low	Clip high
21	*PLTHESR*	V^{-1}	0.000	-	-
22	*PWTHESR*	V^{-1}	0.000	-	-
23	*PLWTHESR*	V^{-1}	0.000	-	-
24	*POTHEPH*	V^{-1}	1.290×10^{-2}	-	-
25	*PLTHEPH*	V^{-1}	0.000	-	-
26	*PWTHEPH*	V^{-1}	0.000	-	-
27	*PLWTHEPH*	V^{-1}	0.000	-	-
28	*POETAMOB*	-	1.400	-	-
29	*PLETAMOB*	-	0.000	-	-
30	*PWETAMOB*	-	0.000	-	-
31	*PLWETAMOB*	-	0.000	-	-
32	*POTHER*	V^{-1}	8.120×10^{-2}	-	-
33	*PLTHER*	V^{-1}	0.000	-	-
34	*PWTHER*	V^{-1}	0.000	-	-
35	*PLWTHER*	V^{-1}	0.000	-	-
36	*THER1*	V	0.000	-	-
37	*THER2*	V	1.000	-	-
38	*POTHESAT*	V^{-1}	2.513×10^{-1}	-	-
39	*PLTHESAT*	V^{-1}	0.000	-	-
40	*PWTHESAT*	V^{-1}	0.000	-	-
41	*PLWTHESAT*	V^{-1}	0.000	-	-
42	*POTHETH*	V^{-3}	1.0×10^{-5}	-	-
43	*PLTHETH*	V^{-3}	0.000	-	-
44	*PWTHETH*	V^{-3}	0.000	-	-

No.	Parameter	Units	Default	Clip low	Clip high
45	*PLWTHETH*	V^{-3}	0.000	-	-
46	*POSDIBL*	$V^{-1/2}$	8.530×10^{-4}	-	-
47	*PLSDIBL*	$V^{-1/2}$	0.000	-	-
48	*PWSDIBL*	$V^{-1/2}$	0.000	-	-
49	*PLWSDIBL*	$V^{-1/2}$	0.000	-	-
50	*POMO*	-	0.000	-	-
51	*PLMO*	-	0.000	-	-
52	*PWMO*	-	0.000	-	-
53	*PLWMO*	-	0.000	-	-
54	*POSSF*	$V^{-1/2}$	1.200×10^{-2}	-	-
55	*PLSSF*	$V^{-1/2}$	0.000	-	-
56	*PWSSF*	$V^{-1/2}$	0.000	-	-
57	*PLWSSF*	$V^{-1/2}$	0.000	-	-
58	*POALP*	-	2.500×10^{-2}	-	-
59	*PLALP*	-	0.000	-	-
60	*PWALP*	-	0.000	-	-
61	*PLWALP*	-	0.000	-	-
62	*VP*	V	5.000×10^{-2}	-	-
63	*POMEXP*	-	0.200	-	-
64	*PLMEXP*	-	0.000	-	-
65	*PWMEXP*	-	0.000	-	-
66	*PLWMEXP*	-	0.000	-	-
67	*POA1*	-	6.022	-	-
68	*PLA1*	-	0.000	-	-
69	*PWA1*	-	0.000	-	-

No.	Parameter	Units	Default	Clip low	Clip high
70	*PLWA1*	-	0.000	-	-
71	*POA2*	V	3.802×10^{1}	-	-
72	*PLA2*	V	0.000	-	-
73	*PWA2*	V	0.000	-	-
74	*PLWA2*	V	0.000	-	-
75	*POA3*	-	6.407×10^{-1}	-	-
76	*PLA3*	-	0.000	-	-
77	*PWA3*	-	0.000	-	-
78	*PLWA3*	-	0.000	-	-
79	*POIGINV*	AV^{-2}	0.000	-	-
80	*PLIGINV*	-	0.000	-	-
81	*PWIGINV*	-	0.000	-	-
82	*PLWIGINV*	-	0.000	-	-
83	*POBINV*	V	4.800×10^{1}	-	-
84	*PLBINV*	V	0.000	-	-
85	*PWBINV*	V	0.000	-	-
86	*PLWBINV*	V	0.000	-	-
87	*POIGACC*	AV^{-2}	0.000	-	-
88	*PLIGACC*	AV^{-2}	0.000	-	-
89	*PWIGACC*	AV^{-2}	0.000	-	-
90	*PLWIGACC*	AV^{-2}	0.000	-	-
91	*POBACC*	V	4.800×10^{1}	-	-
92	*PLBACC*	V	0.000	-	-
93	*PWBACC*	V	0.000	-	-
94	*PLWBACC*	V	0.000	-	-
95	*VFBOV*	V	0.000	-	-

No.	Parameter	Units	Default	Clip low	Clip high
96	*KOV*	$V^{1/2}$	2.500	1.0×10^{-12}	-
97	*POIGOV*	AV^{-2}	0.000	-	-
98	*PLIGOV*	AV^{-2}	0.000	-	-
99	*PWIGOV*	AV^{-2}	0.000	-	-
100	*PLWIGOV*	AV^{-2}	0.000	-	-
101	*POAGIDL*	AV^{-3}	0.000	-	-
102	*PLAGIDL*	AV^{-3}	0.000	-	-
103	*PWAGIDL*	AV^{-3}	0.000	-	-
104	*PLWAGIDL*	AV^{-3}	0.000	-	-
105	*POBGIDL*	V	$4.100 \times 10^{+1}$	-	-
106	*PLBGIDL*	V	0.000	-	-
107	*PWBGIDL*	V	0.000	-	-
108	*PLWBGIDL*	V	0.000	-	-
109	*POCGIDL*	-	0.000	-	-
110	*PLCGIDL*	-	0.000	-	-
111	*PWCGIDL*	-	0.000	-	-
112	*PLWCCGIDL*	-	0.000	-	-
113	*TOX*	m	3.200×10^{-9}	1.0×10^{-12}	-
114	*POCOX*	F	2.980×10^{-14}	-	-
115	*PLCOX*	F	0.000	-	-
116	*PWCOX*	F	0.000	-	-
117	*PLWCOX*	F	0.000	-	-
118	*POCGDO*	F	6.392×10^{-15}	-	-
119	*PLCGDO*	F	0.000	-	-
120	*PWCGDO*	F	0.000	-	-

No.	Parameter	Units	Default	Clip low	Clip high
121	*PLWCGDO*	F	0.000	-	-
122	*POCGSO*	F	6.392×10^{-15}	-	-
123	*PLCGSO*	F	0.000	-	-
124	*PWCGSO*	F	0.000	-	-
125	*PLWCGSO*	F	0.000	-	-
126	*GATENOISE*	-	0.000	0.000	1.000
127	*NT*	J	1.656×10^{-20}	0.000	-
128	*PONFA*	$V^{-1}m^{-4}$	8.323×10^{22}	-	-
129	*PLNFA*	$V^{-1}m^{-4}$	0.000	-	-
130	*PWNFA*	$V^{-1}m^{-4}$	0.000	-	-
131	*PLWNFA*	$V^{-1}m^{-4}$	0.000	-	-
132	*PONFB*	$V^{-1}m^{-2}$	2.514×10^{7}	-	-
133	*PLNFB*	$V^{-1}m^{-2}$	0.000	-	-
134	*PWNFB*	$V^{-1}m^{-2}$	0.000	-	-
135	*PLWNFB*	$V^{-1}m^{-2}$	0.000	-	-
136	*PONFC*	V^{-1}	0.000	-	-
137	*PLNFC*	V^{-1}	0.000	-	-
138	*PWNFC*	V^{-1}	0.000	-	-
139	*PLWNFC*	V^{-1}	0.000	-	-
140	*POTVFB*	VK^{-1}	5.000×10^{-4}	-	-
141	*PLTVFB*	VK^{-1}	0.000	-	-
142	*PWTVFB*	VK^{-1}	0.000	-	-
143	*PLWTVFB*	VK^{-1}	0.000	-	-
144	*POTPHIB*	VK^{-1}	-8.500×10^{-4}	-	-

No.	Parameter	Units	Default	Clip low	Clip high
145	*PLTPHIB*	VK^{-1}	0.000	-	-
146	*PWTPHIB*	VK^{-1}	0.000	-	-
147	*PLWTPHIB*	VK^{-1}	0.000	-	-
148	*POTETABET*	-	1.300	-	-
149	*PLTETABET*	-	0.000	-	-
150	*PWTETABET*	-	0.000	-	-
151	*PLWTETABET*	-	0.000	-	-
152	*POTETASR*	-	0.650	-	-
153	*PLTETASR*	-	0.000	-	-
154	*PWTETASR*	-	0.000	-	-
155	*PLWETASR*	-	0.000	-	-
156	*POTETAPH*	-	1.350	-	-
157	*PLTETAPH*	-	0.000	-	-
158	*PWTETAPH*	-	0.000	-	-
159	*PLWETAPH*	-	0.000	-	-
160	*POTETAMOB*	K^{-1}	0.000	-	-
161	*PLTETAMOB*	K^{-1}	0.000	-	-
162	*PWTETAMOB*	K^{-1}	0.000	-	-
163	*PLWTETAMOB*	K^{-1}	0.000	-	-
164	*NU*	-	2.000	1.000	-
165	*POTNUEXP*	-	5.250	-	-
166	*PLTNUEXP*	-	0.000	-	-
167	*PWTNUEXP*	-	0.000	-	-
168	*PLWTNUEXP*	-	0.000	-	-
169	*POTETAR*	-	0.950	-	-
170	*PLTETAR*	-	0.000	-	-

No.	Parameter	Units	Default	Clip low	Clip high
171	*PWTETAR*	-	0.000	-	-
172	*PLWTETAR*	-	0.000	-	-
173	*POTETASAT*	-	1.040	-	-
174	*PLTETASAT*	-	0.000	-	-
175	*PWTETASAT*	-	0.000	-	-
176	*PLWTETASAT*	-	0.000	-	-
177	*POTA1*	K^{-1}	0.000	-	-
178	*PLTA1*	K^{-1}	0.000	-	-
179	*PWTA1*	K^{-1}	0.000	-	-
180	*PLWTA1*	K^{-1}	0.000	-	-
181	*POTBGIDL*	VK^{-1}	$-3.638x10^{-4}$	-	-
182	*PLTBGIDL*	VK^{-1}	0.000	-	-
183	*PWTBGIDL*	VK^{-1}	0.000	-	-
184	*PLWTBGIDL*	VK^{-1}	0.000	-	-
185	*L*	m	2.000×10^{-6}	-	-
186	*W*	m	1.000×10^{-5}	-	-
187	*DTA*	K	0.000	-	-
188	*MULT*	-	1.000	0.000	-

The default values and clipping values for the parameters of the binning geometrical scaling rules of MOS model, level 1101 (p-channel) are listed below.

No.	Parameter	Units	Default	Clip low	Clip high
0	*LEVEL*	-	11011	-	-
1	*LVAR*	m	0.000	-	-
2	*LAP*	m	4.0×10^{-8}	-	-
3	*WVAR*	m	0.000	-	-
4	*WOT*	m	0.000	-	-
5	*TR*	°C	21.0	-273.15	-
6	*VFB*	V	-1.050	-	-
7	*POKO*	$V^{1/2}$	0.500	-	-
8	*PLKO*	$V^{1/2}$	0.000	-	-
9	*PWKO*	$V^{1/2}$	0.000	-	-
10	*PLWKO*	$V^{1/2}$	0.000	-	-
11	*KPINV*	$V^{-1/2}$	0.000	-	-
12	*POPHIB*	V	0.950	-	-
13	*PLPHIB*	V	0.000	-	-
14	*PWPHIB*	V	0.000	-	-
15	*PLWPHIB*	V	0.000	-	-
16	*POBET*	AV^{-2}	3.814×10^{-4}	-	-
17	*PLBET*	AV^{-2}	0.000	-	-
18	*PWBET*	AV^{-2}	0.000	-	-
19	*PLWBET*	AV^{-2}	0.000	-	-
20	*POTHESR*	V^{-1}	7.300×10^{-1}	-	-
21	*PLTHESR*	V^{-1}	0.000	-	-

No.	Parameter	Units	Default	Clip low	Clip high
22	*PWTHESR*	V^{-1}	0.000	-	-
23	*PLWTHESR*	V^{-1}	0.000	-	-
24	*POTHEPH*	V^{-1}	1.000×10^{-3}	-	-
25	*PLTHEPH*	V^{-1}	0.000	-	-
26	*PWTHEPH*	V^{-1}	0.000	-	-
27	*PLWTHEPH*	V^{-1}	0.000	-	-
28	*POETAMOB*	-	3.000	-	-
29	*PLETAMOB*	-	0.000	-	-
30	*PWETAMOB*	-	0.000	-	-
31	*PLWETAMOB*	-	0.000	-	-
32	*POTHER*	V^{-1}	7.900×10^{-2}	-	-
33	*PLTHER*	V^{-1}	0.000	-	-
34	*PWTHER*	V^{-1}	0.000	-	-
35	*PLWTHER*	V^{-1}	0.000	-	-
36	*THER1*	V	0.000	-	-
37	*THER2*	V	1.000	-	-
38	*POTHESAT*	V^{-1}	1.728×10^{-1}	-	-
39	*PLTHESAT*	V^{-1}	0.000	-	-
40	*PWTHESAT*	V^{-1}	0.000	-	-
41	*PLWTHESAT*	V^{-1}	0.000	-	-
42	*POTHETH*	V^{-3}	0.000	-	-
43	*PLTHETH*	V^{-3}	0.000	-	-
44	*PWTHETH*	V^{-3}	0.000	-	-
45	*PLWTHETH*	V^{-3}	0.000	-	-

No.	Parameter	Units	Default	Clip low	Clip high
46	*POSDIBL*	$V^{-1/2}$	3.551×10^{-5}	-	-
47	*PLSDIBL*	$V^{-1/2}$	0.000	-	-
48	*PWSDIBL*	$V^{-1/2}$	0.000	-	-
49	*PLWSDIBL*	$V^{-1/2}$	0.000	-	-
50	*POMO*	-	0.000	-	-
51	*PLMO*	-	0.000	-	-
52	*PWMO*	-	0.000	-	-
53	*PLWMO*	-	0.000	-	-
54	*POSSF*	$V^{-1/2}$	1.000×10^{-2}	-	-
55	*PLSSF*	$V^{-1/2}$	0.000	-	-
56	*PWSSF*	$V^{-1/2}$	0.000	-	-
57	*PLWSSF*	$V^{-1/2}$	0.000	-	-
58	*POALP*	-	2.500×10^{-2}	-	-
59	*PLALP*	-	0.000	-	-
60	*PWALP*	-	0.000	-	-
61	*PLWALP*	-	0.000	-	-
62	*VP*	V	5.000×10^{-2}	-	-
63	*POMEXP*	-	0.200	-	-
64	*PLMEXP*	-	0.000	-	-
65	*PWMEXP*	-	0.000	-	-
66	*PLWMEXP*	-	0.000	-	-
67	*POA1*	-	6.858	-	-
68	*PLA1*	-	0.000	-	-
69	*PWA1*	-	0.000	-	-
70	*PLWA1*	-	0.000	-	-

No.	Parameter	Units	Default	Clip low	Clip high
71	*POA2*	V	5.732×10^{1}	-	-
72	*PLA2*	V	0.000	-	-
73	*PWA2*	V	0.000	-	-
74	*PLWA2*	V	0.000	-	-
75	*POA3*	-	4.254×10^{-1}	-	-
76	*PLA3*	-	0.000	-	-
77	*PWA3*	-	0.000	-	-
78	*PLWA3*	-	0.000	-	-
79	*POIGINV*	AV^{-2}	0.000	-	-
80	*PLIGINV*	-	0.000	-	-
81	*PWIGINV*	-	0.000	-	-
82	*PLWIGINV*	-	0.000	-	-
83	*POBINV*	V	87.50	-	-
84	*PLBINV*	V	0.000	-	-
85	*PWBINV*	V	0.000	-	-
86	*PLWBINV*	V	0.000	-	-
87	*POIGACC*	AV^{-2}	0.000	-	-
88	*PLIGACC*	AV^{-2}	0.000	-	-
89	*PWIGACC*	AV^{-2}	0.000	-	-
90	*PLWIGACC*	AV^{-2}	0.000	-	-
91	*POBACC*	V	48.00	-	-
92	*PLBACC*	V	0.000	-	-
93	*PWBACC*	V	0.000	-	-
94	*PLWBACC*	V	0.000	-	-
95	*VFBOV*	V	0.000	-	-
96	*KOV*	$V^{1/2}$	2.500	-	-

No.	Parameter	Units	Default	Clip low	Clip high
97	*POIGOV*	AV^{-2}	0.000	-	-
98	*PLIGOV*	AV^{-2}	0.000	-	-
99	*PWIGOV*	AV^{-2}	0.000	-	-
100	*PLWIGOV*	AV^{-2}	0.000	-	-
101	*POAGIDL*	AV^{-3}	0.000	-	-
102	*PLAGIDL*	AV^{-3}	0.000	-	-
103	*PWAGIDL*	AV^{-3}	0.000	-	-
104	*PLWAGIDL*	AV^{-3}	0.000	-	-
105	*POBGIDL*	V	$4.100 \times 10^{+1}$	-	-
106	*PLBGIDL*	V	0.000	-	-
107	*PWBGIDL*	V	0.000	-	-
108	*PLWBGIDL*	V	0.000	-	-
109	*POCGIDL*	-	0.000	-	-
110	*PLCGIDL*	-	0.000	-	-
111	*PWCGIDL*	-	0.000	-	-
112	*PLWCCGIDL*	-	0.000	-	-
113	*TOX*	m	3.200×10^{-9}	-	-
114	*POCOX*	F	2.717×10^{-14}	-	-
115	*PLCOX*	F	0.000	-	-
116	*PWCOX*	F	0.000	-	-
117	*PLWCOX*	F	0.000	-	-
118	*POCGDO*	F	6.358×10^{-15}	-	-
119	*PLCGDO*	F	0.000	-	-
120	*PWCGDO*	F	0.000	-	-
121	*PLWCGDO*	F	0.000	-	-

No.	Parameter	Units	Default	Clip low	Clip high
122	*POCGSO*	F	6.358×10^{-15}	-	-
123	*PLCGSO*	F	0.000	-	-
124	*PWCGSO*	F	0.000	-	-
125	*PLWCGSO*	F	0.000	-	-
126	*GATENOISE*	-	0.000	0.000	1.000
127	*NT*	J	1.656×10^{-20}	-	-
128	*PONFA*	$V^{-1}m^{-4}$	1.900×10^{22}	-	-
129	*PLNFA*	$V^{-1}m^{-4}$	0.000	-	-
130	*PWNFA*	$V^{-1}m^{-4}$	0.000	-	-
131	*PLWNFA*	$V^{-1}m^{-4}$	0.000	-	-
132	*PONFB*	$V^{-1}m^{-2}$	5.043×10^{6}	-	-
133	*PLNFB*	$V^{-1}m^{-2}$	0.000	-	-
134	*PWNFB*	$V^{-1}m^{-2}$	0.000	-	-
135	*PLWNFB*	$V^{-1}m^{-2}$	0.000	-	-
136	*PONFC*	V^{-1}	3.627×10^{-10}	-	-
137	*PLNFC*	V^{-1}	0.000	-	-
138	*PWNFC*	V^{-1}	0.000	-	-
139	*PLWNFC*	V^{-1}	0.000	-	-
140	*POTVFB*	VK^{-1}	0.5×10^{-3}	-	-
141	*PLTVFB*	VK^{-1}	0.000	-	-
142	*PWTVFB*	VK^{-1}	0.000	-	-
143	*PLWTVFB*	VK^{-1}	0.000	-	-
144	*POTPHIB*	VK^{-1}	-8.5×10^{-4}	-	-
145	*PLTPHIB*	VK^{-1}	0.000	-	-

No.	Parameter	Units	Default	Clip low	Clip high
146	*PWTPHIB*	VK^{-1}	0.000	-	-
147	*PLWTPHIB*	VK^{-1}	0.000	-	-
148	*POTETABET*	-	0.500	-	-
149	*PLTETABET*	-	0.000	-	-
150	*PWTETABET*	-	0.000	-	-
151	*PLWTETABET*	-	0.000	-	-
152	*POTETASR*	-	0.500	-	-
153	*PLTETASR*	-	0.000	-	-
154	*PWTETASR*	-	0.000	-	-
155	*PLWTETASR*	-	0.000	-	-
156	*POTETAPH*	-	3.750	-	-
157	*PLTETAPH*	-	0.000	-	-
158	*PWTETAPH*	-	0.000	-	-
159	*PLWTETAPH*	-	0.000	-	-
160	*POTETAMOB*	K^{-1}	0.000	-	-
161	*PLTETAMOB*	K^{-1}	0.000	-	-
162	*PWTETAMOB*	K^{-1}	0.000	-	-
163	*PLWTETAMOB*	K^{-1}	0.000	-	-
164	*NU*	-	2.000	-	-
165	*POTNUEXP*	-	3.230	-	-
166	*PLTNUEXP*	-	0.000	-	-
167	*PWTNUEXP*	-	0.000	-	-
168	*PLWTNUEXP*	-	0.000	-	-
169	*POTETAR*	-	0.400	-	-
170	*PLTETAR*	-	0.000	-	-
171	*PWTETAR*	-	0.000	-	-

No.	Parameter	Units	Default	Clip low	Clip high
172	*PLWTETAR*	-	0.000	-	-
173	*POTETASAT*	-	0.860	-	-
174	*PLTETASAT*	-	0.000	-	-
175	*PWTETASAT*	-	0.000	-	-
176	*PLWTETASAT*	-	0.000	-	-
177	*POTA1*	K^{-1}	0.000	-	-
178	*PLTA1*	K^{-1}	0.000	-	-
179	*PWTA1*	K^{-1}	0.000	-	-
180	*PLWTA1*	K^{-1}	0.000	-	-
181	*POTBGIDL*	VK^{-1}	-3.638×10^{-4}	-	-
182	*PLTBGIDL*	VK^{-1}	0.000	-	-
183	*PWTBGIDL*	VK^{-1}	0.000	-	-
184	*PLWTBGIDL*	VK^{-1}	0.000	-	-
185	*L*	m	2.000×10^{-6}	-	-
186	*W*	m	1.000×10^{-5}	-	-
187	*DTA*	K	0.000	-	-
188	*MULT*	-	1.000	0.000	-

Parameters of the electrical model

These parameter correspond to the electrical model (MNE, MPE).

No.	Symbol	Progr. Name	Units	Description
0		LEVEL	-	Must be 1101
1	T_R	TR	^oC	Reference temperature
2	V_{FB}	VFB	V	Flat-band voltage for the actual transistor at the reference temperature
3	$S_{T;V_{FB}}$	STVFB	VK^{-1}	Coefficient of the temperature dependence of V_{FB}
4	k_0	K0	$V^{1/2}$	Body-effect factor for the actual transistor
5	*1/kp*	KPINV	$V^{-1/2}$	Inverse of body-effect of the poly-silicon gate for the actual transistor
6	ϕ_B	PHIB	V	Surface potential at the onset of strong inversion for the actual transistor at the reference temperature
7	$S_{T;\phi_B}$	STPHIB	VK^{-1}	Coefficient of the temperature dependence of ϕ_B
8	β	BET	AV^{-2}	Gain factor for the actual transistor at the reference temperature
9	η_β	ETABET	-	Exponent of the temperature dependence of the gain factor
10	θ_{sr}	THESR	V^{-1}	Coefficient of the mobility reduction due to surface roughness scattering for the actual transistor at the reference temperature
11	η_{sr}	ETASR	-	Exponent of the temperature dependence of θ_{sr}
12	θ_{ph}	THEPH	V^{-1}	Coefficient of the mobility reduction due to phonon scattering for the actual transistor at the reference temperature
13	η_{ph}	ETAPH	-	Exponent of the temperature dependence of θ_{ph}

No.	Symbol	Progr. Name	Units	Description
14	η_{mob}	ETAMOB	-	Effective field parameter for dependence on depletion/ inversion charge for the actual transistor at the reference temperature
15	$S_{T;\eta_{mob}}$	STETAMOB	K^{-1}	Coefficient of the temperature dependence of η_{mob}
16	ν	NU	-	Exponent of field dependence of mobility model at the reference temperature
17	υ_{exp}	NUEXP	-	Exponent of the temperature dependence of υ
18	θ_R	THER	V^{-1}	Coefficient of the series resistance for the actual transistor at the reference temperature: $\theta_R = 2 \cdot \beta \cdot R_S$
19	η_r	ETAR	-	Exponent of the temperature dependence of θ_R
20	θ_{R1}	THER1	V	Numerator of the gate voltage dependent part of series resistance for the actual transistor
21	θ_{R2}	THER2	V	Denominator of the gate voltage dependent part of series resistance for the actual transistor
22	θ_{sat}	THESAT	V^{-1}	Velocity saturation parameter due to optical/acoustic phonon scattering for the actual transistor at the reference temperature
23	η_{sat}	ETASAT	-	Exponent of the temperature dependence of θ_{sat}
24	θ_{Th}	THETH	V^{-3}	Coefficient of self-heating for the actual transistor at the reference temperature
25	σ_{dibl}	SDIBL	$V^{-1/2}$	Drain-induced barrier-lowering parameter for the actual transistor
26	m_0	MO	-	Parameter for (short-channel) subthreshold slope for the actual transistor
27	σ_{sf}	SSF	$V^{-1/2}$	Static-feedback parameter for the actual transistor

No.	Symbol	Progr. Name	Units	Description
28	α	ALP	-	Factor of the channel-length modulation for the actual transistor
29	V_P	VP	V	Characteristic voltage of the channel-length modulation
30	m	MEXP	-	Smoothing factor for the actual transistor
31	a_1	A1	-	Factor of the weak-avalanche current for the actual transistor at the reference temperature
32	$S_{T;a_1}$	STA1	K^{-1}	Coefficient of the temperature dependence of a_1
33	a_2	A2	V	Exponent of the weak-avalanche current for the actual transistor
34	a_3	A3	-	Factor of the drain-source voltage above which weak-avalanche occurs for the actual transistor
35	I_{GINV}	IGINV	AV^{-2}	Gain factor for intrinsic gate tunnelling current in inversion for the actual transistor
36	B_{INV}	BINV	V	Probability factor for intrinsic gate tunnelling current in inversion
37	I_{GACC}	IGACC	AV^{-2}	Gain factor for intrinsic gate tunnelling current in accumulation for the actual transistor
38	B_{ACC}	BACC	V	Probability factor for intrinsic gate tunnelling current in accumulation
39	V_{FBov}	VFBOV	V	Flat-band voltage for the source/drain overlap extensions
40	k_{ov}	KOV	$V^{1/2}$	Body-effect factor for the sourcedrain overlap extensions
41	I_{GOV}	IGOV	AV^{-2}	Gain factor for source/drain overlap gate tunnelling current for the actual transistor
42	A_{GIDL}	AGIDL	AV^{-3}	Gain factor for gate-induced drain leakage current for the actual transistor
43	B_{GIDL}	BGIDL	V	Probability factor for gate-induced leakage current at the reference temperature

No.	Symbol	Progr. Name	Units	Description
44	$S_{T;B_{GIDL}}$	STBGIDL	VK^{-1}	Coefficient of the temperature dependence of B_{GIDL}
45	C_{GIDL}	CGIDL	-	Factor for the lateral field dependence of the gate-induced drain leakage current
46	C_{ox}	COX	F	Oxide capacitance for the intrinsic channel for the actual transistor
47	C_{GDO}	CGDO	F	Oxide capacitance for the gate-drain overlap for the actual transistor
48	C_{GSO}	CGSO	F	Oxide capacitance for the gate-source overlap for the actual transistor
49	-	GATENOISE		Flag for in/exclusion of induced gate thermal noise
50	N_T	NT	J	Coefficient of the thermal noise at the reference temperature
51	N_{FA}	NFA	$V^{-1}m^{-4}$	First coefficient of the flicker noise for the actual transistor
52	N_{FB}	NFB	$V^{-1}m^{-2}$	Second coefficient of the flicker noise for the actual transistor
53	N_{FC}	NFC	V^{-1}	Third coefficient of the flicker noise for the actual transistor
54	t_{ox}	TOX	m	Thickness of the gate-oxide layer
55	ΔT_A	DTA	K	Temperature offset of the device with respect to ambient circuit temperature T_A
56	N_{MULT}	MULT	-	Number of devices operating in parallel

✓ Note

The parameter t_{ox} is used for calculation of the effective oxide thickness (due to quantum-mechanical effects) and the 1/f noise, not for the calculation of β !!!

Default and clipping values (electrical model)

The default values and clipping values as used for the parameters of the electrical MOS model, level 1101 (n-channel) are listed below.

No.	**Parameter**	Units	**Default**	Clip low	**Clip high**
0	*LEVEL*	-	1101	-	-
1	*TR*	^{o}C	21.0	-273.15	-
2	*VFB*	V	-1.0500	-	-
3	*STVFB*	VK^{-1}	0.5×10^{-3}	-	-
4	*KO*	$V^{1/2}$	0.5000	1.0×10^{-12}	-
5	*KPINV*	$V^{-1/2}$	0.000	0.000	-
6	*PHIB*	V	0.9500	1.0×10^{-12}	-
7	*STPHIB*	VK^{-1}	-8.5×10^{-4}	-	-
8	*BET*	AV^{-2}	1.9215×10^{-3}	0.0	-
9	*ETABET*	-	1.300	-	-
10	*THESR*	V^{-1}	0.3562	1.0×10^{-12}	-
11	*ETASR*	-	0.650	-	-
12	*THEPH*	V^{-1}	1.29×10^{-2}	1.0×10^{-12}	-
13	*ETAPH*	-	1.350	-	-
14	*ETAMOB*	-	1.4000	0.000	-
15	*STETAMOB*	K^{-1}	0.000	-	-
16	*NU*	-	2.0000	1.000	-
17	*NUEXP*	-	5.250	-	-
18	*THER*	V^{-1}	8.12×10^{-2}	0.000	-
19	*ETAR*	-	0.950	-	-
20	*THER1*	V	0.0000	0.000	-
21	*THER2*	V	1.0000	0.000	-

No.	**Parameter**	Units	**Default**	Clip low	**Clip high**
22	*THESAT*	V^{-1}	0.2513	0.000	-
23	*ETASAT*	-	1.040	-	-
24	*THETH*	V^{-3}	1.0×10^{-5}	0.000	-
25	*SDIBL*	$V^{-1/2}$	8.53×10^{-4}	1.0×10^{-12}	-
26	*MO*	V	0.0000	0.000	0.500
27	*SSF*	$V^{-1/2}$	0.0120	1.0×10^{-12}	-
28	*ALP*	-	0.0250	0.000	-
29	*VP*	V	0.0500	1.0×10^{-12}	-
30	*MEXP*	-	5.0000	1.000	-
31	*A1*	-	6.0221	0.000	-
32	*STA1*	K^{-1}	0.000	-	-
33	*A2*	V	38.017	1.0×10^{-12}	-
34	*A3*	-	0.6407	0.000	-
35	*IGINV*	AV^{-2}	0.0000	0.000	-
36	*BINV*	V	48.000	0.000	-
37	*IGACC*	AV^{-2}	0.0000	0.000	-
38	*BACC*	V	48.000	0.000	-
39	*VFBOV*	V	0.0000	-	-
40	*KOV*	$V^{1/2}$	2.5000	1.0×10^{-12}	-
41	*IGOV*	AV^{-2}	0.0000	0.000	-
42	*AGIDL*	AV^{-3}	0.0000	0.000	-
43	*BGIDL*	V	41.000	0.000	-
44	*STBGIDL*	VK^{-1}	-3.638×10^{-4}	-	-
45	*CGIDL*	-	0.000	0.000	-
46	*COX*	F	2.98×10^{-14}	0.000	-

No.	**Parameter**	Units	**Default**	Clip low	**Clip high**
47	*CGDO*	F	6.392×10^{-15}	0.000	-
48	*CGSO*	F	6.392×10^{-15}	0.000	-
49	*GATENOISE*	-	0.0000	0.000	1.000
50	*NT*	J	1.656×10^{-20}	0.000	-
51	*NFA*	$V^{-1}m^{-4}$	8.323×10^{22}	0.000	-
52	*NFB*	$V^{-1}m^{-2}$	2.514×10^{7}	-	-
53	*NFC*	V^{-1}	0.0000	-	-
54	*TOX*	m	3.2×10^{-9}	1.0×10^{-12}	-
55	*DTA*	K	0.000	-	-
56	*MULT*	-	1.000	0.000	-

The default values and clipping values as used for the parameters of the electrical MOS model, level 1101(p-channel) are listed below.

No.	**Parameter**	Units	**Default**	Clip low	**Clip high**
0	*LEVEL*	-	1101	-	-
1	*TR*	^{o}C	21.0	-273.15	-
2	*VFB*	V	-1.0500	-	-
3	*STVFB*	VK^{-1}	0.5×10^{-3}	-	-
4	*KO*	$V^{1/2}$	0.5000	1.0×10^{-12}	-
5	*KPINV*	$V^{-1/2}$	0.000	0.000	-
6	*PHIB*	V	0.9500	1.0×10^{-12}	-
7	*STPHIB*	VK^{-1}	-8.5×10^{-4}	-	-
8	*BET*	AV^{-2}	3.8140×10^{-4}	0.0	-
9	*ETABET*	-	0.500	-	-
10	*THESR*	V^{-1}	0.7300	1.0×10^{-12}	-
11	*ETASR*	-	0.500	-	-
12	*THEPH*	V^{-1}	0.0010	1.0×10^{-12}	-
13	*ETAPH*	-	3.750	-	-
14	*ETAMOB*	-	3.0000	0.000	-
15	*STETAMOB*	K^{-1}	0.000	-	-
16	*NU*	-	2.0000	1.000	-
17	*NUEXP*	-	3.230	-	-
18	*THER*	V^{-1}	7.90×10^{-2}	0.000	-
19	*ETAR*	-	0.400	-	-
20	*THER1*	V	0.0000	0.000	-
21	*THER2*	V	1.0000	0.000	-
22	*THESAT*	V^{-1}	0.1728	0.000	-

No.	**Parameter**	Units	**Default**	Clip low	**Clip high**
23	*ETASAT*	-	0.860	-	-
24	*THETH*	V^{-3}	0.000	0.000	-
25	*SDIBL*	$V^{-1/2}$	3.551×10^{-5}	1.0×10^{-12}	-
26	*MO*	V	0.0000	0.000	0.500
27	*SSF*	$V^{-1/2}$	0.0100	1.0×10^{-12}	-
28	*ALP*	-	0.0250	0.000	-
29	*VP*	V	0.0500	1.0×10^{-12}	-
30	*MEXP*	-	5.0000	1.000	-
31	*A1*	-	6.8583	0.000	-
32	*STA1*	K^{-1}	0.000	-	-
33	*A2*	V	57.324	1.0×10^{-12}	-
34	*A3*	-	0.4254	0.000	-
35	*IGINV*	AV^{-2}	0.0000	0.000	-
36	*BINV*	V	87.500	0.000	-
37	*IGACC*	AV^{-2}	0.0000	0.000	-
38	*BACC*	V	48.000	0.000	-
39	*VFBOV*	V	0.0000	-	-
40	*KOV*	$V^{1/2}$	2.5000	1.0×10^{-12}	-
41	*IGOV*	AV^{-2}	0.0000	0.000	-
42	*AGIDL*	AV^{-3}	0.0000	0.000	-
43	*BGIDL*	V	41.000	0.000	-
44	*STBGIDL*	VK^{-1}	-3.638×10^{-4}	-	-
45	*CGIDL*	-	0.000	0.000	-
46	*COX*	F	2.717×10^{-14}	0.000	-
47	*CGDO*	F	6.358×10^{-15}	0.000	-

No.	**Parameter**	Units	**Default**	Clip low	**Clip high**
48	*CGSO*	F	6.358×10^{-15}	0.000	-
49	*GATENOISE*	-	0.0000	0.000	1.000
50	*NT*	J	1.656×10^{-20}	0.000	-
51	*NFA*	$V^{-1}m^{-4}$	1.900×10^{22}	0.000	-
52	*NFB*	$V^{-1}m^{-2}$	5.043×10^{6}	-	-
53	*NFC*	V^{-1}	3.627×10^{-10}	-	-
54	*TOX*	m	3.2×10^{-9}	1.0×10^{-12}	-
55	*DTA*	K	0.000	-	-
56	*MULT*	-	1.000	0.000	-

12.2.3 Model constants

The following is a list of constants hardcoded in the model.

No.	Constant	Progr. Name	Units	Description
1	T_0	TO	K	Offset for conversion from Celsius to Kelvin temperature scale (273.15)
2	k_B	KB	JK^{-1}	Boltzmann constant $(1.3806226 \cdot 10^{-23})$
3	q	Q	C	Elementary unit charge $(1.6021918 \cdot 10^{-19})$
4	ε_{ox}	EPSOX	Fm^{-1}	Absolute permittivity of the oxide layer $(3.453143800 \cdot 10^{-11})$
5	QM_N	QMN	$Vm^{4/3}C^{-2/3}$	Constant of quantum-mechanical behavior of electrons $(5.951993.10^{+00})$
6	QM_p	QMP	$Vm^{4/3}C^{-2/3}$	Constant of quantum-mechanical behavior of holes $(7.448711.10^{+00})$
7	χ_{BN}	CHIBN	V	Tunnelling barrier height for electrons for Si/SiO2-structure $(3.1.10^{+00})$
8	χ_{Bp}	CHIBP	V	Tunnelling barrier height for holes for Si/SiO2-structure $(4.5.10^{+00})$

12.3 Pstar specific items

12.3.1 Syntax

n-channel geometrical model	:	MN_n (D, G, S, B)	<parameters>
p-channel geometrical model	:	MP_n (D, G, S, B)	<parameters>
n-channel electrical model	:	MNE_n (D, G, S, B)	<parameters>
p-channel electrical model	:	MPE_n (D, G, S, B)	<parameters>

n	:	occurrence indicator
<parameters>	:	list of model parameters

D, G, S and B are drain, gate, source and bulk terminals respectively.

12.3.2 The ON/OFF condition

The solution for a circuit involves a process of successive calculations. The calculations are started from a set of 'initial guesses' for the electrical quantities of the non-linear elements. A simplified DCAPPROX mechanism for devices using ON/OFF keywords is mentioned in [9]. By default the devices start in the default state.

n-channel			
	Default	ON	OFF
V_{DS}	1.25	1.25	2.5
V_{GS}	1.25	1.25	0.0
V_{SB}	0.0	0.0	0.0

p-channel			
	Default	ON	OFF
V_{DS}	-1.25	-1.25	-2.5
V_{GS}	-1.25	-1.25	0.0
V_{SB}	0.0	0.0	0.0

12.3.3 Numerical adaptation

To implement the model in a circuit simulator, care must be taken of the numerical stability of the simulation program. A small non-physical conductance, G_{min}, is connected between the nodes *D* and *S*. The value of the conductance is 10^{-15} [1/Ω].

12.3.4 DC operating point

The DC operating point output facility gives information on the state of a device at its operation point. Besides terminal currents and voltages, the magnitudes of linearized internal elements are given. In some cases meaningful quantities can be derived which are then also given (e.g. f_T). The objective of the DC operating-facility is twofold:

- Calculate small-signal equivalent circuit element values.
- Open a window on the internal bias conditions of the device and its basic capabilities.

Below the printed items are described. $C_{x(y)}$ indicates the derivate of the charge Q at terminal x to the voltage at terminal y, when all other terminals remain constant.

Quantity	Equation	Description
Level	1101	Model level
IDS	I_{DS}	Drain current, excluding avalanche and tunnel currents
IAVL	I_{avl}	Substrate current due to weak-avalanche
IGS	I_{GS}	Gate-to-source current due to direct tunnelling
IGD	I_{GD}	Gate-to-drain current due to direct tunnelling
IGB	I_{GB}	Gate-to-bulk current due to direct tunnelling
VDS	V_{DS}	Drain-Source voltage
VGS	V_{GS}	Gate-Source voltage
VSB	V_{SB}	Source-Bulk voltage
VTO	V_{TO}	Zero-bias threshold voltage
VTS	V_{TS}	Threshold voltage including back-bias effects

Quantity	Equation	Description
VTH	V_{TH}	Threshold voltage including back-bias and drain-bias effects
VGT	V_{inv_0}	Effective gate drive including back-bias and drain voltage effects
VDSS	V_{DSAT}	Drain saturation voltage at actual bias
VSAT	$V_{DS} - V_{DSAT}$	Saturation limit
GM	dI_{DS}/dV_{GS}	Transconductance (assumed V_{ds}>0)
GMB	dI_{DS}/dV_{BS}	Substrate-transconductance (assumed V_{ds}>0)
GDS	dI_{DS}/dV_{DS}	Output conductance
CD(D)	dQ_D/dV_D	
CD(G)	$- dQ_D/dV_G$	
CD(S)	$- dQ_D/dV_S$	
CD(B)	$- dQ_D/dV_B$	
CG(D)	$- dQ_G/dV_D$	
CG(G)	$+dQ_G/dV_G$	
CG(S)	$- dQ_G/dV_S$	
CG(B)	$- dQ_G/dV_B$	
CS(D)	$- dQ_S/dV_D$	
CS(G)	$- dQ_S/dV_G$	
CS(S)	$+dQ_S/dV_S$	
CS(B)	$- dQ_S/dV_B$	
CB(D)	$- dQ_B/dV_D$	
CB(G)	$- dQ_B/dV_G$	
CB(S)	$- dQ_B/dV_S$	

Quantity	Equation	Description
CB(B)	dQ_B/dV_B	
CGDOL	$-\partial Q_{ov_L}/\partial V_{DS}$	Gate-drain overlap capacitance of the actual transistor
CGSOL	$\partial Q_{ov_0}/\partial V_{GS}$	Gate-source overlap capacitance of the actual transistor
WEFF		Effective channel width for geometrical models
LEFF		Effective channel length for geometrical models
U	g_m/g_{ds}	Transistor gain
ROUT	$1/g_{ds}$	Small-signal output resistance
VEARLY	$\lvert I_{DS}\rvert/g_{ds}$	Equivalent Early voltage
KEFF	k_0	Body effect parameter
BEFF	$\frac{2\lvert I_{DS}\rvert}{V_{inv_0}^2}$	Gain factor
FUG	$\frac{g_m}{2\cdot\pi\cdot(C_{G(G)}+C_{GS_{ov}}+C_{GD_{ov}})}$	Unity gain frequency at actual bias
SQRT(SFW)	$\sqrt{S_{th}}/g_m$	Input-referred RMS white noise voltage density
SQRT(SFF)	$\sqrt{S_{fl}(1kHz)}/g_m$	Input-referred RMS white noise voltage density at 1 kHz
FKNEE	$1Hz\cdot S_{fl}(1Hz)/S_{th}$	Cross-over frequency above which white noise is dominant

Remarks:

- When V_{ds}<0, g_m and g_{mb} are calculated with drain and source terminals interchanged. The terminal voltages and I_{DS} keep their sign.

- The signs of *VTO* and *VTS* follow the conventions of the model parameter set. The parameter set is always assumed to correspond to an n-channel device.

- *W* and *L* are not available for the electrical MOS models.

- *MULT* is a scaling parameter that multiplies all currents and charges by the value of *MULT*. This is equivalent to putting *MULT* (a number) MOS transistors in parallel. And as a consequence *MULT* effects the operating point output.

A non-existent conductance, G_{min}, is connected between the nodes *D* and *S*. This conductance G_{min} does not influence the DC-operating point.

- Zero-bias threshold voltage:

$$V_{TO} = V_{FB} + P_D \cdot (\phi_B + 2 \cdot \phi_T) + k_0 \cdot \sqrt{\phi_B + 2 \cdot \phi_T}$$

- Threshold voltage including back-bias effects :

$$V_{TS} = V_{FB} + P_D \cdot (V_{SB_t} + 2 \cdot \phi_T) - (V_{SB_t} - \phi_B) + k_0 \cdot \sqrt{V_{SB_t} + 2 \cdot \phi_T}$$

- Threshold voltage including back-bias and drain-bias effects:

$$V_{TH} = V_{FB} + P_D \cdot (V_{SB_t} + 2 \cdot \phi_T) - (V_{SB_t} - \phi_B) + k_0 \cdot \sqrt{V_{SB_t} + 2 \cdot \phi_T} - \Delta V_G$$

12.4 Physics

12.4.1 Comments and Physical Background

In this section some physical background on the current, charge and noise description of MOS Model 1101 will be given. For the full details of the physical background of the drain-source channel current equations the reader is referred to [33], [34], [36] - [38]. The gate current, charge and noise equations have been newly developed and their physical background will be discussed in a future report. All equations referred to are to be found in section 12.4.2

Comments on Current Equations

Conventional MOS models such as MOS Model 9 and BSIM4 are threshold-voltage-based models, which make use of approximate expressions of the drain-source channel current I_{DS} in the weak-inversion region (i.e. subthreshold) and in the strong-inversion region (i.e. well above threshold). These approximate equations are tied together using a mathematical smoothing function, resulting in neither a physical nor an accurate description of I_{DS} in the moderate inversion region (i.e. around threshold). With the constant downscaling of supply voltage the moderate inversion region becomes more and more important, and an accurate description of this region is thus essential.

A more accurate type of model is the surface-potential-based model, where the channel current I_{DS} is split up in a drift (I_{drift}) and a diffusion (I_{diff}) component, which are a function of the gate bias V_{GB} and the surface potential at the source (ψ_{s_0}) and the drain (ψ_{s_L}) side. In this way I_{DS} can be accurately described using one equation for all operating regions (i.e. weak, moderate and strong-inversion). MOS Model 1101 is a surface-potential-based model.

Surface Potential

The surface potential ψ_s is defined as the electrostatic potential at the gate oxide/substrate interface with respect to the neutral bulk (due to the band bending, see Figure 73a). For an n-MOS transistor with uniform doping concentration it can be calculated from the following implicit relation:

$$\left(\frac{V_{GB}-V_{FB}-\psi_p-\psi_s}{k_0}\right)^2 = \psi_s + \phi_T \cdot \left[\exp\left(-\frac{\psi_s}{\phi_T}\right) - 1\right]$$

$$+ \phi_T \cdot \exp\left(-\frac{\phi_B + V}{(1+m_0)\cdot\phi_T}\right) \cdot \left[\exp\left(\frac{\psi_s}{(1+m_0)\cdot\phi_T}\right) - 1\right]$$

where V is the quasi-Fermi potential, which ranges from V_{SB} at the source side to V_{DB} at the drain side. The parameter m_0 has been added to model the non-ideal sub-threshold behaviour of short-channel transistors[1], and ψ_p is the potential drop in the polysilicon gate material due to the poly-depletion effect. The latter is given by[2]:

$$\psi_p = \begin{cases} 0 & V_{GB} \le V_{FB} \\ \left(\sqrt{V_{GB}-V_{FB}-\psi_s+\frac{k_p^2}{4}}-\frac{k_p}{2}\right)^2 & V_{GB} > V_{FB} \end{cases}$$

In Figure 73b the surface potential is shown as a function of gate bias for a typical n-type MOS device. The surface potential ψ_s is implicitly related to the gate bias V_{GB} and the quasi-Fermi potential V , and cannot be calculated analytically. It can only be calculated using an iterative solution, which in general is computation-time consuming. In MOS Model 1101 an explicit approximation of the surface potential is used, which has partly been treated in [34]. In the inversion region $V_{GB} > V_{FB}$ the surface potential is approximated by $\psi_{s_{inv}}$ given by eqs. 12.18 - 12.20 and 12.27 - 12.32, where variable Δacc is used to describe the influence of majority carriers. In the accumulation region ($V_{GB} < V_{FB}$) the surface potential is approximated by $\psi_{s_{acc}}$ given by eqs. 12.33 - 12.35. The total surface potential ψ_s is simply given by $\psi_{s_{inv}} + \psi_{s_{acc}}$.

1. Parameter $m_0 = 0$ for the ideal long-channel case.

2. For $V_{GB} < V_{FB}$ an accumulation layer is formed in both the substrate silicon and the gate polysilicon, in this case ψ_p is slightly negative and weakly dependent on V_{GB}. This effect has been neglected.

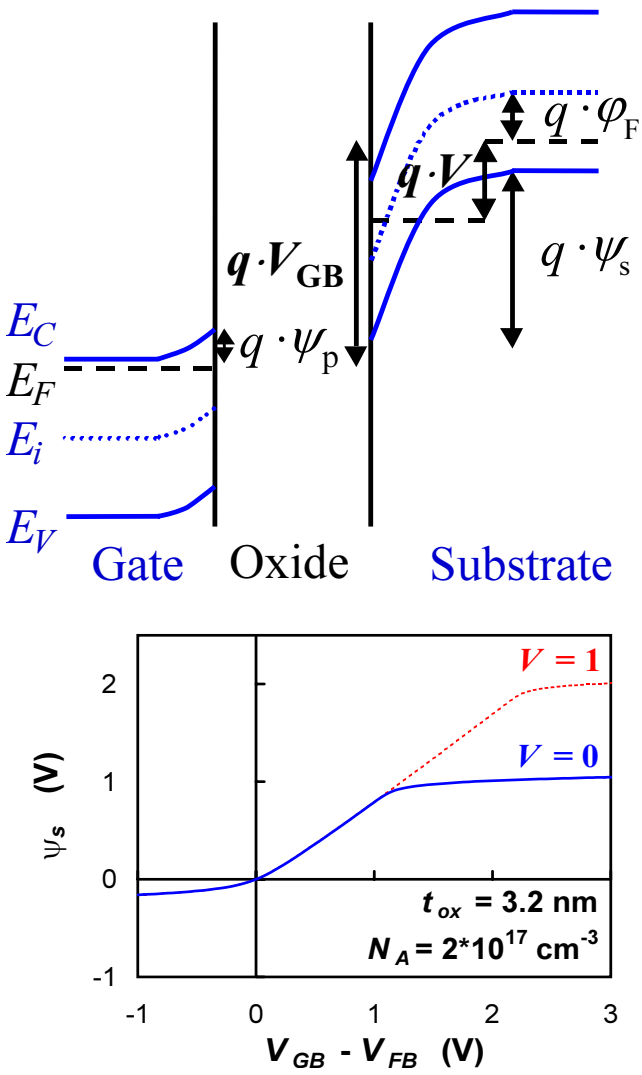

Figure 73: Upper figure: The energy band diagram of an n-type MOS transistor in inversion $V_{GB} > V_{FB}$, *where* ψ_s *is the surface potential,* ψ_p *is the potential drop in the gate due to the poly-depletion effect,* V *is the quasi-Fermi potential and* ϕ_F *is the intrinsic Fermi-potential (*$\phi_B = 2 \cdot \phi_F$*). Lower figure: The surface potential as a function of gate bias for different values of quasi-Fermi potential* V *(*$m_0 = 0$*).*

A surface-potential-based model automatically incorporates the pinch-off condition at the drain side, and as a result it gives a description of both the linear (or ohmic) region and the saturation region for the ideal long-channel case. In this case the saturation voltage V_{DSAT} (i.e. the drain-source voltage above which saturation occurs) corresponds to eq. (12.21). For short-channel devices, however, no real pinch-off occurs and the saturation voltage is affected by velocity saturation and series-resistance. In this case the saturation voltage V_{DSAT} is calculated using eqs. (12.21)-(12.25). The transition from linear to saturation region is no longer automatically described by the surface-potential-based model. This has been solved in the same way as in [39] by introducing an effective drain-source bias V_{DS_x} which changes smoothly from V_{DS} in the linear region to V_{DSAT} in the saturation region, see eq. (12.26).

A surface-potential-based model makes no use of threshold voltage V_T. Circuit designers, however, are used to think in terms of threshold voltage, and as a consequence it would be useful to have a description of V_T in the framework of a surface-potential-model. It has been found that an accurate expression of threshold voltage is simply given by:

$$V_T = V_{FB} + \left(1 + \frac{k_0^2}{k_p^2}\right) \cdot (V_{SB} + \phi_B + 2 \cdot \phi_T) - V_{SB} + k_0 \cdot \sqrt{V_{SB} + \phi_B + 2 \cdot \phi_T}$$

The threshold voltage and other important parameters for circuit design are part of the operating point output as given in Section 12.3.4.

Channel Current

Neglecting the influence of gate and bulk current, the channel current can be written as: $I_{DS} = I_{drift} + I_{diff}$ where ideally the drift component I_{drift} can be approximated by (for $V_{GB} > V_{FB}$):

$$I_{drift} = \beta \cdot \left(\frac{2 \cdot \left[V_{GB} - V_{FB} - \frac{\psi_{s_L} + \psi_{s_0}}{2} \right]}{1 + \sqrt{1 + \frac{4}{k_p^2} \cdot \left[V_{GB} - V_{FB} - \frac{\psi_{s_L} + \psi_{s_0}}{2} \right]}} - k_0 \cdot \sqrt{\frac{\psi_{s_L} + \psi_{s_0}}{2}} \right) \cdot (\psi_{s_L} - \psi_{s_0})$$

and the diffusion component I_{diff} can be approximated by (for $V_{GB} > V_{FB}$):

$$I_{diff} = \beta \cdot \phi_T \cdot (Q_{inv_L} - Q_{inv_0}) \cdot \frac{t_{ox}}{\varepsilon_{ox}}$$

In the latter equation Q_{inv_0} and Q_{inv_L} denote the inversion-layer charge density at the source and drain side, respectively, which are given by eqs. (12.55)-(12.57) (where $Q_{inv} = -\varepsilon_{ox}/t_{ox} \cdot V_{inv}$).

In the non-ideal case the channel current is affected by several physical effects, such as drain-induced barrier lowering, static feedback, mobility reduction, series-resistance, velocity saturation, channel length modulation and self-heating, which have to be taken into account in the channel current expression:

- In threshold-voltage-based models drain-induced barrier lowering and static feedback are traditionally implemented as a decrease in threshold voltage with drain bias. Here these effects have been implemented as an increase in effective gate bias ΔV_G given by eqs. (12.11)-(12.17). An effective drain-source voltage $V_{DS_{eff}}$ has been used to preserve non-singular behaviour in the higher-order derivatives of I_{DS} at $V_{DS} = 0$ V.

- The effects of mobility reduction and series-resistance on channel current have been described in [37], and have consequently been implemented using eqs. (12.48) and (12.52), respectively.

- The effect of velocity saturation has been modelled along the same lines as was done in [38] with the exception of the electrical field distribution. In [38] the influence of the electron velocity saturation expression

  $$v = \frac{\mu \cdot E_{\parallel}}{\sqrt{1 + (\mu/v_{sat} \cdot E_{\parallel})^2}}$$

  was approximated assuming that the lateral electric field $E_{\parallel}$ in the denominator is constant and equal to $(\psi_{s_L} - \psi_{s_0})/L$. Here we assume that $E_{\parallel}$ (in the denominator) increases linearly along the channel (from 0 at the source to $2 \cdot (\psi_{s_L} - \psi_{s_0})/L$ at the drain), and obtain a more accurate expression for velocity saturation, which has been implemented using eq. (12.50).

- The effect of channel length modulation and self-heating on channel current have been described in [38], and have consequently been implemented using eqs. (12.51) and (12.53), respectively.

All the above effects can be incorporated into the channel current expression using eq. (12.54) and eq. (12.60).

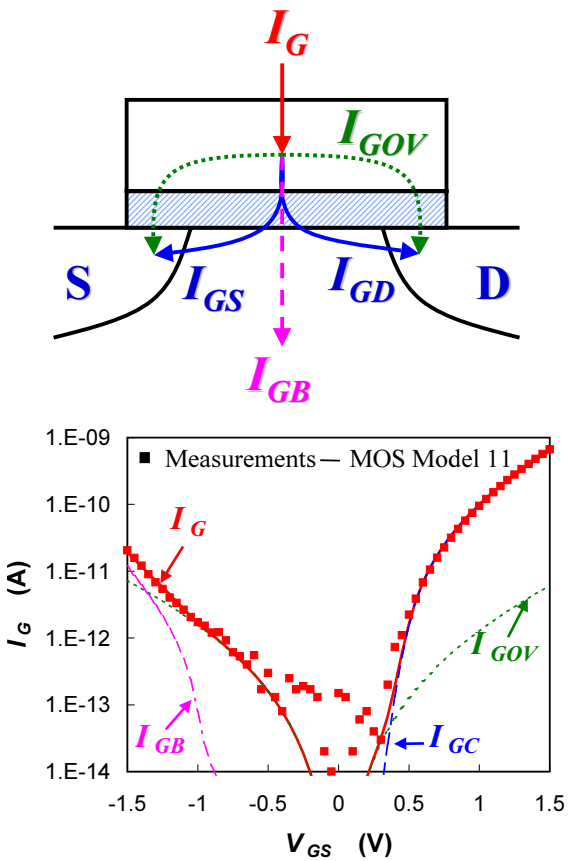

Figure 74: Upper figure: The different gate current components in a MOS transistor. One can distinguish the intrinsic components, i.e. the gate-to-channel current $I_{GC}(= I_{GS} + I_{GD})$ *and the gate-to-bulk current* I_{GB} *, and the extrinsic, i.e. the gate/source and gate/drain overlap components* $I_{G_{ov}}$ *.*
Lower figure: Measured and modelled gate current as a function of gate bias V_{GS} *at* $V_{DS} = V_{SB} = 0$ *V, the different gate current components are also shown. NMOS-transistor,* $W/L = 10/0.6\mu$ *m and* $t_{ox} = 2$ *nm.*

Weak-Avalanche Current

At high drain bias, owing to the weak-avalanche effect (or impact ionization), a current I_{avl} will flow between drain and bulk[1]. The description of the weak-avalanche current has been taken from MOS Model 9 [35], and is given by eq. (12.61). With the down-scaling of supply voltage for modern CMOS technologies, weak-avalanche becomes less and less important.

Gate Tunnelling Current

With CMOS technology scaling the gate oxide thickness is reduced and, due to the direct-tunnelling of carriers through the oxide, the gate current is no longer negligible, and has to be taken into account. Several gate current components can be distinguished, three components (I_{GS}, I_{GD} and I_{GB}) due to the intrinsic MOS channel, and two components (I_{Gov_0} and I_{Gov_L}) due to gate/source and gate/drain overlap region, see Figure 74(a).

For an n-type MOS transistor operating in inversion, the intrinsic gate current density J_G consists of electrons tunnelling from the inversion layer to the gate, the so-called conductance band tunnelling, which in general can be written as [40] (for $V_{GB} > V_{FB}$):

$$J_G \propto -V_{ox} \cdot Q_{inv} \cdot P_{tun}\{V_{ox};\chi_B;B\}$$

where V_{ox} is the oxide voltage given by $V_{ox} = V_{GB} - V_{FB} - \psi_p - \psi_s$. The carrier tunnelling probability P_{tun} is a function of the oxide voltage V_{ox}, the oxide energy barrier χ_B as observed by the inversion-layer carriers, and a parameter B. This probability is given by eq. (12.62), where both direct-tunnelling for $V_{ox} < \chi_B$ and Fowler-Nordheim tunnelling for $V_{ox} > \chi_B$ have been taken into account.

Owing to quantum-mechanical energy quantization in the potential well at the SiO_2-surface, the electrons in the inversion layer are not situated at the bottom of the conduction band, but in the lowest energy subband which lies $\Delta\chi_B$ above the conduction band. Assuming that only the lowest energy subband is occupied by electrons,

1. In reality part of the generated avalanche current will also flow from drain to source [33], this has been neglected

the value of $\Delta\chi_B$ can be given by eq. (12.79)[41]. As a result the oxide barrier $\chi_{B_{eff}}$ has to be lowered by an amount of $\Delta\chi_B$, see eq. (12.80).

In inversion the total intrinsic gate current consists of electrons tunnelling from inversion layer to gate, the so-called gate-to-channel current I_{GC}. These electrons are supplied by both source (I_{GS}) and drain (I_{GD}). The gate-to-channel current I_{GC} can be calculated from:

$$I_{GC} = W \cdot \int_0^L J_G \cdot dx$$

where x is the coordinate along the channel. Using a first-order perturbation approximation, i.e. assuming the gate current is small enough so that it does not change the distribution of surface potential along the channel, I_{GC} can be calculated by eqs. (12.79)-(12.89). In the same way the partitioning of I_{GC} into I_{GS} and I_{GD} can be calculated using:

$$I_{GS} = W \cdot \int_0^L \left(1 - \frac{x}{L}\right) \cdot J_G \cdot dx$$

$$I_{GD} = W \cdot \int_0^L \frac{x}{L} \cdot J_G \cdot dx$$

which results in expressions for I_{GS} and I_{GD} as given by eqs. (12.90)-(12.92). The gate-to-channel current I_{GC} can be seen in Fig. 74 (b) as a function of gate bias for a typical n-MOS transistor at $V_{DS} = 0$ (i.e. $I_{GS} = I_{GD} = 1/2 \cdot I_{GC}$).

For an n-type MOS transistor operating in accumulation, an accumulation layer of holes is formed in the p-type substrate and an accumulation layer of electrons is formed in the n^+-type polysilicon gate. Since the oxide energy barrier for electrons χ_{B_N} is considerably lower than that for holes χ_{B_P}, the gate current will mainly consist of electrons tunnelling from the gate to the bulk silicon, where they are swept to the bulk terminal. In this case the (intrinsic) gate current density J_G can be written as [40] (for $V_{GB} < V_{FB}$):

$$J_G \propto -V_{ox} \cdot Q_{acc} \cdot P_{tun}\{-V_{ox};\chi_B;B\}$$

where Q_{acc} is the accumulation charge density in the gate given by $\varepsilon_{ox}/t_{ox} \cdot V_{ox}$. In order to limit calculation time the quantum-mechanical oxide barrier lowering in this case is neglected, and the resulting expression for I_{GB} is given by eqs. (12.77)-(12.78). The gate-to-bulk current I_{GB} can be seen in Fig. 74 (b) as a function of gate bias for a typical n-MOS transistor at $V_{DS} = 0$.

Apart from the intrinsic components I_{GC} and I_{GB}, considerable gate current can be generated in the gate/source- and gate/drain-overlap regions. Concentrating on the gate/source[1]-overlap region, in order to calculate the overlap gate current, the overlap region is treated as an n^+-gate/oxide/n^+-bulk MOS capacitance where the source acts as bulk. Although the impurity doping concentration in the n^+-source extension region is non-uniform in both lateral and transversal direction, it is assumed that an effective flat-band voltage V_{FBov} and body-factor k_{ov} can be defined for this structure. Furthermore assuming that only accumulation and depletion occur in the n^+-source region[2], a surface potential $\psi_{s_{ov}}$ can be calculated using:

$$\left(\frac{V_{GS} - V_{FBov} - \psi_{p_{ov}} - \psi_{s_{ov}}}{k_{ov}}\right)^2 = -\psi_{s_{OV}} + \phi_T \cdot \left[\exp\left(\frac{\psi_{S_{OV}}}{\phi_T}\right) - 1\right]$$

where the potential drop in the polysilicon gate material due to the poly-depletion effect $\psi_{p_{ov}}$ is given by:

$$\psi_{p_{ov}} = \begin{cases} 0 & V_{GS} \le V_{GBov} \\ \left(\sqrt{V_{GS} - V_{FBov} - \psi_{s_{ov}} + \frac{k_p^2}{4}} - \frac{k_p}{2}\right)^2 & V_{GS} > V_{FBov} \end{cases}$$

Again the surface potential $\psi_{p_{ov}}$ can be explicitly approximated, this is done by using eqs. (12.63)-(12.69).

1. In the following derivation, the same can be done for the gate/drain-overlap region by replacing the source by the drain.

2. Since the source extension has a very high doping concentration, an inversion layer in the gate/source overlap will only be formed at very negative gate-source bias values. This effect has been neglected.

For $V_{GS} > V_{FBov}$ a negatively charged accumulation layer is formed in the overlapped n^+-source extension and a positively charged depletion layer is formed in the overlapping gate. In this case the overlap gate current will mostly consist of electrons tunnelling from the source accumulation layer to the gate, it is given by:

$$I_{G_{ov}} \propto -V_{ov} \cdot Q_{ov} \cdot P_{tun}\{V_{ov};\chi_B;B\}$$

where V_{ov} is the oxide voltage for the gate/source-overlap ($= V_{GS} - V_{FBov} - \psi_{p_{ov}} - \psi_{s_{ov}}$), given by eqs. (12.70)-(12.72), and Q_{ov} is the total charge density in the n^+-source region ($= \varepsilon_{ox}/t_{ox} \cdot V_{ov}$). For $V_{GS} < V_{FBov}$ the situation is reversed, a positively charged depletion layer is formed in the overlapped n^+-source extension and a negatively charged accumulation layer is formed in the overlapping gate. In this case the overlap gate current will mostly consist of electrons tunnelling from the gate accumulation layer to the source, it is given by:

$$I_{G_{ov}} \alpha \cdot V_{ov} \cdot Q_{ov} \cdot P_{tun}\{-V_{ov};\chi_B;B\}$$

The overlap gate current components can now be given by eqs. (12.73)-(12.76). In Fig. 74 (b) the gate overlap current $I_{G_{ov}}$ is shown as a function of gate bias for a typical n-MOS transistor at $V_{DS} = 0$ (i.e. $I_{Gov_L} = I_{Gov_0}$). For n-type and p-type MOS transistors the gate current behaviour is different due to the type of carriers that constitute the different gate current components[1]. The difference is summarized in Table 6.

1. It is assumed here that the gate current is only determined by conductance band tunnelling. For high values of gate bias (i.e. $q \cdot V_{ox} > E_g$) electrons in the bulk valence band may also tunnel through the oxide to the gate conduction band. This mechanism is referred to as valence band tunnelling, and it has not been taken into account in MOS Model 1101.

Table 6: The type of carriers that contribute to the gate tunnelling current in the various operation regions for the intrinsic MOSFET, the gate/drain- and gate/source-overlap regions. The type of carriers determine the value of oxide energy barrier χ_B that has to be used (χ_{B_N} for electrons, χ_{B_P} for holes). In the last row the direction of gate current is indicated.

Type	Intrinsic MOSFET		Overlap Regions
	Accumulation	Inversion	
NMOS	electrons	electrons	electrons
PMOS	electrons	holes	holes
	I_{GB}	I_{GS}/I_{GD}	I_{GS}/I_{GD}

Comments on Charge Equations

In a typical MOS structure we can distinguish intrinsic and extrinsic charges. The latter are due to the gate/source and gate/drain overlap regions. The drain/source junctions also contribute to the capacitance behaviour of a MOSFET, but this is not taken into account in MOS Model 1101; it is described by a separate junction diode model.

Intrinsic Charges

In the intrinsic MOS transistor charges can be attributed to the four terminals. The bulk charge Q_B , which is determined by either the depletion charge (for $V_{GB} > V_{FB}$) or the accumulation charge (for $V_{GB} < V_{FB}$), can be calculated from:

$$Q_B = W \cdot \int_0^L (Q_{tot} - Q_{inv}) \cdot dx$$

where Q_{tot} is the total charge density in the silicon bulk ($Q_{tot} = -\varepsilon_{ox}/t_{ox} \cdot V_{ox}$). The total inversion-layer charge Q_{inv} is split up in a source Q_S and a drain Q_D charge, they can be calculated using the Ward-Dutton charge partitioning scheme [42]:

$$Q_S = W \cdot \int_0^L \left(1 - \frac{x}{L}\right) \cdot Q_{inv} \cdot dx$$

$$Q_D = W \cdot \int_0^L \frac{x}{L} \cdot Q_{inv} \cdot dx$$

Since charge neutrality holds for the complete transistor, the gate charge is simply given by:

$$Q_G = -Q_S - Q_D - Q_B$$

The above equations have been solved, and the charges are given by eqs. (12.99)-(12.105). In these equations $C_{ox_{eff}}$ is the effective oxide capacitance, which is smaller than the ideal oxide capacitance C_{ox} due to quantum-mechanical effects: Quantum-mechanically, the inversion/accumulation charge concentration is not maximum at the Si-SiO_2-interface (as it would be in the classical case), but reaches a maximum at a distance Δz from the interface [41]. This quantum-mechanical effect can be taken into account by an effective oxide thickness $t_{ox} + \varepsilon_{ox}/\varepsilon_{si} \cdot \Delta z$, where Δz is dependent on the effective electric field E_{eff} [41], [43]($E_{eff} = -\varepsilon_{ox}/\varepsilon_{si} \cdot V_{eff}/t_{ox}$). The effective oxide thickness results in an effective oxide capacitance $C_{ox_{eff}}$, see eq. (12.99).

It should be noted that the above charge model is quasi-static. A phase-shift between drain channel current and gate voltage is not taken into account. This implies that for a few applications at high frequencies approaching the cut-off frequency, errors have to be expected due to non-quasi-static effects. Nevertheless non-quasi-effects can be taken into account using a segmentation model as described in [44].

Extrinsic Charges

The gate/source- and gate/drain-overlap regions act as bias-dependent capacitances. In order to take this bias-dependence into account the overlap regions are treated as an n^+-gate/ oxide/n^+-bulk MOS capacitance along the same lines as was done for the overlap gate current, see the section: *Comments on Current Equations.* The charge in the overlap regions can simply be given by eqs. (12.97)-(12.98). The quantum-mechanical effect on oxide thickness has been neglected here in order to reduce calculation time.

Comments on Noise Equations

In a MOS transistor generally three different types of noise can be observed: $1/f$ noise, thermal noise and induced gate noise. The gate tunnel current and the bulk

avalanche current will also exhibit noisy behaviour (due to shot noise), however this has been neglected in MOS Model 1101.

$1/f$ -Noise

At low frequencies flicker (or $1/f$) noise becomes dominant in MOSFETs. In the past this type of noise has been interpreted either in terms of trapping and detrapping of charge carriers in the gate oxide or in terms of mobility fluctuations. Over the past years, a general model for $1/f$ -noise which combines both of the above physical origins [30], [31], has found wide acceptance in the field of MOS modelling. The model assumes that the carrier number in the channel fluctuates due to trapping / detrapping in the gate oxide, and that these number fluctuations also affect the carrier mobility resulting in (correlated) mobility fluctuations.

The same model is part of MOS Model 9 [32], and has been used to calculate the $1/f$ -noise for MOS Model 1101. The calculations have been performed in such a way that the resulting expression for spectral density is valid for all operation regions (i.e. both in subthreshold and above threshold), it is given by eqs. (12.110)-(12.113).

Thermal Noise

Since the MOSFET channel can be considered as a non linear resistor, the channel current is subject to thermal noise. Let thermal noise current sources be parallel connected to each infinitesimal short element of the channel, it can be shown that the noise spectral density, which is defined by [45]:

$$\langle \Delta i_{th}^2 \rangle = \int_0^\infty s_{th}(f)df$$

is given by a generalized Nyquist relation:

$$S_{th} = \frac{N_T}{L^2} \cdot \int_0^L g(x)dx$$

where N_T is equal to $4 \cdot k_B \cdot T$ and $g(x)$ is the local specific channel conductance:

$$g(x) = -\mu(x) \cdot W \cdot Q_{inv}(x)$$

Here the mobility $\mu(x)$ is position dependent mainly due to the effect of velocity saturation. Elaborating the latter integral via a transform of the x variable into the quasi-Fermi potential $V(x)$, we obtain the spectral density given by eqs. (12.107)-

(12.109). Again continuity of the noise model is assured along all modes of operation. The above thermal noise model has been found to accurately describe experimental results for various CMOS technologies without having to invoke carrier heating effects [46].

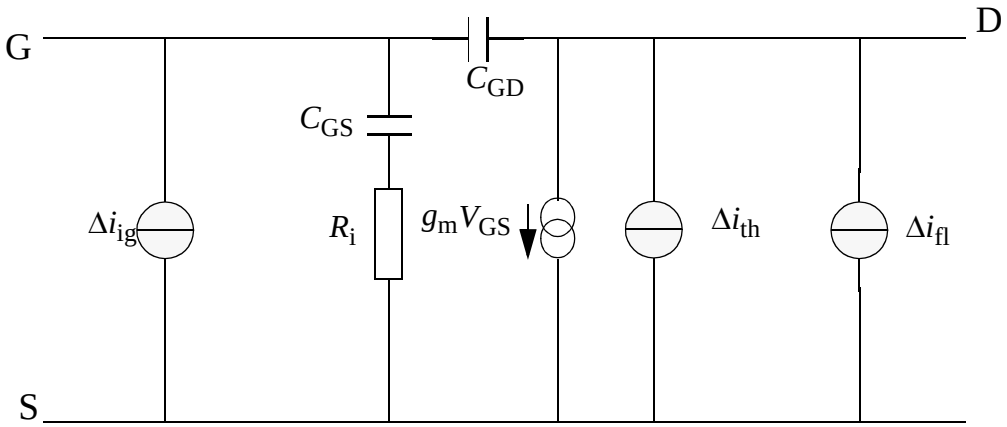

Figure 75: Noise current sources in the electrical scheme of the MOS transistor

Induced Gate Noise

Owing to capacitive coupling between gate and channel, the fluctuating channel current induces noise in the gate terminal at high frequencies. Unfortunately the calculation of this component from first principles is too complicated to provide a result applicable to circuit simulation. It is more practical to derive the desired result from an equivalent circuit presentation given in Fig. 75. Owing to the mentioned capacitive coupling, a part of the channel is present as a resistance in series with the gate input capacitance. In saturation this resistance is approximately equal to:

$$R_i = \frac{1}{3 \cdot g_m}$$

It can be easily shown that the latter resistance produces an input noise current with a spectral density given by eq. (12.114). In addition, since Δi_{th} and Δi_{ig} have the same physical source, both spectral densities are correlated. This is expressed by eqs. (12.115) and (12.116). The induced gate noise S_{ig} is a so-called non-quasi static (NQS)

effect. Since the use of the channel current noise description in an NQS segmentation model [44] would automatically result in a correct description of induced gate noise, S_{ig} can be made equal to zero by using parameter GATENOISE, see eq. (12.114).

12.4.2 Basic Equations

The equations listed in the following sections, are the basic equations of MOS model 1101 without any adaptation necessary for numerical reasons. As such they form the base for parameter extraction. In the following, a function is denoted by *F*{*variable*, ...}, where *F* denotes the function name and the function variables are enclosed by braces {}.

Internal Parameters

$$P_D = 1 + (k_0 / k_p)^2 \tag{12.1}$$

$$V_{limit} = 4 \cdot \phi_T \tag{12.2}$$

$$\theta_{R_{eff}} = \frac{1}{2} \cdot \theta_{R_T} \cdot \left(1 + \frac{\theta_{R1}}{1/2 + \theta_{R2}}\right) \tag{12.3}$$

$$Acc = \left.\frac{\partial \psi_s}{\partial V_{GB}}\right|_{V_{GB} = V_{FB_T}} = \frac{1}{1 + k_0 / (\sqrt{2 \cdot \phi_T})} \tag{12.4}$$

$$N_{\phi_T} = (2.6)^2 / k_0 \tag{12.5}$$

$$Acc_{ov} = \left.\frac{\partial \psi_{sov}}{\partial V_{GB}}\right|_{V_{GB} = V_{FBov}} = \frac{1}{1 + k_{ov} / (\sqrt{2 \cdot \phi_T})} \tag{12.6}$$

$$QM_\psi = \begin{cases} QM_N \cdot (\varepsilon_{ox} / t_{ox})^{2/3} & \text{for NMOS} \\ QM_N \cdot (\varepsilon_{ox} / t_{ox})^{2/3} & \text{for PMOS} \end{cases} \tag{12.7}$$

$$QM_{tox} = \frac{2}{5} \cdot QM_{\psi} \tag{12.8}$$

$$\chi_{B_{inv}} = \begin{cases} \chi_{B_N} & \text{for NMOS} \\ \chi_{B_P} & \text{for PMOS} \end{cases} \tag{12.9}$$

$$\chi_{B_{acc}} = \chi_{B_N} \tag{12.10}$$

Basic Current Equations

Drain induced barrier lowering and Static Feedback:

$$V_{GB_{eff}} = \begin{cases} 0 & V_{GS} + V_{SB} - V_{FB_T} \le 0 \\ V_{GS} + V_{SB} - V_{FB} & V_{GS} + V_{SB} - V_{FB_T} > 0 \end{cases} \tag{12.11}$$

$$\psi_{sat_0} = \left(\frac{\sqrt{P_D \cdot V_{GB_{eff}} + k_0^2/4} - k_0/2}{P_D} \right)^2 \tag{12.12}$$

$$D_{dibl} = \sigma_{dibl} \cdot \sqrt{V_{SB} + \phi_B} \tag{12.13}$$

$$D_{sf} = \begin{cases} 0 & \psi_{sat_0} - V_{SB} - \phi_{B_T} \le 0 \\ \sigma_{sf} \cdot \sqrt{\psi_{sat_0} - V_{SB} - \phi_B} & \psi_{sat_0} - V_{SB} - \phi_{B_T} > 0 \end{cases} \tag{12.14}$$

$$D = \begin{cases} D_{dibl} & D_{sf} \le D_{dibl} \\ D_{sf} & D_{sf} > D_{dibl} \end{cases} \tag{12.15}$$

$$V_{DS_{eff}} = \frac{V_{DS}^4}{(V_{limit}^2 + V_{DS}^2)^{3/2}} \tag{12.16}$$

$$\Delta V_G = D \cdot V_{DS_{eff}} \tag{12.17}$$

Redefinition of $V_{GB_{eff}}$, equation (12.11)

$$V_{GB_{eff}} = \begin{cases} 0 & V_{GS} + V_{SB} + \Delta V_G - V_{FB_T} \le 0 \\ V_{GS} + V_{SB} + \Delta V_G - V_{FB} & V_{GS} + V_{SB} + \Delta V_G - V_{FB_T} > 0 \end{cases} \tag{12.18}$$

$$\Delta_{acc} = \phi_T \cdot \left[\exp\left(-\frac{Acc \cdot V_{GB_{eff}}}{\phi_T} \right) - 1 \right] \tag{12.19}$$

$$\psi_{sat_1} = \left(\frac{\sqrt{P_D \cdot (V_{GB_{eff}} + \Delta_{acc}) + k_0^2/4} - k_0/2}{P_D} \right)^2 - \Delta_{acc} \tag{12.20}$$

Drain Saturation Voltage:

$$V_{DSAT_{long}} = \begin{cases} 0 & \psi_{sat_1} - V_{SB} - \phi_{B_T} \le 0 \\ \psi_{sat_1} - V_{SB} - \phi_B & \psi_{sat_1} - V_{SB} - \phi_{B_T} > 0 \end{cases} \tag{12.21}$$

$$T_{sat} = \begin{cases} \theta_{sat_T} & \text{for NMOS} \\ \dfrac{\theta_{sat_T}}{(1 + \theta_{sat_T}^2 \cdot V_{DSAT_{long}}^2)^{1/4}} & \text{for PMOS} \end{cases} \tag{12.22}$$

$$\Delta_{SAT} = \frac{T_{sat} - \theta_{R_{eff}}}{\sqrt{\frac{2}{V_{DSAT_{long}}^2} + T_{sat}^2} + \theta_{R_{eff}}} \tag{12.23}$$

$$V_{DSAT_{short}} = V_{DSAT_{long}} \cdot \left(1 - \frac{9}{10} \cdot \frac{\Delta_{SAT}}{1 + \sqrt{1 - \Delta_{SAT}^2}}\right) \tag{12.24}$$

$$V_{DSAT} = \begin{cases} V_{limit} & V_{DSAT_{short}} \le V_{limit} \\ V_{DSAT_{short}} & V_{DSAT_{short}} > V_{limit} \end{cases} \tag{12.25}$$

$$V_{DS_x} = \frac{V_{DS} \cdot V_{DSAT}}{[V_{DS}^{2m} + V_{DSAT}^{2m}]^{1/(2m)}} \tag{12.26}$$

Surface Potential:

$$f_1\{\psi\} = \begin{cases} \psi_{sat_1} & \psi_{sat_1} \le \psi \\ \psi & \psi_{sat_1} > \psi \end{cases} \tag{12.27}$$

$$f_2\{\psi\} = f_1\{\psi\} + \frac{\psi_{sat_1} - f_1\{\psi\}}{\sqrt{1 + \frac{[\psi_{sat_1} - f_1\{\psi\}]^2}{N_{\phi_T} \cdot \phi_T^2}}} \tag{12.28}$$

$$f_3\{\psi\} = \frac{2 \cdot [V_{GB_{eff}} - f_2\{\psi\}]}{1 + \sqrt{1 + 4/k_p^2 \cdot [V_{GB_{eff}} - f_2\{\psi\}]}} \tag{12.29}$$

$$\psi_{s_{inv}}\{\psi\} = f_1\{\psi\} + \phi_T \cdot [1 + m_0] \cdot \ln\left[\frac{\left[\frac{f_3\{\psi\}}{k_0}\right]^2 - f_1\{\psi\} - \Delta_{acc} + \phi_T}{\phi_T}\right]$$

(12.30)

$$\psi^*_{s_0} = \psi_{s_{inv}} \cdot \{V_{SB} + \phi_{B_T}\} \tag{12.31}$$

$$\psi^*_{s_L} = \psi_{s_{inv}} \cdot \{V_{DS_x} + V_{SB} + \phi_{B_T}\} \tag{12.32}$$

Surface Potential in Accumulation:

$$f_1 = \begin{cases} Acc \cdot (V_{GS} + V_{SB} + \Delta V_G - V_{FB}) & V_{GS} + V_{SB} + \Delta V_G - V_{FB_T} \le 0 \\ 0 & V_{GS} + V_{SB} + \Delta V_G - V_{FB_T} > 0 \end{cases} \tag{12.33}$$

$$f_2 = \frac{f_1}{\sqrt{1 + \frac{f_1^2}{N_{\phi_T} \cdot \phi_T^2}}} \tag{12.34}$$

$$\psi_{s_{acc}} = -\phi_T \cdot \ln\left[\frac{\left\{\frac{f_1 / Acc - f_2}{k_0}\right\}^2 - f_2 + \phi_T}{\phi_T}\right] \tag{12.35}$$

Auxiliary Variables:

$$\Delta\psi = \psi^*_{s_L} - \psi^*_{s_0} \tag{12.36}$$

$$\overline{\psi}_{inv} = \frac{\psi^*_{s_L} + \psi^*_{s_0}}{2} \tag{12.37}$$

$$V_{G_T}\{\psi_{s_{inv}}\} = \frac{2 \cdot [V_{GB_{eff}} - \psi_{s_{inv}}]}{1 + \sqrt{1 + 4/k_p^2 \cdot [V_{GB_{eff}} - \psi_{s_{inv}}]}} - k_0 \cdot \sqrt{\psi_{s_{inv}} + \Delta_{acc}} \tag{12.38}$$

$$V_{GT_0} = V_{G_T}\left\{\psi^*_{s_0}\right\} \tag{12.39}$$

$$V_{GT_L} = V_{G_T}\left\{\psi^*_{s_L}\right\} \tag{12.40}$$

$$\overline{V}_{G_T} = V_{G_T}\{\overline{\psi}_{inv}\} \tag{12.41}$$

$$V_{ox} = \frac{2 \cdot [V_{GS} + V_{SB} + \Delta V_G - V_{FB_T} - \overline{\psi}_{inv} - \psi_{acc}]}{1 + \sqrt{1 + 4/k_p^2 \cdot [V_{GB_{eff}} - \overline{\psi}_{inv}]}} \tag{12.42}$$

$$\partial V_{ox} = \frac{2}{1 + \sqrt{1 + 4/k_p^2 \cdot [V_{GB_{eff}} - \overline{\psi}_{inv}]}} \tag{12.43}$$

$$V_{eff} = V_{G_T} + \eta_{mob_T} \cdot (V_{ox} - V_{G_T}) \tag{12.44}$$

$$\xi_{ox} = -\phi_T \cdot \frac{\partial V_{ox}}{\partial \bar{\psi}_{inv}} = \phi_T \cdot \frac{1}{\sqrt{1 + 4/k_p^2 \cdot [V_{GB_{eff}} - \bar{\psi}_{inv}]}} \tag{12.45}$$

$$\xi = \phi_T \cdot \frac{\partial \bar{V}_{G_T}}{\partial \bar{\psi}_{inv}} = \phi_T \cdot \left[\frac{1}{\sqrt{1 + 4/k_p^2 \cdot [V_{GB_{eff}} - \bar{\psi}_{inv}]}} + \frac{k_0}{2 \cdot \sqrt{\bar{\psi}_{inv} + \Delta_{acc}}} \right]$$

(12.46)

$$\bar{V}^*_{G_T} = \frac{V_{GT_0} + V_{GT_L}}{2} + \xi \tag{12.47}$$

Second-Order Effects

Mobility Degradation:

$$G_{mob} = \frac{\mu_0}{\mu} = \begin{cases} 1 + [(\theta_{ph_T} \cdot V_{eff})^{\nu_T/3} + (\theta_{sr_T} \cdot V_{eff})^{2\nu_T}]^{1/\nu_T} & \text{for NMOS} \\ 1 + [(\theta_{ph_T} \cdot V_{eff})^{\nu_T/3} + (\theta_{sr_T} \cdot V_{eff})^{\nu_T}]^{1/\nu_T} & \text{for PMOS} \end{cases} \tag{12.48}$$

Velocity Saturation:

$$x = \begin{cases} \dfrac{2 \cdot \theta_{sat_T} \cdot \Delta\psi}{\sqrt{G_{mob}}} & \text{for NMOS} \\ \dfrac{2 \cdot \theta_{sat_T}}{\sqrt{G_{mob}}} \cdot \dfrac{\Delta\psi}{(1 + \theta_{sat}^2 \cdot \Delta\psi^2)^{1/4}} & \text{for PMOS} \end{cases} \tag{12.49}$$

$$G_{vsat} = \frac{G_{mob}}{2} \cdot \left[\sqrt{1 + x^2} + \frac{\ln(x + \sqrt{1 + x^2})}{x} \right] \tag{12.50}$$

Channel Length Modulation:

$$G_{\Delta L} = 1 - \frac{\Delta L}{L} = 1 - \alpha \cdot \ln \left[\frac{V_{DS} - V_{DS_x} + \sqrt{(V_{DS} - V_{DS_x})^2 + V_p^2}}{V_P} \right] \tag{12.51}$$

Series Resistance and Self-Heating:

$$G_R = \theta_{R_T} \cdot \left(1 + \frac{\theta_{R1}}{\theta_{R2} + \bar{V}_{G_T}} \right) \cdot \bar{V}_{G_T} \tag{12.52}$$

$$G_{Th} = \theta_{Th} \cdot V_{DS} \cdot \Delta\psi \cdot V_{G_T} \tag{12.53}$$

$$G_{tot} = G_{Th} + \frac{[G_{\Delta L} \cdot G_{vsat} + G_R]}{2} \cdot \left[1 + \sqrt{1 - \frac{4 \cdot G_R / G_{vsat}}{[G_{\Delta L} \cdot G_{vsat} + G_R]^2} \cdot (G_{vsat}^2 - G_{mob}^2)} \right] \tag{12.54}$$

Inversion-Layer Charge

$(Q_{inv} = -\varepsilon_{ox}/t_{ox} \cdot V_{inv})$:

$$V_{inv}\{\psi_{s_{inv}},\psi\} = \frac{k_0 \cdot \phi_T \cdot \exp\left[\frac{\psi_{s_{inv}} - \psi}{(1+m_0)\cdot\phi_T}\right]}{\sqrt{\psi_{s_{inv}} + \Delta_{acc} + \phi_T \cdot \exp\left[\frac{\psi_{s_{inv}} - \psi}{(1+m_0)\cdot\phi_T}\right]} + \sqrt{\psi_{s_{inv}} + \Delta_{acc}}} \tag{12.55}$$

$$V_{inv_0} = V_{inv}\left\{\psi^*_{s_0}, V_{SB} + \phi_{B_T}\right\} \tag{12.56}$$

$$V_{inv_L} = V_{inv}\left\{\psi^*_{s_L}, V_{DS_x} + V_{SB} + \phi_{B_T}\right\} \tag{12.57}$$

Drain Current

$$I_{drift} = \beta_T \cdot V_{G_T} \cdot \Delta\psi \tag{12.58}$$

$$I_{diff} = \beta_T \cdot \phi_T \cdot (V_{inv_0} - V_{inv_L}) \tag{12.59}$$

$$I_{DS} = \frac{I_{drift} + I_{diff}}{G_{tot}} \tag{12.60}$$

Weak-Avalanche

$$I_{avl} = \begin{cases} 0 & V_{DS} \le a_3 \cdot V_{DSAT} \\ a_{1_T} \cdot I_{DS} \cdot \exp\left(-\frac{a_2}{V_{DS} - a_3 \cdot V_{DSAT}}\right) & V_{DS} > a_3 \cdot V_{DSAT} \end{cases} \tag{12.61}$$

Gate Current Equations

The tunnelling probability is given by:

$$P_{tun}\{V_{ox};\chi_B;B\} = \begin{cases} \exp\left(-B \cdot \dfrac{[1-(1-V_{ox}/\chi_B)^{3/2}]}{V_{ox}}\right) & V_{ox} < \chi_B \\ \exp(-B/V_{ox}) & V_{ox} \geq \chi_B \end{cases} \quad (12.62)$$

Source/Drain Gate Overlap Current:

First calculate the oxide voltage V_{ov} at both Source and Drain overlap:

$$V_{GX_{eff}}\{V_{GX}\} = \begin{cases} V_{GX} - V_{FBov} & V_{GX} - V_{FBov} \leq 0 \\ 0 & V_{GX} - V_{FBov} > 0 \end{cases} \quad (12.63)$$

$$\Delta_{ov}\{V_{GX}\} = \phi_T \cdot \left[\exp\left(\frac{Acc_{ov} \cdot V_{GX_{eff}}\{V_{GX}\}}{\phi_T}\right) - 1\right] \quad (12.64)$$

$$\psi_{sat_{ov}}\{V_{GX}\} = -\left[\sqrt{\frac{k_{ov}^2}{4} - V_{G_{eff}}\{V_{GX}\} + \Delta_{ov}\{V_{GX}\}} - \frac{k_{ov}}{2}\right]^2 + \Delta_{ov}\{V_{GX}\} \quad (12.65)$$

$$f_1\{V_{GX}\} = \begin{cases} 0 & V_{GX} - V_{FBov} \leq 0 \\ Acc_{ov} \cdot [V_{GX} - V_{FBov}] & V_{GX} - V_{FBov} > 0 \end{cases} \quad (12.66)$$

$$f_2\{V_{GX}\} = \frac{f_1\{V_{GX}\}}{\sqrt{1 + \frac{[f_1\{V_{GX}\}]^2}{N_{\phi_T} \cdot \phi_T^2}}} \tag{12.67}$$

$$f_3\{V_{GX}\} = \frac{2 \cdot \left[\frac{f_1\{V_{GX}\}}{Acc_{ov}} - f_2\{V_{GX}\}\right]}{1 + \sqrt{1 + 4/k_p^2 \cdot \left[\frac{f_1\{V_{GX}\}}{Acc_{ov}} - f_2\{V_{GX}\}\right]}} \tag{12.68}$$

$$\psi^*_{s_{ov}}\{V_{GX}\} = \phi_T \cdot \ln\left[\frac{\left(\frac{f_3\{V_{GX}\}}{k_{ov}}\right)^2 + f_2\{V_{GX}\} + \phi_T}{\phi_T}\right] \tag{12.69}$$

$$V_{ov}\{V_{GX}\} = \frac{2 \cdot [V_{GX} - V_{FBov} - \psi^*_{s_{ov}}\{V_{GX}\} - \psi_{sat_{ov}}\{V_{GX}\}]}{1 + \sqrt{1 + 4/k_p^2 \cdot [(f_1\{V_{GX}\})/Acc_{ov} - \psi^*_{s_{ov}}\{V_{GX}\}]}} \tag{12.70}$$

$$V_{ov_0} = V_{ov}\{V_{GS}\} \tag{12.71}$$

$$V_{ov_L} = V_{ov}\{V_{GS} - V_{DS}\} \tag{12.72}$$

Next calculate the gate tunnelling current in both Source and Drain overlap:

$$P_{ov}\{V_{ov}\} = P_{tun}\{V_{ov}; \chi_{B_{inv}}; B_{inv}\} \tag{12.73}$$

$$I_{Gov}\{V_{GX}, V_{ov}\} = I_{GOV} \cdot V_{GX} \cdot V_{ov} \cdot [P_{ov}\{V_{ov}\} - P_{ov}\{-V_{ov}\}] \tag{12.74}$$

$$I_{Gov_0} = I_{Gov}\{V_{GS}, V_{ov_0}\} \tag{12.75}$$

$$I_{Gov_L} = I_{Gov}\{V_{GS} - V_{DS}, V_{ov_L}\} \tag{12.76}$$

Intrinsic Gate Current

The gate tunnelling current in accumulation:

$$P_{acc} = P_{tun}\{-V_{ov}; \chi_{B_{acc}}; B_{acc}\} \tag{12.77}$$

$$I_{GB} = \begin{cases} -I_{GACC} \cdot (V_{GS} + V_{SB}) \cdot V_{ox} \cdot P_{acc} & V_{ox} \le 0 \\ 0 & V_{ox} > 0 \end{cases} \tag{12.78}$$

The tunnelling current in inversion, including quantum-mechanical barrier lowering $\Delta\chi_B$:

$$\Delta\chi_B = QM_\psi \cdot (\overline{V}_{G_T}/3 + V_{ox} - \overline{V}_{G_T})^{2/3} \tag{12.79}$$

$$\chi_{B_{eff}} = \chi_{B_{inv}} - \Delta\chi_B \tag{12.80}$$

$$B_{eff} = B_{inv} \cdot (\chi_{B_{eff}}/\chi_{B_{inv}})^{3/2} \tag{12.81}$$

$$P_{inv} = P_{tun}\{V_{ox}; \chi_{B_{eff}}; B_{eff}\} \tag{12.82}$$

$$B^*_{inv} = \frac{3}{8} \cdot \chi^{-2}_{B_{eff}} \cdot B_{eff} \cdot \partial V_{ox} \tag{12.83}$$

$$\xi^* = \frac{\xi}{\phi_T \cdot \bar{V}_{G_T}^*} \tag{12.84}$$

$$\partial V_{ox}^* = \frac{\partial V_{ox}}{V_{ox}} \tag{12.85}$$

$$P_{GC} = 1 + \frac{[(B_{inv}^*)^2 + 4 \cdot B_{inv}^* \cdot \xi^* + 2 \cdot B_{inv}^* \cdot \partial V_{ox}^* + 2 \cdot \xi^{*2} + 4 \cdot \partial V_{ox}^* \cdot \xi^*] \cdot \Delta\psi^2}{24}$$

(12.86)

$$\bar{I}_{GC} = I_{GINV} \cdot G_{\Delta L} \cdot \left(V_{GS} - \frac{1}{2} \cdot V_{DS_x}\right) \cdot P_{inv} \tag{12.87}$$

$$\bar{V}_{inv} = \frac{V_{inv_0} + V_{inv_L}}{2} \tag{12.88}$$

The total intrinsic gate current I_{GC} :

$$I_{GC} = IGC \cdot V_{inv} \cdot P_{GC} \tag{12.89}$$

$$P_{GS} = [B_{inv}^* + \partial V_{ox}^*] \cdot \frac{\Delta\psi}{12} + [(B_{inv}^*)^2 \cdot (B_{inv}^* + 5 \cdot \xi^* + 3 \cdot \partial V_{ox}^*) + 2 \cdot \xi^{*2} \cdot (B_{inv}^* - \xi^* + \partial V_{ox}^*) + 10 \cdot B_{inv}^* \cdot \xi^* \cdot \partial V_{ox}^*] \cdot \frac{\Delta\psi^3}{480} \tag{12.90}$$

$$I_{GS} = \frac{1}{2} \cdot I_{GC} + \left(P_{GS} \cdot \bar{V}_{inv} + \frac{V_{inv_0} - V_{inv_L}}{12}\right) \cdot \bar{I}_{GC} + I_{Gov_0} \tag{12.91}$$

$$I_{GD} = I_{GC} - I_{GS} + I_{Gov_0} + I_{Gov_L} \tag{12.92}$$

Gate-Induced Drain/Source Leakage Current:

$$V_{tov}\{V_{ov};V\} = \sqrt{V_{ov}{}^2 + C_{GIDL}{}^2 \cdot V^2} \tag{12.93}$$

$$I_{gixl}\{V_{ov};V\} = A_{GIDL} \cdot V \cdot V_{tov}\{V_{ov};V\}{}^2 \cdot \exp\left(-\frac{B_{GIDL_T}}{V_{tov}\{V_{ov};V\}}\right) \tag{12.94}$$

$$I_{gisl} = I_{gixl}\{V_{ov_0};V_{SB}\} \tag{12.95}$$

$$I_{gidl} = I_{gixl}\{V_{ov_L};V_{DS} + V_{SB}\} \tag{12.96}$$

Basic Charge Equations

Bias-Dependent Overlap Capacitance:

$$Q_{ov_0} = C_{GSO} \cdot V_{ov_0} \tag{12.97}$$

$$Q_{ov_L} = C_{GDO} \cdot V_{ov_L} \tag{12.98}$$

Intrinsic Charges:

$$C_{ox_{eff}} = \frac{C_{ox}}{1 + QM_{t_{ox}} \cdot \left[\frac{V_{eff}}{\eta_{mob_T}}\right]^{-1/3}} \tag{12.99}$$

$$\Delta V_{G_T} = \frac{V_{GT_0} - V_{GT_L}}{2 \cdot \left(1 + \theta_{R_T} \cdot \frac{\overline{V}^{*}_{G_T}}{G_{tot}}\right)} \tag{12.100}$$

$$F_j = \frac{\Delta V_{G_T}}{\overline{V}^{*}_{G_T}} \tag{12.101}$$

$$Q_S = -\frac{C_{ox_{eff}}}{2} \cdot \left[\overline{V}^{*}_{G_T} + \frac{\Delta V_{G_T}}{3} \cdot \left(F_j - \frac{F_j^2}{5} + 1\right) - \xi\right] \tag{12.102}$$

$$Q_D = -\frac{C_{ox_{eff}}}{2} \cdot \left[\overline{V}^{*}_{G_T} + \frac{\Delta V_{G_T}}{3} \cdot \left(F_j + \frac{F_j^2}{5} - 1\right) - \xi\right] \tag{12.103}$$

$$Q_G = -C_{ox_{eff}} \cdot \left[V_{ox} + \frac{\Delta V_{G_T}}{3} \cdot F_j \cdot \frac{\xi_{ox}}{\xi}\right] \tag{12.104}$$

$$Q_B = -[Q_S + Q_D + Q_G] \tag{12.105}$$

Noise Equations

In these equations f represents the operation frequency of the transistor.

$$g_m = \frac{\partial I_{DS}}{\partial V_{GS}} \tag{12.106}$$

$$T_{sat} = \begin{cases} \theta_{sat_T}^2 & \text{for NMOS} \\ \dfrac{\theta_{sat_T}^2}{\sqrt{1 + \theta_{sat_T}^2 \cdot \Delta\psi^2}} & \text{for PMOS} \end{cases} \tag{12.107}$$

$$R_{ideal} = \frac{\beta \cdot G_{vsat}^2}{G_{tot}} \cdot \left[\bar{V}_{G_T} + \frac{\frac{\Delta\psi^2}{12} - \xi \cdot \left(\bar{V}_{G_T} - \frac{V_{inv_0} + V_{inv_L}}{2} \right)}{\bar{V}_{G_T} + \xi} \right] \tag{12.108}$$

$$S_{th} = \frac{N_{T_T}}{G_{mob}^2} \cdot (R_{ideal} - T_{sat} \cdot I_{DS} \cdot \Delta\psi) \tag{12.109}$$

$$N_0 = \frac{\varepsilon_{ox}}{qt_{ox}} \cdot V_{inv_0} \tag{12.110}$$

$$N_L = \frac{\varepsilon_{ox}}{qt_{ox}} \cdot V_{inv_L} \tag{12.111}$$

$$N^* = \frac{\varepsilon_{ox}}{qt_{ox}} \cdot \xi \tag{12.112}$$

$$S_{fl} = \frac{q \cdot \phi_T^2 \cdot t_{ox} \cdot \beta_T \cdot I_{DS}}{f \cdot \varepsilon_{ox} \cdot G_{mob} \cdot N^*} \cdot [(N_{FA} - N^* \cdot N_{FB} + N^{*2} \cdot N_{FC}) \cdot \ln\frac{N_0 + N^*}{N_L + N^*} + (N_{FB} - N^* \cdot N_{FC}) \cdot (N_0 - N_L) + \frac{N_{FC}}{2} \cdot (N_0^2 - N_L^2)] + \frac{\phi_T \cdot I_{DS}^2}{f} \cdot (1 - G_{\Delta L}) \cdot \left[\frac{N_{FA} + N_{FB} \cdot N_L + N_{FC} \cdot N_L^2}{(N_L + N^*)^2}\right]$$

(12.113)

$$S_{ig} = \begin{cases} \dfrac{\frac{1}{3} \cdot N_{T_T} \cdot (2 \cdot \pi \cdot f \cdot C_{ox})^2 / g_m}{1 + 0.075 \cdot (2 \cdot \pi \cdot f \cdot C_{ox} / g_m)^2} & \text{GATENOISE = 0} \\ 0 & \text{GATENOISE = 1} \end{cases} \quad (12.114)$$

$$\rho_{igth} = 0.4j \quad (12.115)$$

$$S_{igth} = \rho_{igth} \cdot \sqrt{S_{ig} \cdot S_{th}} \quad (12.116)$$

12.5 Parameter scaling

12.5.1 Geometrical scaling and temperature scaling

Calculation of Transistor Geometry

$$L_E = L - \Delta L = L + \Delta L_{PS} - 2 \cdot \Delta L_{\text{overlap}} \tag{12.117}$$

$$W_E = W - \Delta W = W + \Delta W_{OD} - 2 \cdot \Delta W_{\text{narrow}} \tag{12.118}$$

WARNING : L_E and W_E after calculation can not be less than 0 !

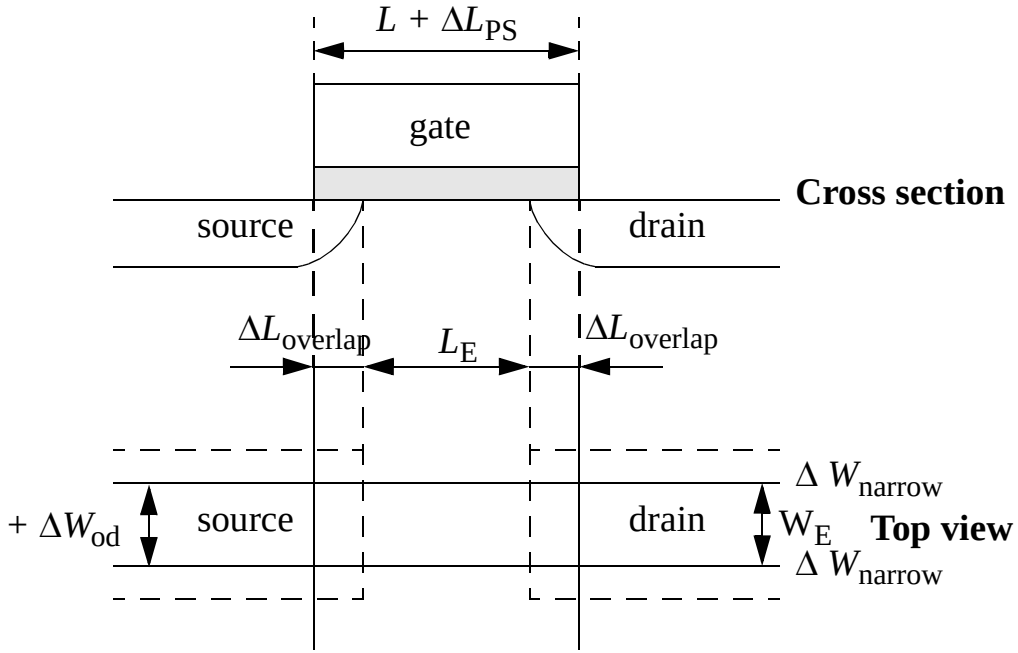

Figure 76: Specification of the dimensions of a MOS transistor

Calculation of Geometry-Dependent Parameters

In MOS Model 11, Level 1101, parameter binning has been facilitated by adding a second, separate set of geometry scaling rules. Consequently, besides the physical geometrical scaling rules there is also a set of binning geometrical scaling rules. The physical geometry scaling rules. The physical geometry scaling rules of Level 1101 have been developed to give a good description over the whole geometry range of CMOS technologies. For processes under development, however, it is sometimes useful to have more flexible scaling relations. In this case one could opt for a binning strategy, where the accuracy with geometry is mostly determined by the number of bins used. The physical scaling rules of Level 1101 are not straightforwardly applicable to binning strategies, since they may result in discontinuities in parameter values at the bin boundaries. Consequently, special binning geometrical scaling relations have been developed, which guarantee continuity in the model parameters at the bin boundaries.
It should be noted that using the source code of the Modelkit on the Philips' website (which can be found at http://www.semiconductors.philips.com/Philips_Models)

1. The physical geometry scaling rules can be selected by using Level 11010, while
2. The binning geometry scaling rules can be selected by using Level 11011.

Three types of binning geometrical scaling rules can be distinguished:

1. Type I

$$P(W_E,L_E) = P_0 + \frac{L_{EN}}{L_E}\cdot P_L + \frac{W_{EN}}{W_E}\cdot P_W + \frac{L_{EN}}{L_E}\cdot\frac{W_{EN}}{W_E}\cdot P_{LW} \qquad (12.119)$$

2. Type II

$$P(W_E,L_E) = P_0 + \frac{L_E}{L_{EN}}\cdot P_L + \frac{W_E}{W_{EN}}\cdot P_W + \frac{L_E}{L_{EN}}\cdot\frac{W_E}{W_{EN}}\cdot P_{LW} \qquad (12.120)$$

3. Type III

$$P(W_E,L_E) = P_0 + \frac{L_{EN}}{L_E}\cdot P_L + \frac{W_E}{W_{EN}}\cdot P_W + \frac{W_E}{L_E}\cdot P_{LW} \qquad (12.121)$$

In these equations L_{EN} and W_{EN} are constants, equal to 10^{-6}.

Table 7 gives a survey of the parameters scaling.

#	Parameter	physical scaling	binning	#	parameter	physical scaling	binning
0	$LEVEL$	no	no	1	T_R	no	no
2	V_{FB}	no	no	3	$S_{T;V_{FB}}$	no	type I
4	k_0	yes	type I	5	$1/k_P$	no	no
6	ϕ_B	yes	type I	7	$S_{T;\phi_B}$	no	type I
8	β	yes	type III	9	η_β	yes	type I
10	θ_{sr}	yes	type I	11	η_{sr}	no	type I
12	θ_{ph}	yes	type I	13	η_{ph}	no	type I
14	η_{mob}	yes	type I	15	$S_{T;\eta_{mob}}$	no	type I
16	υ	no	no	17	υ_{EXP}	no	
18	θ_R	yes	type I	19	η_R	no	type I
20	θ_{R1}	no	no	21	θ_{R2}	no	no
22	θ_{sat}	yes	type I	23	η_{sat}	no	type I
24	θ_{Th}	yes	type I	25	σ_{dibl}	yes	type I
26	m_0	yes	type I	27	σ_{sf}	yes	type I
28	α	yes	type I	29	V_P	no	no
30	m	yes	type I	31	a_1	yes	type I

32	$S_{T;a_1}$	no	type I	33	a_2	yes	type I
34	a_3	yes	type I	35	I_{GINV}	yes	type II
36	B_{INV}	no	type I	37	I_{GACC}	yes	type II
38	B_{ACC}	no	type I	39	V_{RFBov}	no	no
40	k_{ov}	no	no	41	I_{GOV}	yes	type III
42	A_{GIDL}	yes	type III	43	B_{GIDL}	yes	type I
44	$S_{T;B_{GIDL}}$	yes	type I	45	C_{GIDL}	yes	type I
46	C_{ox}	yes	type II	47	C_{GDO}	yes	type III
48	C_{GSO}	yes	type III	49	$GATENOISE$	no	no
50	N_T	no	no	51	N_{FA}	yes	type I
52	N_{FB}	yes	type I	53	N_{FC}	yes	type I
54	t_{ox}	no	no	55	ΔT_A	no	no
56	N_{MULT}	no	no				

Table 7: Survey of parameters scaling. In the third column is indicated if there is a physical geometrical scaling rule for the parameter; in the fourth column the type of binning geometrical scaling rule for the parameter is indicated.

Calculation of Geometry-Dependent Parameters using the Physical Scaling Rules

$$L_{EN} = 10^{-6} \tag{12.122}$$

$$W_{EN} = 10^{-6} \tag{12.123}$$

Calculation of Threshold-Voltage Parameters

$$k_0 = k_{0R} \cdot \left[1 + \frac{L_{EN}}{L_E} \cdot S_{L;k_0} + \left(\frac{L_{EN}}{L_E}\right)^2 \cdot S_{L2;k_0}\right] \cdot \left[1 + \frac{W_{EN}}{W_E} \cdot S_{W;k_0}\right]$$

$$\phi_B = \phi_{BR} \cdot \left[1 + \frac{L_{EN}}{L_E} \cdot S_{L;\phi_B} + \left(\frac{L_{EN}}{L_E}\right)^2 \cdot S_{L2;\phi_B}\right] \cdot \left[1 + \frac{W_{EN}}{W_E} \cdot S_{W;\phi_B}\right]$$

Calculation of Mobility/Series-Resistance Parameters

$$G_{P,E} = 1 + f_{\beta,1} \cdot \frac{L_{P,1}}{L_E} \cdot \left\{1 - \exp\left(-\frac{L_E}{L_{P,1}}\right)\right\} + \tag{12.124}$$

$$f_{\beta,2} \cdot \frac{L_{P,2}}{L_E} \cdot \left\{1 - \exp\left(-\frac{L_E}{L_{P,2}}\right)\right\}$$

$$\bar{\beta} = \frac{\beta_{sq}}{G_{P,E}} \cdot \frac{W_E}{L_E} \tag{12.125}$$

$$\bar{\theta}_{sr} = \theta_{srR} \cdot \left[1 + \frac{W_{EN}}{W_E} \cdot S_{W;\theta_{sr}}\right] \tag{12.126}$$

$$\tilde{\theta}_{ph} = \theta_{phR} \cdot \left[1 + \frac{W_{EN}}{W_E} \cdot S_{W;\theta_{ph}}\right] \tag{12.127}$$

$$\bar{\eta}_{mob} = \theta_{srR} \cdot \left[1 + \frac{W_{EN}}{W_E} \cdot S_{W;\eta_{mob}}\right] \tag{12.128}$$

$$\bar{\theta}_R = \theta_{RR} \cdot \left[1 + \frac{W_{EN}}{W_E} \cdot S_{W;\theta_R} \right] \cdot \frac{L_{EN}}{L_E} \cdot \frac{1}{G_{P,E}} \tag{12.129}$$

$$\tilde{\theta}_{sat} = \theta_{satR} \cdot \left[1 + \frac{W_{EN}}{W_E} \cdot S_{W;\theta_{sat}} \right] \cdot \left[1 + S_{L;\theta_{sat}} \cdot \left\{ \left(\frac{L_{EN}}{L_E} \right)^{\theta_{satEXP}} - 1 \right\} \right] \tag{12.130}$$

Calculation of Conductance Parameters

$$\bar{\theta}_{Th} = \theta_{ThR} \cdot \left[1 + \frac{W_{EN}}{W_E} \cdot S_{W;\theta_{Th}} \right] \cdot \left[\frac{L_{EN}}{L_E} \right]^{\theta_{ThEXP}} \tag{12.131}$$

$$\sigma_{sf} = \sigma_{sfR} \cdot \left[1 + \frac{W_{EN}}{W_E} \cdot S_{W;\sigma_{sf}} \right] \cdot \left[1 + \frac{L_{EN}}{L_E} \cdot S_{L;\sigma_{sf}} \right] \tag{12.132}$$

$$\alpha = \alpha_R \cdot \left[1 + \frac{W_{EN}}{W_E} \cdot S_{W;\alpha} \right] \cdot \left[1 + S_{L;\alpha} \cdot \left\{ \left(\frac{L_{EN}}{L_E} \right)^{\alpha_{EXP}} - 1 \right\} \right] \tag{12.133}$$

Calculation of Sub-Threshold Parameters

$$\sigma_{dibl} = \sigma_{dibl0} \cdot \left(\frac{L_{EN}}{L_E} \right)^{\sigma_{diblEXP}} \tag{12.134}$$

$$m_0 = m_{00} + m_{0R} \cdot \left(\frac{L_{EN}}{L_E} \right)^{m_{0EXP}} \tag{12.135}$$

Calculation of Smoothing Parameters

$$L_{max} = 10 \cdot 10^{-6} \tag{12.136}$$

$$m = \frac{8 \cdot (L_{max} - L_{min})}{L_{max} - 4 \cdot L_{min} + 3 \cdot \frac{L_{max} \cdot L_{min}}{L_E}} \tag{12.137}$$

Calculation of Weak-Avalanche Parameters

$$a_1 = a_{1R} \cdot \left[1 + \frac{L_{EN}}{L_E} \cdot S_{L;a_1}\right] \cdot \left[1 + \frac{W_{EN}}{W_E} \cdot S_{W;a_1}\right] \tag{12.138}$$

$$a_2 = a_{2R} \cdot \left[1 + \frac{L_{EN}}{L_E} \cdot S_{L;a_2}\right] \cdot \left[1 + \frac{W_{EN}}{W_E} \cdot S_{W;a_2}\right] \tag{12.139}$$

$$a_3 = a_{3R} \cdot \left[1 + \frac{L_{EN}}{L_E} \cdot S_{L;a_3}\right] \cdot \left[1 + \frac{W_{EN}}{W_E} \cdot S_{W;a_3}\right] \tag{12.140}$$

Calculation of Gate Current Parameters

$$I_{GINV} = \frac{W_E \cdot L_E}{W_{EN} \cdot L_{EN}} \cdot I_{GINVR} \tag{12.141}$$

$$I_{GACC} = \frac{W_E \cdot L_E}{W_{EN} \cdot L_{EN}} \cdot I_{GACCR} \tag{12.142}$$

$$I_{GOV} = \frac{W_E}{W_{EN}} \cdot I_{GOVR} \tag{12.143}$$

Calculation of Gate-Induced Drain Leakage Parameters

$$A_{GIDL} = \frac{W_E}{W_{EN}} \cdot A_{GIDLR} \tag{12.144}$$

Calculation of Charge Parameters

$$C_{ox} = \varepsilon_{ox} \cdot \frac{W_E \cdot L_E}{t_{ox}} \tag{12.145}$$

$$C_{GD0} = \frac{W_E}{W_{EN}} \cdot C_{ol} \tag{12.146}$$

$$C_{GS0} = \frac{W_E}{W_{EN}} \cdot C_{ol} \tag{12.147}$$

Calculation of Noise Parameters

$$N_{FA} = \frac{W_{EN} \cdot L_{EN}}{W_E \cdot L_E} \cdot N_{FAR} \tag{12.148}$$

$$N_{FB} = \frac{W_{EN} \cdot L_{EN}}{W_E \cdot L_E} \cdot N_{FBR} \tag{12.149}$$

$$N_{FC} = \frac{W_{EN} \cdot L_{EN}}{W_E \cdot L_E} \cdot N_{FCR} \tag{12.150}$$

Calculation of Mobility/Series-Resistance Temperature-Scaling Coefficients

$$\eta_\beta = \eta_{\beta R} + S_{L;\eta_\beta} \cdot \frac{L_{EN}}{L_E} \tag{12.151}$$

Calculation of Geometry-Dependent Parameters using the Binning Scaling Rules

Note that for each bin (W_{min},W_{max},L_{min},L_{max}) there is a separate parameter set, which is valid for (W,L) values with $W_{min} \le W \le W_{max}$ and $L_{min} \le L \le L_{max}$.

$$L_{EN} = 10^{-6} \tag{12.152}$$

$$W_{EN} = 10^{-6} \tag{12.153}$$

Calculation of Threshold-Voltage Parameters

$$k_0 = P_{0;k_0} + \frac{L_{EN}}{L_E} \cdot P_{L;k_0} + \frac{W_{EN}}{W_E} \cdot P_{W;k_0} + \frac{L_{EN} \cdot W_{EN}}{L_E \cdot W_E} \cdot P_{LW;k_0} \tag{12.154}$$

$$\phi_B = P_{0;\phi_B} + \frac{L_{EN}}{L_E} \cdot P_{L;\phi_B} + \frac{W_{EN}}{W_E} \cdot P_{W;\phi_B} + \frac{L_{EN} \cdot W_{EN}}{L_E \cdot W_E} \cdot P_{LW;\phi_B} \tag{12.155}$$

Calculation of Mobility/Series-Resistance Parameters

$$\beta = P_{0;\beta} + \frac{L_{EN}}{L_E} \cdot P_{L;\beta} + \frac{W_E}{W_{EN}} \cdot P_{W;\beta} + \frac{W_E}{L_E} \cdot P_{LW;\beta} \tag{12.156}$$

$$\theta_{sr} = P_{0;\theta_{sr}} + \frac{L_{EN}}{L_E} \cdot P_{L;\theta_{sr}} + \frac{W_{EN}}{W_E} \cdot P_{W;\theta_{sr}} + \frac{L_{EN} \cdot W_{EN}}{L_E \cdot W_E} \cdot P_{LW;\theta_{sr}} \quad (12.157)$$

$$\theta_{ph} = P_{0;\theta_{ph}} + \frac{L_{EN}}{L_E} \cdot P_{L;\theta_{ph}} + \frac{W_{EN}}{W_E} \cdot P_{W;\theta_{ph}} + \frac{L_{EN} \cdot W_{EN}}{L_E \cdot W_E} \cdot P_{LW;\theta_{ph}} \quad (12.158)$$

$$\eta_{mob} = P_{0;\eta_{mob}} + \frac{L_{EN}}{L_E} \cdot P_{L;\eta_{mob}} + \frac{W_{EN}}{W_E} \cdot P_{W;\eta_{mob}} + \frac{L_{EN} \cdot W_{EN}}{L_E \cdot W_E} \cdot P_{LW;\eta_{mob}} \quad (12.159)$$

$$\theta_R = P_{0;\theta_R} + \frac{L_{EN}}{L_E} \cdot P_{L;\theta_R} + \frac{W_{EN}}{W_E} \cdot P_{W;\theta_R} + \frac{L_{EN} \cdot W_{EN}}{L_E \cdot W_E} \cdot P_{LW;\theta_R} \quad (12.160)$$

$$\theta_{sat} = P_{0;\theta_{sat}} + \frac{L_{EN}}{L_E} \cdot P_{L;\theta_{sat}} + \frac{W_{EN}}{W_E} \cdot P_{W;\theta_{sat}} + \frac{L_{EN} \cdot W_{EN}}{L_E \cdot W_E} \cdot P_{LW;\theta_{sat}} \quad (12.161)$$

Calculation of Conductance Parameters

$$\theta_{Th} = P_{0;\theta_{Th}} + \frac{L_{EN}}{L_E} \cdot P_{L;\theta_{Th}} + \frac{W_{EN}}{W_E} \cdot P_{W;\theta_{Th}} + \frac{L_{EN} \cdot W_{EN}}{L_E \cdot W_E} \cdot P_{LW;\theta_{Th}} \quad (12.162)$$

$$\sigma_{sf} = P_{0;\sigma_{sf}} + \frac{L_{EN}}{L_E} \cdot P_{L;\sigma_{sf}} + \frac{W_{EN}}{W_E} \cdot P_{W;\sigma_{sf}} + \frac{L_{EN} \cdot W_{EN}}{L_E \cdot W_E} \cdot P_{LW;\sigma_{sf}} \quad (12.163)$$

$$\alpha = P_{0;\alpha} + \frac{L_{EN}}{L_E} \cdot P_{L;\alpha} + \frac{W_{EN}}{W_E} \cdot P_{W;\alpha} + \frac{L_{EN} \cdot W_{EN}}{L_E \cdot W_E} \cdot P_{LW;\alpha} \quad (12.164)$$

Calculation of Sub-Threshold Parameters

$$\sigma_{dibl} = P_{0;\sigma_{dibl}} + \frac{L_{EN}}{L_E} \cdot P_{L;\sigma_{dibl}} + \frac{W_{EN}}{W_E} \cdot P_{W;\sigma_{dibl}} + \frac{L_{EN} \cdot W_{EN}}{L_E \cdot W_E} \cdot P_{LW;\sigma_{dibl}} \quad (12.165)$$

$$m_0 = P_{0;m_0} + \frac{L_{EN}}{L_E} \cdot P_{L;m_0} + \frac{W_{EN}}{W_E} \cdot P_{W;m_0} + \frac{L_{EN} \cdot W_{EN}}{L_E \cdot W_E} \cdot P_{LW;m_0} \quad (12.166)$$

Calculation of Smoothing Parameters

$$\frac{1}{m} = P_{0;m} + \frac{L_{EN}}{L_E} \cdot P_{L;m} + \frac{W_{EN}}{W_E} \cdot P_{W;m} + \frac{L_{EN} \cdot W_{EN}}{L_E \cdot W_E} \cdot P_{LW;m} \quad (12.167)$$

Calculation of Weak-Avalanche Parameters

$$a_1 = P_{0;a_1} + \frac{L_{EN}}{L_E} \cdot P_{L;a_1} + \frac{W_{EN}}{W_E} \cdot P_{W;a_1} + \frac{L_{EN} \cdot W_{EN}}{L_E \cdot W_E} \cdot P_{LW;a_1} \quad (12.168)$$

$$a_2 = P_{0;a_2} + \frac{L_{EN}}{L_E} \cdot P_{L;a_2} + \frac{W_{EN}}{W_E} \cdot P_{W;a_2} + \frac{L_{EN} \cdot W_{EN}}{L_E \cdot W_E} \cdot P_{LW;a_2} \quad (12.169)$$

$$a_3 = P_{0;a_3} + \frac{L_{EN}}{L_E} \cdot P_{L;a_3} + \frac{W_{EN}}{W_E} \cdot P_{W;a_3} + \frac{L_{EN} \cdot W_{EN}}{L_E \cdot W_E} \cdot P_{LW;a_3} \quad (12.170)$$

Calculation of Gate Current Parameters

$$I_{GINV} = P_{0;I_{GINV}} + \frac{L_E}{L_{EN}} \cdot P_{L;I_{GINV}} + \frac{W_E}{W_{EN}} \cdot P_{W;I_{GINV}} + \frac{L_E \cdot W_E}{L_{EN} \cdot W_{EN}} \cdot P_{LW;I_{GINV}}$$

(12.171)

$$B_{INV} = P_{0;B_{INV}} + \frac{L_{EN}}{L_E} \cdot P_{L;B_{INV}} + \frac{W_{EN}}{W_E} \cdot P_{W;B_{INV}} + \frac{L_{EN} \cdot W_{EN}}{L_E \cdot W_E} \cdot P_{LW;B_{INV}}$$

(12.172)

$$I_{GACC} = P_{0;I_{GACC}} + \frac{L_E}{L_{EN}} \cdot P_{L;I_{GACC}} + \frac{W_E}{W_{EN}} \cdot P_{W;I_{GACC}} + \frac{L_E \cdot W_E}{L_{EN} \cdot W_{EN}} \cdot P_{LW;I_{GACC}}$$

(12.173)

$$B_{acc} = P_{0;B_{acc}} + \frac{L_{EN}}{L_E} \cdot P_{L;B_{acc}} + \frac{W_{EN}}{W_E} \cdot P_{W;B_{acc}} + \frac{L_{EN} \cdot W_{EN}}{L_E \cdot W_E} \cdot P_{LW;B_{acc}}$$

(12.174)

$$I_{GOV} = P_{0;I_{GOV}} + \frac{L_{EN}}{L_E} \cdot P_{L;I_{GOV}} + \frac{W_E}{W_{EN}} \cdot P_{W;I_{GOV}} + \frac{W_E}{L_E} \cdot P_{LW;I_{GOV}} \quad (12.175)$$

Calculation of Gate-Induced Drain Leakage Parameters

$$A_{GIDL} = P_{0;A_{GIDL}} + \frac{L_{EN}}{L_E} \cdot P_{L;A_{GIDL}} + \frac{W_E}{W_{EN}} \cdot P_{W;A_{GIDL}} + \frac{W_E}{L_E} \cdot P_{LW;A_{GIDL}} \quad (12.176)$$

$$B_{GIDL} = P_{0;B_{GIDL}} + \frac{L_{EN}}{L_E} \cdot P_{L;B_{GIDL}} + \frac{W_{EN}}{W_E} \cdot P_{W;B_{GIDL}} + \frac{L_{EN} \cdot W_{EN}}{L_E \cdot W_E} \cdot P_{LW;B_{GIDL}}$$

(12.177)

$$C_{GIDL} = P_{0;C_{GIDL}} + \frac{L_{EN}}{L_E} \cdot P_{L;C_{GIDL}} + \frac{W_{EN}}{W_E} \cdot P_{W;C_{GIDL}} + \frac{L_{EN} \cdot W_{EN}}{L_E \cdot W_E} \cdot P_{LW;C_{GIDL}}$$

(12.178)

Calculation of Charge Parameters

$$C_{ox} = P_{0;C_{ox}} + \frac{L_E}{L_{EN}} \cdot P_{L;C_{ox}} + \frac{W_E}{W_{EN}} \cdot P_{W;C_{ox}} + \frac{L_E \cdot W_E}{L_{EN} \cdot W_{EN}} \cdot P_{LW;C_{ox}} \quad (12.179)$$

$$C_{GD0} = P_{0;C_{GD0}} + \frac{L_{EN}}{L_E} \cdot P_{L;C_{GD0}} + \frac{W_E}{W_{EN}} \cdot P_{W;C_{GD0}} + \frac{W_E}{L_E} \cdot P_{LW;C_{GD0}} \quad (12.180)$$

$$C_{GS0} = P_{0;C_{GS0}} + \frac{L_{EN}}{L_E} \cdot P_{L;C_{GS0}} + \frac{W_E}{W_{EN}} \cdot P_{W;C_{GS0}} + \frac{W_E}{L_E} \cdot P_{LW;C_{GS0}} \quad (12.181)$$

Calculation of Noise Parameters

$$N_{FA} = P_{0;N_{FA}} + \frac{L_{EN}}{L_E} \cdot P_{L;N_{FA}} + \frac{W_{EN}}{W_E} \cdot P_{W;N_{FA}} + \frac{L_{EN} \cdot W_{EN}}{L_E \cdot W_E} \cdot P_{LW;N_{FA}} \quad (12.182)$$

$$N_{FB} = P_{0;N_{FB}} + \frac{L_{EN}}{L_E} \cdot P_{L;N_{FB}} + \frac{W_{EN}}{W_E} \cdot P_{W;N_{FB}} + \frac{L_{EN} \cdot W_{EN}}{L_E \cdot W_E} \cdot P_{LW;N_{FB}} \quad (12.183)$$

$$N_{FC} = P_{0;N_{FC}} + \frac{L_{EN}}{L_E} \cdot P_{L;N_{FC}} + \frac{W_{EN}}{W_E} \cdot P_{W;N_{FC}} + \frac{L_{EN} \cdot W_{EN}}{L_E \cdot W_E} \cdot P_{LW;N_{FC}} \quad (12.184)$$

Calculation of Treshold-voltage Temperature-Scaling Coefficients

$$S_{T;V_{FB}} = P_{0;T;V_{FB}} + \frac{L_{EN}}{L_E} \cdot P_{L;T;V_{FB}} + \frac{W_{EN}}{W_E} \cdot P_{W;T;V_{FB}} + \frac{L_{EN} \cdot W_{EN}}{L_E \cdot W_E} \cdot P_{LW;T;V_{FB}}$$

(12.185)

$$S_{T;\phi_B} = P_{0;T;\phi_B} + \frac{L_{EN}}{L_E} \cdot P_{L;T;\phi_B} + \frac{W_{EN}}{W_E} \cdot P_{W;T;\phi_B} + \frac{L_{EN} \cdot W_{EN}}{L_E \cdot W_E} \cdot P_{LW;T;\phi_B}$$

(12.186)

Calculation of Mobility/Series-Resistance Temperature-Scaling Coefficients

$$\eta_\beta = P_{0;T;\eta_\beta} + \frac{L_{EN}}{L_E} \cdot P_{L;T;\eta_\beta} + \frac{W_{EN}}{W_E} \cdot P_{W;T;\eta_\beta} + \frac{L_{EN} \cdot W_{EN}}{L_E \cdot W_E} \cdot P_{LW;T;\eta_\beta}$$ (12.187)

$$\eta_{sr} = P_{0;T;\eta_{sr}} + \frac{L_{EN}}{L_E} \cdot P_{L;T;\eta_{sr}} + \frac{W_{EN}}{W_E} \cdot P_{W;T;\eta_{sr}} + \frac{L_{EN} \cdot W_{EN}}{L_E \cdot W_E} \cdot P_{LW;T;\eta_{sr}}$$

(12.188)

$$\eta_{ph} = P_{0;T;\eta_{ph}} + \frac{L_{EN}}{L_E} \cdot P_{L;T;\eta_{ph}} + \frac{W_{EN}}{W_E} \cdot P_{W;T;\eta_{ph}} + \frac{L_{EN} \cdot W_{EN}}{L_E \cdot W_E} \cdot P_{LW;T;\eta_{ph}}$$

(12.189)

$$S_{T;\eta_{mob}} = P_{0;T;\eta_{mob}} + \frac{L_{EN}}{L_E} \cdot P_{L;T;\eta_{mob}} + \frac{W_{EN}}{W_E} \cdot P_{W;T;\eta_{mob}} + \frac{L_{EN} \cdot W_{EN}}{L_E \cdot W_E} \cdot P_{LW;T;\eta_{mob}}$$

(12.190)

$$\upsilon_{exp} = P_{0;T;\upsilon_{exp}} + \frac{L_{EN}}{L_E} \cdot P_{L;T;\upsilon_{exp}} + \frac{W_{EN}}{W_E} \cdot P_{W;T;\upsilon_{exp}} + \frac{L_{EN} \cdot W_{EN}}{L_E \cdot W_E} \cdot P_{LW;T;\upsilon_{exp}}$$

(12.191)

$$\eta_R = P_{0;T;\eta_R} + \frac{L_{EN}}{L_E} \cdot P_{L;T;\eta_R} + \frac{W_{EN}}{W_E} \cdot P_{W;T;\eta_R} + \frac{L_{EN} \cdot W_{EN}}{L_E \cdot W_E} \cdot P_{LW;T;\eta_R}$$

(12.192)

$$\eta_{sat} = P_{0;T;\eta_{sat}} + \frac{L_{EN}}{L_E} \cdot P_{L;T;\eta_{sat}} + \frac{W_{EN}}{W_E} \cdot P_{W;T;\eta_{sat}} + \frac{L_{EN} \cdot W_{EN}}{L_E \cdot W_E} \cdot P_{LW;T;\eta_{sat}}$$

(12.193)

Calculation of Weak-Avalanche Temperature-Scaling Coefficients

$$S_{T;a_1} = P_{0;T;a_1} + \frac{L_{EN}}{L_E} \cdot P_{L;T;a_1} + \frac{W_{EN}}{W_E} \cdot P_{W;T;a_1} + \frac{L_{EN} \cdot W_{EN}}{L_E \cdot W_E} \cdot P_{LW;T;a_1}$$

(12.194)

Calculation of Gate-Induced Drain Leakage Temperature-Scaling Coefficients

$$S_{T;B_{GIDL}} = P_{0;T;B_{GIDL}} + \frac{L_{EN}}{L_E} \cdot P_{L;T;B_{GIDL}} + \frac{W_{EN}}{W_E} \cdot P_{W;T;B_{GIDL}} + \frac{L_{EN} \cdot W_{EN}}{L_E \cdot W_E} \cdot P_{LW;T;B_{GIDL}}$$

(12.195)

Calculation of Temperature-Dependent Parameters

Calculation of Transistor Temperature

$$T_{KR} = T_0 + T_R$$ (12.196)

$$T_{KD} = T_0 + T_A + \Delta T_A \tag{12.197}$$

Calculation of Threshold-Voltage Parameters

$$\phi_T = \frac{k_B \cdot T_{KD}}{q} \tag{12.198}$$

$$V_{FB_T} = V_{FB} + (T_{KD} - T_{KR}) \cdot S_{T;V_{FB}} \tag{12.199}$$

$$\phi_{B_T} = \phi_B + (T_{KD} - T_{KR}) \cdot S_{T;\phi_B} \tag{12.200}$$

Calculation of Mobility/Series-Resistance Parameters

$$\beta_T = \beta \cdot \left(\frac{T_{KR}}{T_{KD}}\right)^{\eta_\beta} \tag{12.201}$$

$$\theta_{sr_T} = \theta_{sr} \cdot \left(\frac{T_{KR}}{T_{KD}}\right)^{\eta_{sr}} \tag{12.202}$$

$$\theta_{ph_T} = \theta_{ph} \cdot \left(\frac{T_{KD}}{T_{KR}}\right)^{\eta_{ph}} \tag{12.203}$$

$$\eta_{mob_T} = \eta_{mob} \cdot [1 + (T_{KD} - T_{KR}) \cdot S_{T;\eta_{mob}}] \tag{12.204}$$

$$\nu_T = 1 + (\nu - 1) \cdot (T_{KR} / T_{KD})^{\nu_{exp}} \tag{12.205}$$

$$\theta_{R_T} = \theta_R \cdot \left(\frac{T_{KR}}{T_{KD}}\right)^{\eta_R} \tag{12.206}$$

$$\theta_{sat_T} = \theta_{sat} \cdot \left(\frac{T_{KR}}{T_{KD}}\right)^{\eta_{sat}} \tag{12.207}$$

Calculation of Conductance Parameters

$$\theta_{Th_T} = \theta_{Th} \cdot \left(\frac{T_{KR}}{T_{KD}}\right)^{\eta_{\beta}} \tag{12.208}$$

Calculation of Weak-Avalanche Parameters

$$a_{1_T} = a_1 \cdot [1 + (T_{KD} - T_{KR}) \cdot S_{T;a_1}] \tag{12.209}$$

Calculation of Gate-Induced Drain Leakage Parameters

$$B_{GIDL_T} = B_{GIDL} \cdot [1 + (T_{KD} - T_{KR}) \cdot S_{T;B_{GIDL}}] \tag{12.210}$$

Calculation of Noise Parameters

$$N_{T_T} = \frac{T_{KD}}{T_{KR}} \cdot N_T \tag{12.211}$$

12.5.2 MULT scaling

The N_{MULT} factor determines the number of equivalent parallel devices of a specified model. The N_{MULT} factor has to be applied on the electrical parameters. Hence after the temperature scaling and other parameter processing. Some electrical parameters cannot be specified by the user as parameters but must always be computed from geometrical parameters. They are called electrical quantities here. The parameters: β, I_{GINV}, I_{GACC}, I_{GOV}, C_{OX}, C_{GDO}, C_{GSO}, *NF*, *NFA*, *NFB* and *NFC* are affected by the N_{MULT} factor:

$$\beta = \beta \cdot N_{MULT}$$

$$I_{GINV} = I_{GINV} \cdot N_{MULT}$$

$$I_{GACC} = I_{GACC} \cdot N_{MULT}$$

$$I_{GOV} = I_{GOV} \cdot N_{MULT}$$

$$A_{GIDL} = A_{GIDL} \cdot N_{MULT}$$

$$C_{OX} = C_{OX} \cdot N_{MULT}$$

$$C_{GDO} = C_{GDO} \cdot N_{MULT}$$

$$C_{GSO} = C_{GSO} \cdot N_{MULT}$$

$$N_{FA} = \frac{N_{FA}}{N_{MULT}}$$

$$N_{FB} = \frac{N_{FB}}{N_{MULT}}$$

$$N_{FC} = \frac{N_{FC}}{N_{MULT}}$$

Convention:

No distinction is made between the symbol before and after the N_{MULT} scaling, e.g: the symbol β represents the actual parameter after the N_{MULT} processing and temperature scaling. This parameter may be used to put several MOSTs in parallel.

12.6 Model Equations

Although the basic equations, given in section 12.4.2 on page 692, form a complete set of model equations, they are not yet suited for a circuit simulator. Several equations have to be adapted in order to obtain smooth transitions of the characteristics between adjacent regions of operation conditions and to prevent numerical problems during the iteration process for solving the network equations. In the following section a list of numerical adaptations and elucidations is given, followed by the extended set of model equations.

The definition of the hyp function, which provides for a smooth C_∞-continuous clipping, is to be found in the appendix A.

In the following sections , a function is denoted by *F*{*variable*, ...}, where *F* denotes the function name and the function variables are enclosed by braces {}.

Internal Parameters

$$\varepsilon_1 = 2 \cdot 10^{-2} \tag{12.212}$$

$$\varepsilon_2 = 1 \cdot 10^{-2} \tag{12.213}$$

$$\varepsilon_3 = 4 \cdot 10^{-2} \tag{12.214}$$

$$\varepsilon_4 = 1 \cdot 10^{-1} \tag{12.215}$$

$$\varepsilon_5 = 1 \cdot 10^{-4} \tag{12.216}$$

$$P_D = 1 + (k_0 / k_p)^2 \tag{12.217}$$

$$V_{limit} = 4 \cdot \phi_T \tag{12.218}$$

$$\theta_{R_{eff}} = \frac{1}{2} \cdot \theta_{R_T} \cdot \left(1 + \frac{\theta_{R1}}{1/2 + \theta_{R2}}\right) \tag{12.219}$$

$$Acc = \left.\frac{\partial \psi_s}{\partial V_{GB}}\right|_{V_{GB} = V_{FB_T}} = \frac{1}{1 + k_0/(\sqrt{2 \cdot \phi_T})} \tag{12.220}$$

$$N_{\phi_T} = (2.6)^2/k_0 \tag{12.221}$$

$$Acc_{ov} = \left.\frac{\partial \psi_{sov}}{\partial V_{GB}}\right|_{V_{GB} = V_{FBov}} = \frac{1}{1 + k_{ov}/(\sqrt{2 \cdot \phi_T})} \tag{12.222}$$

$$QM_{\psi} = \begin{cases} QM_N \cdot (\varepsilon_{ox}/t_{ox})^{2/3} & \text{for NMOS} \\ QM_N \cdot (\varepsilon_{ox}/t_{ox})^{2/3} & \text{for PMOS} \end{cases} \tag{12.223}$$

$$QM_{tox} = \frac{2}{5} \cdot QM_{\psi} \tag{12.224}$$

$$\chi_{B_{inv}} = \begin{cases} \chi_{B_N} & \text{for NMOS} \\ \chi_{B_P} & \text{for PMOS} \end{cases} \tag{12.225}$$

$$\chi_{B_{acc}} = \chi_{B_N} \tag{12.226}$$

Extended Current Equations

$$V_{GB_{eff}} = \text{hyp}_1(V_{GS} + V_{SB} - V_{FB_T}; \varepsilon_1) \tag{12.227}$$

$$V_{SB_t} = \mathrm{hyp}_1(V_{SB} + 0.9 \cdot \phi_{B_T}; \varepsilon_2) + 0.1 \cdot \phi_{B_T} \tag{12.228}$$

$$\psi_{sat_0} = \left(\frac{\sqrt{P_D \cdot V_{GB_{eff}} + k_0^2/4} - k_0/2}{P_D} \right)^2 \tag{12.229}$$

Drain induced barrier lowering and Static Feedback

$$D_{dibl} = \sigma_{dibl} \cdot \sqrt{V_{SB_t}} \tag{12.230}$$

$$D_{sf} = \sigma_{sf} \cdot \sqrt{\mathrm{hyp}_1(\psi_{sat_0} - V_{SB_t}; \varepsilon_3)} \tag{12.231}$$

$$D = D_{dibl} + \mathrm{hyp}_1(D_{sf} - D_{dibl}; \sigma_{sf} \cdot \varepsilon_4) \tag{12.232}$$

$$V_{DS_{eff}} = \frac{V_{DS}^4}{(V_{limit}^2 + V_{DS}^2)^{3/2}} \tag{12.233}$$

$$\Delta V_G = D \cdot V_{DS_{eff}} \tag{12.234}$$

Redefinition of $V_{GB_{eff}}$, equation (12.227)

$$V_{GB_{eff}} = \mathrm{hyp}_1(V_{GS} + V_{SB} + \Delta V_G - V_{FB_T}; \varepsilon_1) \tag{12.235}$$

$$\Delta_{acc} = \phi_T \cdot \left[\exp\left(-\frac{Acc \cdot [V_{GB_{eff}} - \varepsilon_1]}{\phi_T} \right) - 1 \right] \tag{12.236}$$

$$\psi_{sat_1} = \left(\frac{\sqrt{P_D \cdot (V_{GB_{eff}} + \Delta_{acc}) + k_0^2/4} - k_0/2}{P_D} \right)^2 - \Delta_{acc} \tag{12.237}$$

Drain Saturation Voltage:

$$V_{DSAT_{long}} = \psi_{sat_1} - V_{SB_t} \tag{12.238}$$

$$T_{sat} = \begin{cases} \theta_{sat_T} & \text{for NMOS} \\ \dfrac{\theta_{sat_T}}{(1 + \theta_{sat_T}^2 \cdot V_{DSAT_{long}}^2)^{1/4}} & \text{for PMOS} \end{cases} \tag{12.239}$$

$$\Delta_{SAT} = \frac{T_{sat} - \theta_{R_{eff}}}{\sqrt{\dfrac{2}{V_{DSAT_{long}}^2 + \varepsilon_4} + T_{sat}^2} + \theta_{R_{eff}}} \tag{12.240}$$

$$V_{DSAT_{short}} = V_{DSAT_{long}} \cdot \left(1 - \frac{9}{10} \cdot \frac{\Delta_{SAT}}{1 + \sqrt{1 - \Delta_{SAT}}^2} \right) \tag{12.241}$$

$$V_{DSAT} = V_{limit} + \mathrm{hyp}_1(V_{DSATshort} - V_{limit}; \varepsilon_3) \tag{12.242}$$

$$V_{DS_x} = \frac{V_{DS} \cdot V_{DSAT}}{[V_{DS}^{2m} + V_{DSAT}^{2m}]^{1/(2 \cdot m)}} \tag{12.243}$$

$$V_{DB_t} = \mathrm{hyp}_1(V_{DS_X} + V_{SB} + 0.9 \cdot \phi_{B_T}; \varepsilon_2) + 0.1 \cdot \phi_{B_T} \tag{12.244}$$

Surface Potential:

$$f_1\{\psi\} = \psi_{sat_1} - \mathrm{hyp}_1\{\psi_{sat_1} - \psi; \varepsilon_1\} \tag{12.245}$$

$$f_2\{\psi\} = f_1\{\psi\} + \frac{\psi_{sat_1} - f_1\{\psi\}}{\sqrt{1 + \frac{[\psi_{sat_1} - f_1\{\psi\}]^2}{N_{\phi_T} \cdot \phi_T^2}}} \tag{12.246}$$

$$f_3\{\psi\} = \frac{2 \cdot [V_{GB_{eff}} - f_2\{\psi\}]}{1 + \sqrt{1 + 4/k_p^2 \cdot [V_{GB_{eff}} - f_2\{\psi\}]}} \tag{12.247}$$

$$\psi_{s_{inv}}\{\psi\} = f_1\{\psi\} + \phi_T \cdot [1 + m_0] \cdot \ln\left[\frac{\left[\frac{f_3\{\psi\}}{k_0}\right]^2 - f_1\{\psi\} - \Delta_{acc} + \phi_T}{\phi_T}\right] \tag{12.248}$$

$$\psi^*_{s_0} = \psi_{s_{inv}} \cdot \{V_{SB_t}\} \tag{12.249}$$

$$\psi^*_{s_L} = \psi_{s_{inv}} \cdot \{V_{DB_t}\} \tag{12.250}$$

Surface Potential in Accumulation:

$$f_1 = Acc \cdot [V_{GS} + V_{SB} + \Delta V_G - V_{FB_T} - V_{GB_{eff}}] \tag{12.251}$$

$$f_2 = \frac{f_1}{\sqrt{1 + \frac{f_1^2}{N_{\phi_T} \cdot \phi_T^2}}} \tag{12.252}$$

$$\psi_{s_{acc}} = -\phi_T \cdot \ln\left[\frac{\left\{\frac{f_1/(Acc) - f_2}{k_0}\right\}^2 - f_2 + \phi_T}{\phi_T}\right] \tag{12.253}$$

Auxiliary Variables:

$$\Delta\psi = \psi^*_{s_L} - \psi^*_{s_0} \tag{12.254}$$

$$\overline{\psi}_{inv} = \frac{\psi^*_{s_L} + \psi^*_{s_0}}{2} \tag{12.255}$$

$$V_{G_T}\{\psi_{s_{inv}}\} = \frac{2 \cdot [V_{GB_{eff}} - \psi_{s_{inv}}]}{1 + \sqrt{1 + 4/k_p^2 \cdot [V_{GB_{eff}} - \psi_{s_{inv}}]}} - k_0 \cdot \sqrt{\mathrm{hyp}_1\{\psi_{s_{inv}} + \Delta_{acc}\ ;\varepsilon_2\}}$$

(12.256)

$$V_{GT_0} = \mathrm{hyp}_1\left\{V_{G_T}\left\{\psi^*_{s_0}\right\};\varepsilon_5\right\} \tag{12.257}$$

$$V_{GT_L} = \mathrm{hyp}_1\left\{V_{G_T}\left\{\psi^*_{s_L}\right\};\varepsilon_5\right\} \tag{12.258}$$

$$\bar{V}_{G_T} = V_{G_T}\{\bar{\psi}_{inv}\} \tag{12.259}$$

$$V_{ox} = \frac{2\cdot[V_{GS} + V_{SB} + \Delta V_G - V_{FB} - \bar{\psi}_{inv} - \psi_{acc}]}{1 + \sqrt{1 + 4/k_p^2\cdot[V_{GB_{eff}} - \bar{\psi}_{inv}]}} \tag{12.260}$$

$$\partial V_{ox} = \frac{2}{1 + \sqrt{1 + 4/k_p^2\cdot[V_{GB_{eff}} - \bar{\psi}_{inv}]}} \tag{12.261}$$

$$V_{eff} = V_{G_T} + \eta_{mob}\cdot(V_{ox} - V_{G_T}) \tag{12.262}$$

$$\xi_{ox} = -\phi_T\cdot\frac{\partial V_{ox}}{\partial\bar{\psi}_{inv}} = \phi_T\cdot\frac{1}{\sqrt{1 + 4/k_p^2\cdot[V_{GB_{eff}} - \bar{\psi}_{inv}]}} \tag{12.263}$$

$$\xi = \phi_T\cdot\left[\frac{1}{\sqrt{1 + 4/k_p^2\cdot[V_{GB_{eff}} - \bar{\psi}_{inv}]}} + \frac{k_0}{2\cdot\sqrt{\mathrm{hyp}_1\{\bar{\psi}_{inv} + \Delta_{acc}\ ;\varepsilon_5\}}}\right] \tag{12.264}$$

$$\bar{V}^*_{G_T} = \frac{V_{GT_0} + V_{GT_L}}{2} + \xi \tag{12.265}$$

Second-Order Effects

Mobility Degradation:

$$V_{eff_1} = \mathrm{hyp}_1(V_{eff};\varepsilon_2) \tag{12.266}$$

$$G_{mob} = \frac{\mu_0}{\mu} = \begin{cases} 1 + [(\theta_{ph_T} \cdot V_{eff_1})^{\nu_T/3} + (\theta_{sr_T} \cdot V_{eff_1})^{2\nu_T}]^{1/\nu_T} & \text{for NMOS} \\ 1 + [(\theta_{ph_T} \cdot V_{eff_1})^{\nu_T/3} + (\theta_{sr_T} \cdot V_{eff_1})^{\nu_T}]^{1/\nu_T} & \text{for PMOS} \end{cases} \tag{12.267}$$

Velocity Saturation:

$$x = \begin{cases} \dfrac{2 \cdot \theta_{sat_T} \cdot \Delta\psi}{\sqrt{G_{mob}}} & \text{for NMOS} \\ \dfrac{2 \cdot \theta_{sat_T}}{\sqrt{G_{mob}}} \cdot \dfrac{\Delta\psi}{(1 + \theta_{sat_T}^2 \cdot \Delta\psi^2)^{1/4}} & \text{for PMOS} \end{cases} \tag{12.268}$$

$$G_{vsat} = \begin{cases} \dfrac{G_{mob}}{2} \cdot \left[\sqrt{1 + x^2} + 1 - \dfrac{x^2}{6}\right] & x < 1 \cdot 10^{-4} \\ \dfrac{G_{mob}}{2} \cdot \left[\sqrt{1 + x^2} + \dfrac{\ln(x + \sqrt{1 + x^2})}{x}\right] & x \geq 1 \cdot 10^{-4} \end{cases} \tag{12.269}$$

Channel Length Modulation:

$$G_{\Delta L} = \mathrm{hyp}_1\left(1 - \alpha \cdot \ln\left[\frac{V_{DS} - V_{DS_x} + \sqrt{(V_{DS} - V_{DS_x})^2 + V_p^2}}{V_P}\right]; \varepsilon_5\right) \tag{12.270}$$

Series Resistance and Self-Heating:

$$G_R = \theta_{R_T} \cdot \left(1 + \frac{\theta_{R1}}{\theta_{R2} + \bar{V}_{G_T}}\right) \cdot \bar{V}_{G_T} \tag{12.271}$$

$$G_{Th} = \theta_{Th_T} \cdot V_{DS} \cdot \Delta\psi \cdot V_{G_T} \tag{12.272}$$

$$G_{tot} = G_{Th} + \frac{[G_{\Delta L} \cdot G_{vsat} + G_R]}{2} \cdot \left[1 + \sqrt{\mathrm{hyp}_1\left(1 - \frac{4 \cdot G_R / G_{vsat}}{G_{\Delta L} \cdot G_{vsat} + G_R{}^2} \cdot [G_{vsat}^2 - G_{mob}^2]; \varepsilon_5\right)}\right] \tag{12.273}$$

Inversion-Layer Charge

$(Q_{inv} = -\varepsilon_{ox}/t_{ox} \cdot V_{inv})$:

$$\psi^*_{s_{inv}}\{\psi_{s_{inv}}\} = \mathrm{hyp}_1(\psi_{s_{inv}} + \Delta_{acc}; \varepsilon_5) \tag{12.274}$$

$$V_{inv}\{\psi_{s_{inv}},\psi\} = \frac{k_0 \cdot \phi_T \cdot \exp\left[\frac{\psi_{s_{inv}} - \psi}{(1+m_0)\cdot\phi_T}\right]}{\sqrt{\psi^*_{s_{inv}}\{\psi_{s_{inv}}\} + \phi_T \cdot \exp\left[\frac{\psi_{s_{inv}} - \psi}{(1+m_0)\cdot\phi_T}\right]} + \sqrt{\psi^*_{s_{inv}}\{\psi_{s_{inv}}\}}}$$

(12.275)

$$V_{inv_0} = V_{inv}\left\{\psi^*_{s_0}, V_{SB_t}\right\} \tag{12.276}$$

$$V_{inv_L} = V_{inv}\left\{\psi^*_{s_L}, V_{DB_t}\right\} \tag{12.277}$$

Drain Current

$$x_0 = \frac{2}{\phi_T}\cdot(\psi_{sat_1} + \phi_T - V_{SB_t}) \tag{12.278}$$

$$x_L = \frac{2}{\phi_T}\cdot(\psi_{sat_1} + \phi_T - V_{DB_t}) \tag{12.279}$$

$$G = \frac{\exp(x_0) + \exp(x_L)}{\exp(x_0) + \exp(x_L) + 1} \tag{12.280}$$

$$I_{drift} = \begin{cases} \beta \cdot V_{G_T} \cdot \Delta\psi & x_0 > 80 \text{ or } x_L > 80 \\ \beta \cdot \bar{V}_{G_T} \cdot \Delta\psi \cdot G & x_0 \le 80 \text{ and } x_L \le 80 \end{cases} \tag{12.281}$$

$$I_{diff} = \beta_T \cdot \phi_T \cdot (V_{inv_0} - V_{inv_L}) \tag{12.282}$$

$$I_{DS} = \frac{I_{drift} + I_{diff}}{G_{tot}} \tag{12.283}$$

Weak-Avalanche

$$I_{avl} = \begin{cases} 0 & for: V_{DS} - a_3 \cdot V_{DSAT} \le -a_2/A \\ a_{1_T} \cdot I_{DS} \cdot \exp\left(-\dfrac{a_2}{V_{DS} - a_3 \cdot V_{DSAT}}\right) & for: V_{DS} - a_3 \cdot V_{DSAT} > -a_2/A \end{cases} \tag{12.284}$$

Gate Current Equations

The tunnelling probability is given by:

$$P_{tun}\{V_{ox};\chi_B;B\} = \begin{cases} \exp\left(-\dfrac{B}{\chi_B} \cdot \dfrac{\left[\left(\dfrac{V_{ox}}{\chi_B}\right)^2 - 3 \cdot \dfrac{V_{ox}}{\chi_B} + 3\right]}{1 + \left(1 - \dfrac{V_{ox}}{\chi_B}\right)^{3/2}}\right) & V_{ox} < \chi_B \\ \exp(-B/V_{ox}) & V_{ox} \ge \chi_B \end{cases} \tag{12.285}$$

Source/Drain Gate Overlap Current:

First calculate the oxide voltage V_{ov} at both Source and Drain overlap:

$$V_{G_{eff}}\{V_{GX}\} = V_{GX} - V_{FBov} - \mathrm{hyp}_1(V_{GX} - V_{FBov};\varepsilon_1) \tag{12.286}$$

$$\Delta_{ov}\{V_{GX}\} = \phi_T \cdot \left[\exp\left(\frac{Acc_{ov} \cdot [V_{GX_{eff}}\{V_{GX}\} + \varepsilon_1]}{\phi_T}\right) - 1\right] \tag{12.287}$$

$$\psi_{sat_{ov}}\{V_{GX}\} = -\left[\sqrt{\frac{k_{ov}^2}{4} - V_{G_{eff}}\{V_{GX}\} + \Delta_{ov}\{V_{GX}\}} - \frac{k_{ov}}{2}\right]^2 + \Delta_{ov}\{V_{GX}\} \tag{12.288}$$

$$f_1\{V_{GX}\} = Acc_{ov} \cdot [V_{GX} - V_{FBov} - V_{G_{eff}}\{V_{GX}\}] \tag{12.289}$$

$$f_2\{V_{GX}\} = \frac{f_1\{V_{GX}\}}{\sqrt{1 + \frac{[f_1\{V_{GX}\}]^2}{N_{\phi_T} \cdot \phi_T^2}}} \tag{12.290}$$

$$f_3\{V_{GX}\} = \frac{2 \cdot \left[\frac{f_1\{V_{GX}\}}{Acc_{ov}} - f_2\{V_{GX}\}\right]}{1 + \sqrt{1 + 4/k_p^2 \cdot \left[\frac{f_1\{V_{GX}\}}{Acc_{ov}} - f_2\{V_{GX}\}\right]}} \tag{12.291}$$

$$\psi_{s_{ov}}^*\{V_{GX}\} = \phi_T \cdot \ln\left(\frac{\left(\frac{f_3\{V_{GX}\}}{k_{ov}}\right)^2 + f_2\{V_{GX}\} + \phi_T}{\phi_T}\right) \tag{12.292}$$

$$V_{ov}\{V_{GX}\} = \frac{2 \cdot [V_{GX} - V_{FBov} - \psi_{s_{ov}}^*\{V_{GX}\} - \psi_{sat_{ov}}\{V_{GX}\}]}{1 + \sqrt{1 + 4/k_p^2 \cdot [(f_1\{V_{GX}\})/Acc_{ov} - \psi_{s_{ov}}^*\{V_{GX}\}]}} \tag{12.293}$$

$$V_{ov_0} = V_{ov}\{V_{GS}\} \tag{12.294}$$

$$V_{ov_L} = V_{ov}\{V_{GS} - V_{DS}\} \tag{12.295}$$

Next calculate the gate tunnelling current in both Source and Drain overlap:

$$P_{ov}\{V_{ov}\} = P_{tun}\{V_{ov};\chi_{B_{inv}};B_{inv}\} \tag{12.296}$$

$$I_{Gov}\{V_{GX},V_{ov}\} = I_{GOV}\cdot V_{GX}\cdot V_{ov}\cdot [P_{ov}\{V_{ov}\} - P_{ov}\{-V_{ov}\}] \tag{12.297}$$

$$I_{Gov_0} = I_{Gov}\{V_{GS}\,,\,V_{ov_0}\} \tag{12.298}$$

$$I_{Gov_L} = I_{Gov}\{V_{GS} - V_{DS}\,,\,V_{ov_L}\} \tag{12.299}$$

Intrinsic Gate Current

The gate tunnelling current in accumulation:

$$P_{acc} = P_{tun}\{-V_{ox};\chi_{B_{acc}};B_{acc}\} \tag{12.300}$$

$$V_{acc} = V_{ox} - \mathrm{hyp}_1(V_{ox};\varepsilon_5) \tag{12.301}$$

$$I_{GB} = -I_{GACC}\cdot (V_{GS} + V_{SB})\cdot V_{acc}\cdot P_{acc} \tag{12.302}$$

The tunnelling current in inversion, including quantum-mechanical barrier lowering $\Delta\chi_B$:

$$\Delta\chi_B = QM_{\psi}\cdot [(\overline{V}_{G_T}/3 + V_{ox} - \overline{V}_{G_T})^2 + V_{limit}^2]^{1/3} \tag{12.303}$$

$$\chi_{B_{eff}} = 0.7 \cdot \chi_{B_{inv}} + \mathrm{hyp}_1(0.3 \cdot \chi_{B_{inv}} - \Delta\chi_B;\varepsilon_5) \tag{12.304}$$

$$B_{eff} = B_{inv} \cdot (\chi_{B_{eff}} / \chi_{B_{inv}})^{3/2} \tag{12.305}$$

$$P_{inv} = P_{tun}(V_{ox};\chi_{B_{eff}};B_{eff}) \tag{12.306}$$

$$B^*_{inv} = \frac{3}{8} \cdot \chi^{-2}_{B_{eff}} \cdot B_{eff} \cdot \partial V_{ox} \tag{12.307}$$

$$\xi^* = \frac{\xi}{\phi_T \cdot \bar{V}^*_{G_T}} \tag{12.308}$$

$$\partial V^*_{ox} = \frac{\partial V_{ox}}{\sqrt{V^2_{ox} + V^2_{limit}}} \tag{12.309}$$

$$P_{GC} = 1 + \frac{[(B^*_{inv})^2 + 4 \cdot B^*_{inv} \cdot \xi^* + 2 \cdot B^*_{inv} \cdot \partial V^*_{ox} + 2 \cdot \xi^{*2} + 4 \cdot \partial V^*_{ox} \cdot \xi^*] \cdot \Delta\psi^2}{24}$$

(12.310)

$$\bar{I}_{GC} = I_{GINV} \cdot G_{\Delta L} \cdot \left(V_{GS} - \frac{1}{2} \cdot V_{DS_x}\right) \cdot P_{inv} \tag{12.311}$$

$$\bar{V}_{inv} = \frac{V_{inv_0} + V_{inv_L}}{2} \tag{12.312}$$

The total intrinsic gate current I_{GC} :

$$I_{GC} = I_{GC} \cdot V_{inv} \cdot P_{GC} \tag{12.313}$$

$$P_{GS} = [B^*_{inv} + \partial V^*_{ox}] \cdot \frac{\Delta\psi}{12} + [(B^*_{inv})^2 \cdot (B^*_{inv} + 5 \cdot \xi^* + 3 \cdot \partial V^*_{ox}) + 2 \cdot \xi^{*2} \cdot (B^*_{inv} - \xi^* + \partial V^*_{ox}) + 10 \cdot B^*_{inv} \cdot \xi^* \cdot \partial V^*_{ox}] \cdot \frac{\Delta\psi^3}{480} \tag{12.314}$$

$$I_{GS} = \frac{1}{2} \cdot I_{GC} + \left(P_{GS} \cdot \bar{V}_{inv} + \frac{V_{inv_0} - V_{inv_L}}{12} \right) \cdot \bar{I}_{GC} + I_{Gov_0} \tag{12.315}$$

$$I_{GD} = I_{GC} - I_{GS} + I_{Gov_0} + I_{Gov_L} \tag{12.316}$$

Gate-Induced Drain/Source Leakage Current:

$$V_{tov}\{V_{ov};V\} = \sqrt{(V_{ov} - \ hyp_1\{V_{ov};\varepsilon_5\})^2 + C_{GIDL}{}^2 \cdot V^2} \tag{12.317}$$

$$I_{gixl}\{V_{ov};V\} = \begin{cases} A_{GIDL} \cdot V \cdot V_{tov} \cdot \{V_{ov};V\}^2 \cdot e^{-\frac{B_{GIDL_T}}{V_{tov}\{V_{ov};V\}}} & \text{for: } V_{tov}\{V_{ov};V\} > -\frac{B_{GIDL_T}}{A} \\ 0 & \text{for: } V_{tov}\{V_{ov};V\} \le -\frac{B_{GIDL_T}}{A} \end{cases} \tag{12.318}$$

$$I_{gisl} = I_{gixl}\{V_{ov_0};V_{SB}\} \tag{12.319}$$

$$I_{gidl} = I_{gixl}\{V_{ov_L};V_{DS} + V_{SB}\} \tag{12.320}$$

Extended Charge Equations

Bias-Dependent Overlap Capacitance:

$$Q_{ov_0} = C_{GSO} \cdot V_{ov_0} \tag{12.321}$$

$$Q_{ov_L} = C_{GDO} \cdot V_{ov_L} \tag{12.322}$$

Intrinsic Charges:

$$C_{ox_{eff}} = \frac{C_{ox}}{1 + QM_{t_{ox}} \cdot \left[\left(\frac{V_{eff}}{\eta_{mob}}\right)^2 + (20 \cdot \phi_T)^2\right]^{-1/6}} \tag{12.323}$$

$$\Delta V_{G_T} = \frac{V_{GT_0} - V_{GT_L}}{2 \cdot \left(1 + \theta_{R_T} \cdot \frac{\overline{V}^*_{G_T}}{G_{tot}}\right)} \tag{12.324}$$

$$F_j = \frac{\Delta V_{G_T}}{\overline{V}^*_{G_T}} \tag{12.325}$$

$$Q_S = -\frac{C_{ox_{eff}}}{2} \cdot \left[\overline{V}^*_{G_T} + \frac{\Delta V_{G_T}}{3} \cdot \left(F_j - \frac{F_j^2}{5} + 1\right) - \xi\right] \tag{12.326}$$

$$Q_D = -\frac{C_{ox_{eff}}}{2} \cdot \left[\overline{V}^*_{G_T} + \frac{\Delta V_{G_T}}{3} \cdot \left(F_j + \frac{F_j^2}{5} - 1\right) - \xi\right] \tag{12.327}$$

$$Q_G = -C_{ox_{eff}} \cdot \left[V_{ox} + \frac{\Delta V_{G_T}}{3} \cdot F_j \cdot \frac{\xi_{ox}}{\xi} \right] \tag{12.328}$$

$$Q_B = -[Q_S + Q_D + Q_G] \tag{12.329}$$

Extended Noise Equations

In these equations f represents the operation frequency of the transistor.

$$g_m = \frac{\partial I_{DS}}{\partial V_{GS}} \tag{12.330}$$

$$T_{sat} = \begin{cases} \theta^2_{sat_T} & \text{for NMOS} \\ \dfrac{\theta^2_{sat_T}}{\sqrt{1 + \theta^2_{sat_T} \cdot \Delta\psi^2}} & \text{for PMOS} \end{cases} \tag{12.331}$$

$$R_{ideal} = \frac{\beta \cdot G^2_{vsat}}{G_{tot}} \cdot \left[\bar{V}_{G_T} + \frac{\frac{\Delta\psi^2}{12} - \xi \cdot \left(\bar{V}_{G_T} - \frac{V_{inv_0} + V_{inv_L}}{2} \right)}{\bar{V}_{G_T} + \xi} \right] \tag{12.332}$$

$$S_{th} = \begin{cases} 0 & R_{ideal} \le T_{sat} \cdot I_{DS} \cdot \Delta\psi \\ \dfrac{N_{T_T}}{G_{mob}}^2 \cdot (R_{ideal} - T_{sat} \cdot I_{DS} \cdot \Delta\psi) & R_{ideal} > T_{sat} \cdot I_{DS} \cdot \Delta\psi \end{cases} \tag{12.333}$$

$$N_0 = \frac{\varepsilon_{ox}}{q t_{ox}} \cdot V_{inv_0} \tag{12.334}$$

$$N_L = \frac{\varepsilon_{ox}}{qt_{ox}} \cdot V_{inv_L} \tag{12.335}$$

$$N^* = \frac{\varepsilon_{ox}}{qt_{ox}} \cdot \xi \tag{12.336}$$

$$S_{fl} = \frac{q \cdot \phi_T^2 \cdot t_{ox} \cdot \beta_T \cdot I_{DS}}{f \cdot \varepsilon_{ox} \cdot G_{mob} \cdot N^*} \cdot \left[(N_{FA} - N^* \cdot N_{FB} + N^{*2} \cdot N_{FC}) \cdot \ln \frac{N_0 + N^*}{N_L + N^*} + (N_{FB} - N^* \cdot N_{FC}) \cdot (N_0 - N_L) + \frac{N_{FC}}{2} \cdot (N_0^2 - N_L^2) \right] + \frac{\phi_T \cdot I_{DS}^2}{f} \cdot (1 - G_{\Delta L}) \cdot \left[\frac{N_{FA} + N_{FB} \cdot N_L + N_{FC} \cdot N_L^2}{(N_L + N^*)^2} \right] \tag{12.337}$$

$$S_{ig} = \begin{cases} \dfrac{\frac{1}{3} \cdot N_{T_T} \cdot (2 \cdot \pi \cdot f \cdot C_{ox})^2 / g_m}{1 + 0.075 \cdot (2 \cdot \pi \cdot f \cdot C_{ox} / g_m)^2} & \text{GATENOISE} = 0 \\ 0 & \text{GATENOISE} = 1 \end{cases} \tag{12.338}$$

$$\rho_{igth} = 0.4j \tag{12.339}$$

$$S_{igth} = \rho_{igth} \cdot \sqrt{S_{ig} \cdot S_{th}} \tag{12.340}$$

12.6.1 Numerical adaptations

The implemented electrical equations of MOS Model 1101 are essentially based on the physical description given in section 12.4 on page 677. The following numerical adaptations have been made in order to obtain smooth transitions and prevent numerical problems, leading to the equations given in section 12.6 on page 728:

- The piece-wise eqs. (12.11) and (12.19) for $V_{GB_{eff}}$,(12.14) for D_{sf} ,(12.15) for D ,(12.22)for $V_{DSAT_{long}}$, (12.25) for V_{DSAT} ,(12.27), (12.33) and (12.66) for different functions f_1 ,(12.63) for $V_{GX_{eff}}$ and (12.78) for I_{GB} have been replaced by smooth C_∞ -continuous functions based on hyp-functions.

- Expression (12.13) describing the drain-induced barrier lowering effect has no numerical solution for $V_{SB} + \phi_B < 0$. In order to solve this problem the expression $V_{SB} + \phi_B$ is clipped at a minimum value of $0.1 \cdot \phi_B$ using eq. (12.228). In order to maintain symmetry (with respect to source and drain) the same method must be applied to the drain side, this is done in eq. (12.244).

- The effective voltage V_{eff} given by eq. (12.262) becomes negative in the accumulation region, which leads to strange behaviour in the mobility reduction expression (12.48). In order to prevent V_{eff} from becoming negative, a hyp-smoothing function is used in the actual implementation, see eq. (12.266).

- The theoretical velocity saturation expression (12.50) results in zero divided by zero for $V_{DS} = 0$. This numerical problem has been circumvented by replacing this expression by a third-order Taylor polynomial for small values of V_{DS} , see eq. (12.269).

- The theoretical channel length modulation expression (12.51) can become negative for high values of α and V_{DS} . This corresponds to a negative effective channel length, which is not physical. In order to prevent $G_{\Delta L}$ from becoming negative, a hyp-smoothing function is used in the actual implementation, see eq. (12.270).

- The term in the square root of eq. (12.54) can become negative for very high values of parameter θ_R, which would result in numerical errors. This has been prevented in the actual implementation (12.273) by using a hyp-smoothing function.

- The term $\psi_{s_{inv}} + \Delta_{acc}$ in expression (12.55) may become negative in accumulation for certain parameter values. Since a square root is taken of this term, it has to be prevented that the above term becomes negative; this has been done using a hyp-smoothing function (12.274) in eq. (12.275). The same type of problem occurs in eq. (12.46) for variable ξ, it has been circumvented in the same way, see eq. (12.264).

- Theoretically in subthreshold the drift current given by eq. (12.58) is much smaller than the diffusion current, due to the term $\Delta\psi$ which rapidly approaches zero for decreasing gate bias. Owing to the approximations made in the calculation of surface potential in MOS Model 1101, for certain conditions $\Delta\psi$ may not go to zero rapidly enough. As a result the drift current is forced to very small values in subthreshold by making use of eqs. (12.278) to (12.281).

- The exponent in the tunnelling probability P_{tun}, given by eq. (12.62), results in zero divided by zero for $V_{ox} = 0$. By simply rewriting the exponent, this problem can be circumvented as has been done in eq. (12.285).

- The expression of effective oxide barrier lowering $\Delta\chi_B$, given by eq. (12.79), can become equal to zero (at $V_{GB} = V_{FB}$), resulting in numerical errors in the first-order derivatives of $\Delta\chi_B$ to the terminal voltages. In order to prevent $\Delta\chi_B$ from becoming zero, eq. (12.303) has been used.

- For very high gate bias values, which could occur during the iteration process of the circuit simulator, the expression of effective oxide barrier $\chi_{B_{eff}}$, given by eq. (12.80), can become zero or negative resulting in numerical errors. In order to prevent this problem $\chi_{B_{eff}}$ is clipped at a minimum (arbitrary) value of $0.7 \cdot \chi_{B_{inv}}$ using a hyp-smoothing function, see eq. (12.304).

- The expression of ∂V_{ox}^{*}, given by eq. (12.85), gives numerical problems when the oxide voltage V_{ox} is equal to zero. This problem has been circumvented by replacing V_{ox} by $\sqrt{V_{ox}^2 + V_{limit}^2}$, see eq. (12.309).

- The expression of effective oxide capacitance (12.99) due to quantum-mechanical effects gives erroneous results for $V_{eff} = 0$ (i.e. $V_{GB} = V_{FB}$). This can be prevented by replacing V_{eff}/η_{mob} by $\sqrt{(V_{eff}/\eta_{mob})^2 + (20 \cdot \phi_T)^2}$, where the value of $20 \cdot \phi_T$ is

rather arbitrary but it nevertheless ensures a smooth transition from accumulation to depletion / inversion.

12.7 Model embedding in a circuit simulator

In CMOS technologies both n- and p-channel MOS transistors are supported. It is convenient to use one model for both type of transistors instead of two separate models. This is accomplished by mapping a p-channel device with its bias conditions and parameter set onto an equivalent n-channel device with appropriately changed bias conditions (i.e. currents, voltages and charges) and parameters. In this way both type of transistors can be treated as an n-channel transistor. Nevertheless, the electrical behaviour of electrons and holes is not exactly the same (e.g. the mobility and tunnelling behaviour), and consequently slightly different equations have to be used in case of n- or p-type transistors, see section 12.4.2 on page 692.

As said earlier, any circuit simulator internally identifies the terminals of a MOS transistor by a number. However, designers are used to the standard terminology of source, drain, gate and bulk. Therefore, in the context of a circuit simulator it is traditionally possible to address, say, the drain of MOST number 17, even if in reality the corresponding source is at a higher potential (n channel case). More strongly, most circuit simulators provide for model evaluation a so called V_{DS} , V_{GS} , and V_{SB} based on an a priori assignment of source, drain and bulk that is independent of the actual bias conditions. Since MOS Model 1101 assumes saturation occurs at the drain side of the MOSFET, the basic model cannot cope with bias conditions that correspond to $V_{DS} < 0$. Again a transformation of the bias conditions is necessary. In this case, the transformation corresponds to internally reassigning source and drain, applying the standard electrical model, and then reassigning the currents and charges to the original terminals. In MOS Model 1101care has been taken to preserve symmetry with respect to drain and source at $V_{DS} = 0$. In other words no non-singularities will occur in the higher-order derivatives at $V_{DS} = 0$.

In detail, in order to embed MOS Model 1101 correctly into a circuit simulator, the following procedure, illustrated in figure 77 should be followed. We have assumed that indeed the simulator provides the nodal potentials V_D^e , V_G^e , V_S^e and V_B^e based on an a priori assignment of drain, gate, source and bulk.

Step 1 Calculate the voltages V''_{DS}, V''_{GS} and V''_{SB}, and the additional voltages V''_{DG} and V''_{SG}. The latter are used for calculating the charges associated with overlap capacitances.

Step 2 Based on n- or p-channel devices, calculate the modified voltages V'_{DS}, V'_{GS} and V'_{SB}. From here onwards only n-channel behaviour needs to be considered.

Step 3 Based on a positive or negative V'_{DS}, calculate the internal nodal voltages. At this level, the voltages - and the parameters, see below - comply to all the requirements for input quantities of MOS Model 1101.

Step 4 Evaluate all the internal output quantities - channel current, weak avalanche current, gate current, nodal charges, and noise-power spectral densities - using the standard MOS Model 1101 equations and the internal voltages.

Step 5 Correct the internal output quantities for a possible source-drain interchange. In fact, this directly establishes the external noise power spectral densities.

Step 6 Correct for a possible p-channel transformation.

Step 7 Change from branch current to nodal currents, establishing the external current output quantities. Calculate the overlap charges that are related to the physical regions and add them to the nodal charges, thus forming the external charge output quantities.

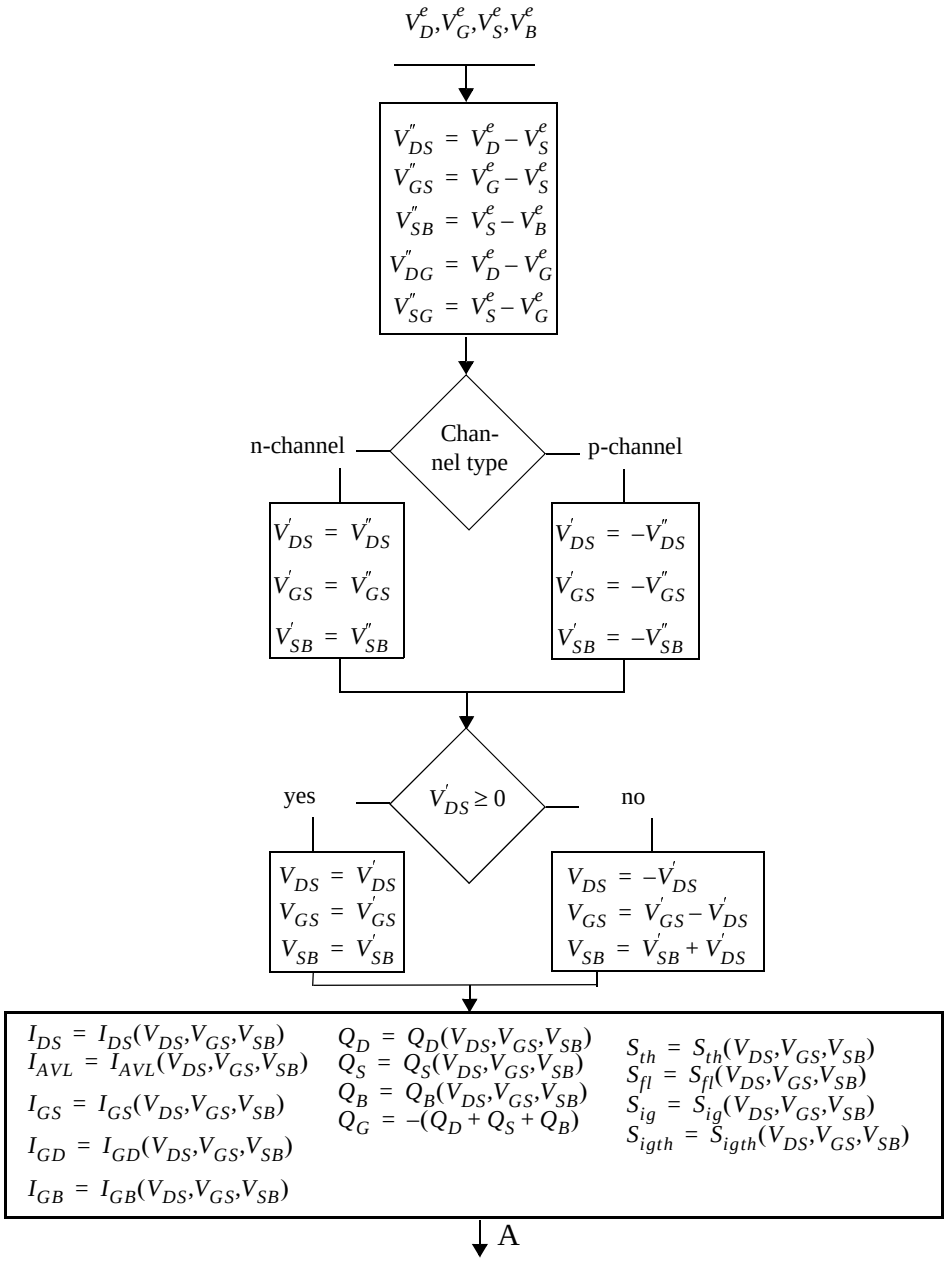
$V_D^e, V_G^e, V_S^e, V_B^e$
$V''_{DS} = V_D^e - V_S^e$
$V''_{GS} = V_G^e - V_S^e$
$V''_{SB} = V_S^e - V_B^e$
$V''_{DG} = V_D^e - V_G^e$
$V''_{SG} = V_S^e - V_G^e$
Chan-nel type
n-channel
p-channel
$V'_{DS} = V''_{DS}$
$V'_{GS} = V''_{GS}$
$V'_{SB} = V''_{SB}$
$V'_{DS} = -V''_{DS}$
$V'_{GS} = -V''_{GS}$
$V'_{SB} = -V''_{SB}$
$V'_{DS} \geq 0$
yes
no
$V_{DS} = V'_{DS}$
$V_{GS} = V'_{GS}$
$V_{SB} = V'_{SB}$
$V_{DS} = -V'_{DS}$
$V_{GS} = V'_{GS} - V'_{DS}$
$V_{SB} = V'_{SB} + V'_{DS}$
$I_{DS} = I_{DS}(V_{DS}, V_{GS}, V_{SB})$
$I_{AVL} = I_{AVL}(V_{DS}, V_{GS}, V_{SB})$
$I_{GS} = I_{GS}(V_{DS}, V_{GS}, V_{SB})$
$I_{GD} = I_{GD}(V_{DS}, V_{GS}, V_{SB})$
$I_{GB} = I_{GB}(V_{DS}, V_{GS}, V_{SB})$
$Q_D = Q_D(V_{DS}, V_{GS}, V_{SB})$
$Q_S = Q_S(V_{DS}, V_{GS}, V_{SB})$
$Q_B = Q_B(V_{DS}, V_{GS}, V_{SB})$
$Q_G = -(Q_D + Q_S + Q_B)$
$S_{th} = S_{th}(V_{DS}, V_{GS}, V_{SB})$
$S_{fl} = S_{fl}(V_{DS}, V_{GS}, V_{SB})$
$S_{ig} = S_{ig}(V_{DS}, V_{GS}, V_{SB})$
$S_{igth} = S_{igth}(V_{DS}, V_{GS}, V_{SB})$
A

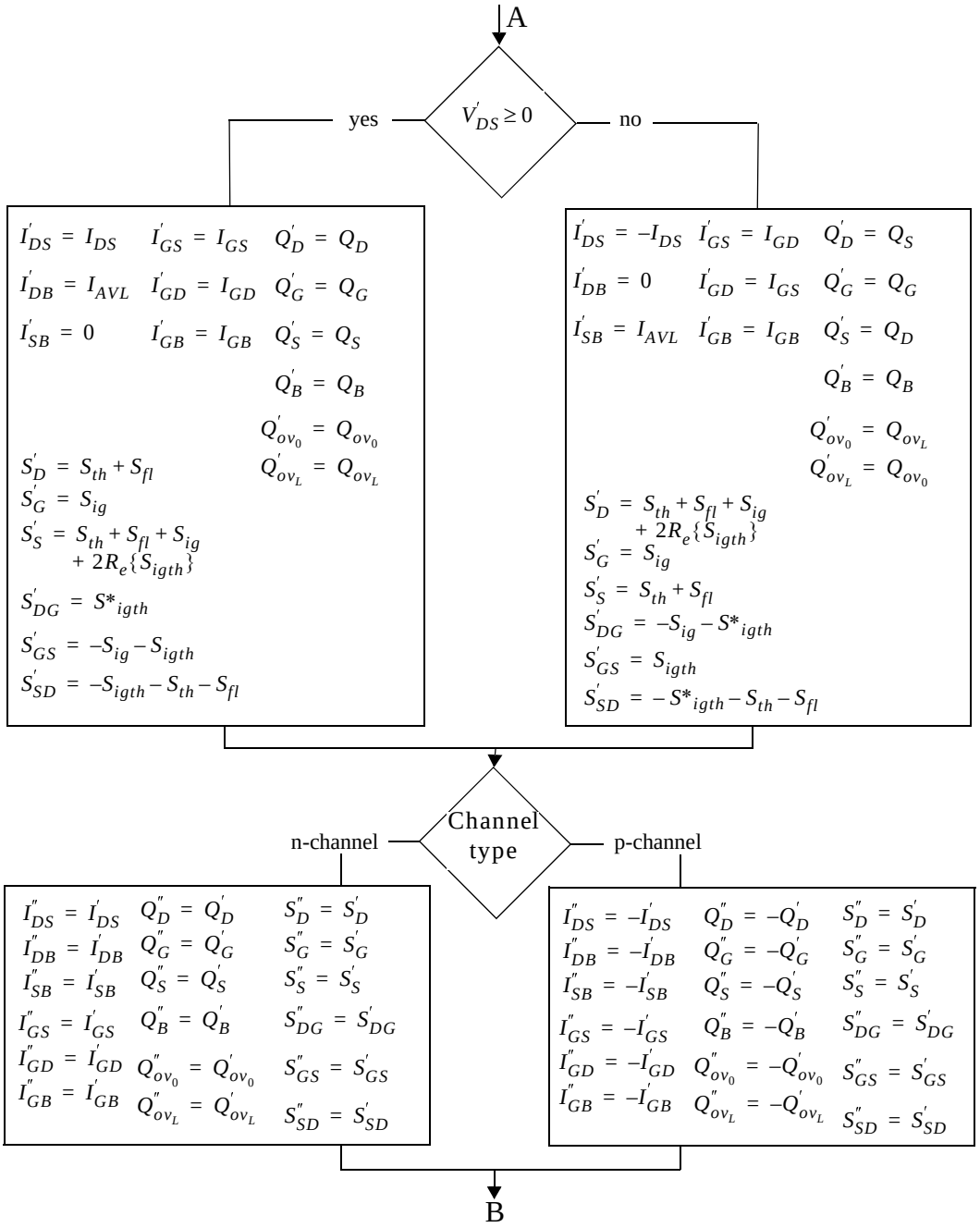
A
$V'_{DS} \geq 0$
yes
no
$I'_{DS} = I_{DS}$ $I'_{GS} = I_{GS}$ $Q'_D = Q_D$
$I'_{DB} = I_{AVL}$ $I'_{GD} = I_{GD}$ $Q'_G = Q_G$
$I'_{SB} = 0$ $I'_{GB} = I_{GB}$ $Q'_S = Q_S$
$Q'_B = Q_B$
$Q'_{ov_0} = Q_{ov_0}$
$Q'_{ov_L} = Q_{ov_L}$
$S'_D = S_{th} + S_{fl}$
$S'_G = S_{ig}$
$S'_S = S_{th} + S_{fl} + S_{ig} + 2R_e\{S_{igth}\}$
$S'_{DG} = S^*_{igth}$
$S'_{GS} = -S_{ig} - S_{igth}$
$S'_{SD} = -S_{igth} - S_{th} - S_{fl}$
$I'_{DS} = -I_{DS}$ $I'_{GS} = I_{GD}$ $Q'_D = Q_S$
$I'_{DB} = 0$ $I'_{GD} = I_{GS}$ $Q'_G = Q_G$
$I'_{SB} = I_{AVL}$ $I'_{GB} = I_{GB}$ $Q'_S = Q_D$
$Q'_B = Q_B$
$Q'_{ov_0} = Q_{ov_L}$
$Q'_{ov_L} = Q_{ov_0}$
$S'_D = S_{th} + S_{fl} + S_{ig} + 2R_e\{S_{igth}\}$
$S'_G = S_{ig}$
$S'_S = S_{th} + S_{fl}$
$S'_{DG} = -S_{ig} - S^*_{igth}$
$S'_{GS} = S_{igth}$
$S'_{SD} = -S^*_{igth} - S_{th} - S_{fl}$
Channel type
n-channel
p-channel
$I''_{DS} = I'_{DS}$ $Q''_D = Q'_D$ $S''_D = S'_D$
$I''_{DB} = I'_{DB}$ $Q''_G = Q'_G$ $S''_G = S'_G$
$I''_{SB} = I'_{SB}$ $Q''_S = Q'_S$ $S''_S = S'_S$
$I''_{GS} = I'_{GS}$ $Q''_B = Q'_B$ $S''_{DG} = S'_{DG}$
$I''_{GD} = I'_{GD}$ $Q''_{ov_0} = Q'_{ov_0}$ $S''_{GS} = S'_{GS}$
$I''_{GB} = I'_{GB}$ $Q''_{ov_L} = Q'_{ov_L}$ $S''_{SD} = S'_{SD}$
$I''_{DS} = -I'_{DS}$ $Q''_D = -Q'_D$ $S''_D = S'_D$
$I''_{DB} = -I'_{DB}$ $Q''_G = -Q'_G$ $S''_G = S'_G$
$I''_{SB} = -I'_{SB}$ $Q''_S = -Q'_S$ $S''_S = S'_S$
$I''_{GS} = -I'_{GS}$ $Q''_B = -Q'_B$ $S''_{DG} = S'_{DG}$
$I''_{GD} = -I'_{GD}$ $Q''_{ov_0} = -Q'_{ov_0}$ $S''_{GS} = S'_{GS}$
$I''_{GB} = -I'_{GB}$ $Q''_{ov_L} = -Q'_{ov_L}$ $S''_{SD} = S'_{SD}$
B

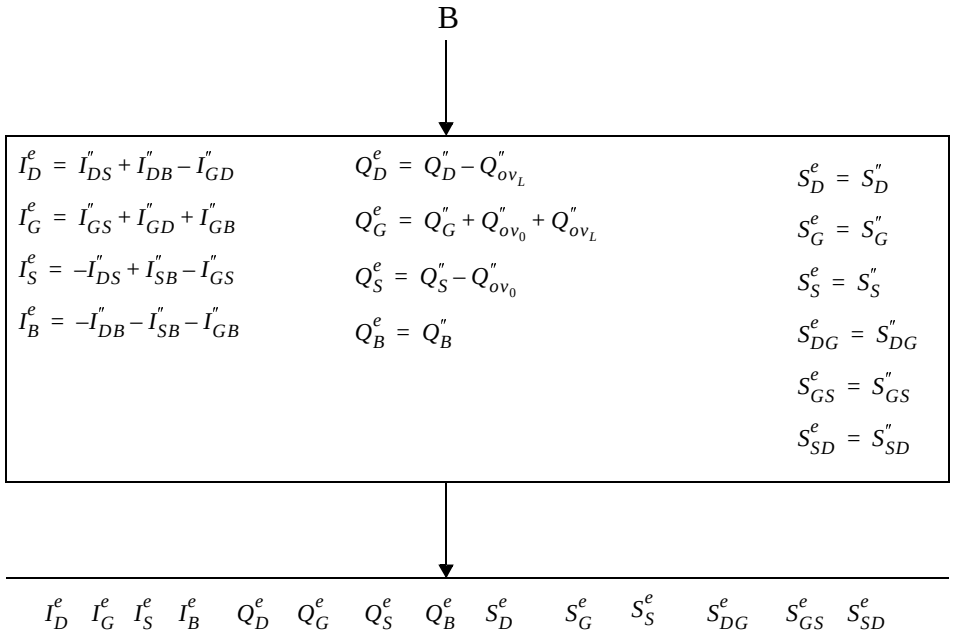

Figure 77: Transformation scheme

It is customary to have separate user models in the circuit simulators for n- and p-channel transistors. In that manner it is easy to use a different set of reference and scaling parameters for the two channel types. As a consequence, the changes in the parameter values necessary for a p-channel type transistor are normally already included in the parameter sets on file. The changes should not be included in the simulator.

12.8 Parameter Extraction

The parameter extraction strategy for MOS Model 11 using an **optimization method** consists of four main steps:

1. measurements
2. extraction of miniset parameters at room temperature
3. extraction of temperature scaling parameters
4. extraction of geometry scaling parameters.

The above steps will be briefly described in the following sections.

12.8.1 Measurements

The parameter extraction reoutine consists of four different dc-measurements and two (optional) capacitance measurements[1]:

- **Measurement I:** $I_D/g_m/I_G$-V_{GS} - characteristics in linear region:

n-channel : V_{GS} = 0 ... V_{sup} (with steps of maximum 50 mV).
V_{DS} = 50 mV
V_{BS} = 0 ... -V_{sup}

p-channel : V_{GS} = 0 ... -V_{sup} (with steps of maximum 50 mV).
V_{DS} = -50 mV
V_{BS} = 0 ... V_{sup}

- **Measurement II:** Subtreshold I_D-V_{GS} - characteristics:

n-channel : V_{GS} = V_T - 0.6 V ... V_T + 0.3 V
V_{DS} = 3 values starting from 100 mV to V_{sup}
V_{BS} = 0 ... -V_{sup}

p-channel : V_{GS} = V_T + 0.6 V ... V_T - 0.3 V
V_{DS} = 3 values starting from -100 mV to -V_{sup}
V_{BS} = 0 ... V_{sup}

1.The bias conditions to be used for the measurements are dependent on the supply voltage of the process. Of course it is adviseable to restrict the range of voltages to this supply voltage Vsup. Otherwise physical effects, atypical for normal transistor operation and therefore less well described by MOS Model 11, may dominate the characteristics.

- **Measurement III:** $I_D/g_{DS}/I_G$-V_{DS} - characteristics:

n-channel : V_{DS} = 0 ... V_{sup} (with steps of maximum 50 mV).
V_{GS} = 4 values starting from V_T + 0.1 V , not above V_{sup}
V_{BS} = 3 values starting from 0 V to -V_{sup}

p-channel : V_{DS} = 0 ... -V_{sup} (with steps of maximum 50 mV).
V_{GS} = 4 values starting from V_T + 0.1 V , not below -V_{sup}
V_{BS} = 3 values starting from 0 V to V_{sup}

- **Measurement IV:** $I_D/I_S/I_G/I_B$-V_{GS} - characteristics in all operation regions:

n-channel : V_{GS} = -V_{sup} ... V_{sup} (with steps of maximum 50 mV).
V_{DS} = 4 values starting from 0 V to V_{sup}
V_{BS} = 0 V

p-channel : V_{GS} = -V_{sup} ... -V_{sup} (with steps of maximum 50 mV).
V_{DS} = 4 values starting from 0 V to -V_{sup}
V_{BS} = 0 V

- **Measurement V:** C_{gg}-V_{GS} - characteristics (optional):

n / p-channel : V_{GS} = -V_{sup} ... V_{sup} (with steps of maximum 50 mV).
V_{DS} = 0 V
V_{BS} = 0 V

- **Measurement VI:** C_{cg}-V_{GS} - characteristics:

n / p-channel : V_{GS} = -V_{sup} ... V_{sup}
V_{DS} = 0 V
V_{BS} = 0 V

The values of transconductance g_m and output conductance g_{DS} are extracted from the I - V-curves by calculating in a numerical way the derivative of I_D to V_{GS} and V_{DS}, respectively. In the subthreshold measurements, Measurement II, use is made of threshold voltage V_T, which has to be determined for all the bulk-source bias values V_{BS}. The determination of V_T is rather arbitrary, and it can be either determined using the lineas extrapolation method or the constant current criterion. The channel-

to-gate capacitance C_{cg} is the summation of the drain-to-gate capacitance C_{dg} and the source-to-gate capacitance C_{sg} (i.e. source and drain are short-circuited), it is needed to extract overlap capacitance parameters.

For the miniset extraction measurements I through IV have to be performed at room temperature for every device. In addition measurements V and VI need to be performed for a long/broad and a short/broad (i.e. $L = L_{min}$) transistor (at room temperature). Furthermore, for the extraction of temperature scaling parameters measurements I, III and IV have to be performed at different temperatures (at least two, typically -40°C and 125°C) for at least a long/broad and a short/broad transistor.

12.8.2 Extraction of Miniset Parameters at Room Temperature

The extraction of miniset parameters is performed for every device. In order to ensure that the temperature scaling relations do not affect the behaviour at room temperature, the reference temperature T_R is chosen equal to room temperture. In general the simultaneous determination of all miniset parameters is not advisable, because the value of some parameters can be wrong due to correlation and suboptimization. Therefore it is more practical to split the parameters into several groups, where each parameter group can be determined using specific measurements.

Although the poly-depletion effect affects the dc-behaviour of a MOSFET, the poly-depletion parameter KPINV can only be determined accurately from *C-V*-measurements. If the (physical) oxide thickness t_{ox} and the polysilicon impurity concentration N_P are known, the parameter KPINV ($= 1/(k_p)$) can be calculated from[1]:

$$k_p = \frac{t_{ox} \cdot \sqrt{2 \cdot q \cdot \varepsilon_{si} \cdot N_p}}{\varepsilon_{ox}} \tag{12.341}$$

If the polysilicon impurity concentration N_P is not known, as a good first-order estimate one can use $N_p = 1 \cdot 10^{26} m^{-3}$ for n^+-polysilicon gates and $N_p = 5 \cdot 10^{25} m^{-3}$ for p^+-polysilicon gates. In the latter case a measured C_{GG}-V_{GS}-characteristic for a long-channel transistor is essential for an accurate determination of KPINV.

1.For metal gates the poly-depletion effect does not occur and in this case KPINV = 0.

Table 8: Starting miniset parameter values for parameter extraction at room temperature T_R of a typical MOSFET with channel length L (m), channel width W(m), oxide thickness t_{ox} (m), polysilicon impurity concentration N_P (m^{-3}) and minimum technology feature size L_{min}. If the polysilicon concentration N_P is not known, one can use $N_p = 1 \cdot 10^{26} m^{-3}$ or $5 \cdot 10^{25} m^{-3}$ for n^+- resp. p^+-polysilicon gates. Parameters C_{ox}, C_{GSO} and C_{GDO} are only important for the charge model, and do not affect the dc-model; they have to be extracted from C-V -characteristics. In order to determine the parameter geometry-scaling, the last column indicates for which conditions the parameters have to be extracted: L=long-channel device (fixed for short-channel devices), S=short-channel devices, A=all devices and F=fixed parameter.

Parameter	Program Name	Parameter Value		Extracted for
		NMOS	PMOS	
V_{FB}	VFB	-1.1	-0.95	L
k_0	KO	0.25	0.25	A
$1/k_p$	KPINV	$6.0 \cdot 10^3/(t_{OX} \cdot \sqrt{N_p})$	$6.0 \cdot 10^3/(t_{OX} \cdot \sqrt{N_p})$	L
ϕ_B	PHIB	0.95	0.95	A
β	BET	$1.7 \cdot 10^{-12}/t_{OX} \cdot W/L$	$4.5 \cdot 10^{-13}/t_{OX} \cdot W/L$	A
θ_{sr}	THESR	$1.5 \cdot 10^{-9}/t_{OX}$	$2.3 \cdot 10^{-9}/t_{OX}$	L
θ_{ph}	THEPH	$.3 \cdot 10^{-10}/t_{OX}$	$.2 \cdot 10^{-10}/t_{OX}$	L
η_{mob}	ETAMOB	1.3	3.0	L
ν	NU	2.0	2.0	A
θ_R	THER	$1.3 \cdot 10^{-7}/L$	$8.0 \cdot 10^{-8}/L$	S
θ_{R1}	THER1	0	0	-
θ_{R2}	THER2	1	1	-
θ_{sat}	THESAT	$4.5 \cdot 10^{-7}/L$	$2.0 \cdot 10^{-7}/L$	A
θ_{Th}	THETH	$1.0 \cdot 10^{-6}$	$1.0 \cdot 10^{-6}$	A
σ_{dib1}	SDIBL	$5.0 \cdot 10^{-2} \cdot (L_{min}/L)^2$	$5.0 \cdot 10^{-2} \cdot (L_{min}/L)^2$	S

Table 8: Starting miniset parameter values for parameter extraction at room temperature T_R of a typical MOSFET with channel length L (m), channel width W(m), oxide thickness t_{ox} (m), polysilicon impurity concentration N_P (m^{-3}) and minimum technology feature size L_{min}. If the polysilicon concentration N_P is not known, one can use $N_p = 1 \cdot 10^{26} m^{-3}$ or $5 \cdot 10^{25} m^{-3}$ for n^+- resp. p^+-polysilicon gates. Parameters C_{ox}, C_{GSO} and C_{GDO} are only important for the charge model, and do not affect the dc-model; they have to be extracted from C-V -characteristics. In order to determine the parameter geometry-scaling, the last column indicates for which conditions the parameters have to be extracted: L=long-channel device (fixed for short-channel devices), S=short-channel devices, A=all devices and F=fixed parameter.

Parameter	Program Name	Parameter Value		Extracted for
		NMOS	PMOS	
m_0	MO	$1.0 \cdot 10^{-3}$	$1.0 \cdot 10^{-3}$	A
σ_{sf}	SSF	$6.0 \cdot 10^{-2} \cdot L_{min}/L$	$6.0 \cdot 10^{-2} \cdot L_{min}/L$	A
α	ALP	$6.0 \cdot 10^{-2} \cdot L_{min}/L$	$6.0 \cdot 10^{-2} \cdot L_{min}/L$	A
V_p	VP	$5.0 \cdot 10^{-2}$	$1.0 \cdot 10^{-1}$	F
m	MEXP	use Eq. (12.132)	use Eq. (12.132)	-
a_1	A1	25	100	A
a_2	A2	25	37	A
a_3	A3	1	1	A
I_{GINV}	IGINV	$3.0 \cdot 10^{-5} \cdot W \cdot L/t_{ox}^2$	$4.0 \cdot 10^{-5} \cdot W \cdot L/t_{ox}^2$	A
B_{INV}	BINV	$2.9 \cdot 10^{+10} \cdot t_{ox}$	$4.3 \cdot 10^{+10} \cdot t_{ox}$	L
I_{GACC}	IGACC	$3.0 \cdot 10^{-5} \cdot W \cdot L/t_{ox}^2$	$2.0 \cdot 10^{-5} \cdot W \cdot L/t_{ox}^2$	A
B_{ACC}	BACC	B_{INV}	$2.9 \cdot 10^{+10} \cdot t_{ox}$	L
$V_{FB_{OV}}$	VFBOV	0.1	0.1	L
k_{ov}	KOV	$9.3 \cdot 10^{+8} \cdot t_{ox}$	$3.8 \cdot 10^{+8} \cdot t_{ox}$	L
I_{GOV}	IGOV	$5.0 \cdot 10^{-13} \cdot W/t_{ox}^2$	$5.0 \cdot 10^{-12} \cdot W/t_{ox}^2$	A
C_{ox}	COX	$\varepsilon_{ox}/t_{ox} \cdot W \cdot L$	$\varepsilon_{ox}/t_{ox} \cdot W \cdot L$	-

Table 8: Starting miniset parameter values for parameter extraction at room temperature T_R of a typical MOSFET with channel length L (m), channel width W(m), oxide thickness t_{ox} (m), polysilicon impurity concentration N_P (m^{-3}) and minimum technology feature size L_{min}. If the polysilicon concentration N_P is not known, one can use $N_p = 1 \cdot 10^{26} m^{-3}$ or $5 \cdot 10^{25} m^{-3}$ for n^+- resp. p^+-polysilicon gates. Parameters C_{ox}, C_{GSO} and C_{GDO} are only important for the charge model, and do not affect the dc-model; they have to be extracted from C-V -characteristics. In order to determine the parameter geometry-scaling, the last column indicates for which conditions the parameters have to be extracted: L=long-channel device (fixed for short-channel devices), S=short-channel devices, A=all devices and F=fixed parameter.

Parameter	Program Name	Parameter Value		Extracted for
		NMOS	PMOS	
C_{GDO}	CGDO	$3.0 \cdot 10^{-10} \cdot W$	$3.0 \cdot 10^{-10} \cdot W$	-
C_{GSO}	CGSO	$3.0 \cdot 10^{-10} \cdot W$	$3.0 \cdot 10^{-10} \cdot W$	-

Before the optimization is started a parameter set has to be determined which contains a first estimation of the parameters to be extracted and the parameters which remain constant. The value of smoothing factor m is calculated from the device length L and from the minimum feature size of the technology L_{min} using eq. (12.132). The parameter set used as a first-order estimation of the parameters to be extracted is given in Table 8. With this parameter set a first optimization following the scheme below, is performed. After this the new parameter set serves as an estimation for the second optimization, which is performed following the same scheme. This method yields a proper set of parameters after the second optimization. Experi-

ments with transistors of different processes show that the parameter set does not change very much after a third optimization.

Table 9: DC-parameter extraction procedure for a long-channel n-MOSFET, where Steps 2 and 12 are optional. For p-type transistors all voltages and currents have to be multiplied by - 1. The optimization is either performed on the absolute or relative deviation between model and measurements. Parameter I_{tst} is 2.5 µA for NMOS and 0.8 µA for PMOS. For n-MOSFETs $B_{acc} = B_{inv}$, and as a result B_{acc} does not have to be extracted. For p-MOSFETs this is not the case, see Table. 10.

Step	Optimised Parameters	Measure -ment	Fitted On	Absolute/ Relative	Specific Conditions
1	ϕ_B, k_0, β, θ_{sr}	I	I_D	Absolute	-
2	V_{FB}, k_0, k_P, C_{ox}	V	C_{gg}	Relative	-
3	ϕ_B, k_0, m_0	II	I_D	Relative	-
4	β, θ_{sr}, θ_{ph}	I	I_D / g_m	Relative	$V_{SB} = 0V$ $V_{GS} > V_T + 0.3V$
5	η_{mob}	I	I_D	Absolute	$I_D > W/L \cdot I_{tst}$
6	θ_{sat}	III	I_D	Absolute	-
7	σ_{sf}, α, θ_{Th}	III	g_{DS}	Relative	-
8	θ_{sat}	III	I_D	Absolute	-
9	I_{GINV}, B_{INV}	I	I_G	Absolute	-
19	I_{GOV}, (B_{ACC}), I_{GACC}, k_{ov}	IV	I_G	Relative	$V_{GS} < 0V$
11	a_1, a_2, a_3	IV	I_B	Absolute	$V_{GS} \geq 0V$
12	V_{FB}, k_p, C_{ox}	V	C_{gg}	Relative	-
13	Repeat steps 3, 4, 5, 6, 7, 8, 9, 10 and 11				

For an accurate extraction of parameter values, the parameter set for a long-channel transistor has to be determined first. In the long-channel case the poly-depletion parameter $1/k_P$, the flat-band voltage VFB, the carrier mobility (i.e. θ_{sr}, θ_{ph} and η_{mob}) and the gate tunnelling probability factors (B_{inv} and B_{acc}) can be determined, and they can subsequently be fixed for the short and narrow-channel devices, see

Tab. 8. In Table 9 the extraction procedure for long-channel transistors is given. Since the value of body-factor k_0 may change much over geometry and over technology, the first-order estimate in Tab. 7.1 is very crude and a more accurate, preliminary value is obtained using Step 1. In Step 2 (optional) more accurate values of the poly-depletion parameter $1/k_P$ and the flat-band voltage V_{FB} (which determines the onset of accumulation) are extracted. Next the subthreshold parameters ϕ_B, k_0 and m_0 are optimized in Step 3, neglecting short-channel effects such as drain-induced barrier-lowering (DIBL). After that the mobility parameters are optimized using Steps 4 and 5, neglecting the influence of series-resistance. In Step 6 a preliminary value of the velocity saturation parameter is obtained, and subsequently the conductance parameters σ_{sf}, α and θ_{Th} are determined in Step 7. A more accurate value of θ_{sat} can now be obtained using Step 8 (which is Step 6 repeated). The gate current parameters are determined in Steps 9 and 10. Finally the weak-avalanche parameters are optimized in Step 11.

Table 10: DC-parameter extraction procedure for a short-channel n-MOSFET. For p-type transistors all voltages and currents have to be multiplied by - 1. Parameters $1/k_P$, V_{FB}, θ_{sr}, θ_{ph}, η_{mob}, B_{inv}, B_{acc} and k_{ov} are taken from the long-channel case. The optimization is either performed on the absolute or relative deviation between model and measurements.

Step	Optimised Parameters	Measure-ment	Fitted On	Absolute/ Relative	Specific Conditions
1	$\phi_B, k_0, \beta, \theta_R$	I	I_D	Absolute	-
2	$\phi_B, k_0, m_0, \sigma_{dibl}$	II	I_D	Relative	-
3	β, θ_R	I	I_D/g_m	Relative	$V_{SB} = 0V$ $V_{GS} > V_T + 0.3V$
4	θ_{sat}	III	I_D	Absolute	-
5	$\sigma_{sf}, \alpha, \theta_{Th}, \sigma_{dibl}$	III	g_{DS}	Relative	-
6	θ_{sat}	III	I_D	Absolute	-
7	$I_{GINV}, I_{GOV}, I_{GACC}$	IV	I_D	Relative	-
8	a_1, a_2, a_3	IV	I_B	Absolute	$V_{GS} \geq 0V$
9	Repeat steps 2, 3, 4, 5, 7 and 8				

For short-channel devices the values of the poly-depletion parameter $1/k_P$, flat-band voltage V_{FB},the carrier mobility parameters (θ_{sr}, θ_{ph} and η_{mob}) and the gate tunnelling probability factors (B_{inv} and B_{acc}) of the long-channel device are copied, and next the extraction procedure as given in Table 10 is executed. In contrast to the long-channel case, the extraction procedure for short-channel devices also optimizes the parameters for series-resistance[1] and DIBL.

AC-parameters: The AC-parameters C_{ox}, C_{GSO}, C_{GDO}, k_{ov} and V_{FBov} cannot be (accurately) de-termined from DC-characteristics, and as a consequence they have to be determined from C–V– characteristics[2]. Since normal MOS transistors are symmetrical devices, one can assume that the oxide capacitance of the source and drain extension are identical, which implies that C_{GSO}=C_{GDO}. The oxide capacitance of the intrisic MOSFET C_{ox} can be extracted from Measurement VI. In Table 11 the extraction procedure for the AC-parameters is given.

12.8.3 Extraction of Temperature Scaling Parameters

For a specific device the temperature scaling parameters can be extracted after the miniset at room temperature has been extracted. In order to so, measurements I, III and IV need to be performed at various temperature values (at least two values different from room temperature, typically - 40^o C and 125^o C).

Table 11: AC-parameter extraction procedure for a MOSFET. Here it is assumed that C_{GSO} = C_{GDO}. In the first instance flat-band voltage V_{FBov} is not optimised, although it may be optimised during Step 1 in order to ob-tain more accurate results. The optimization is either performed on the absolute or relative deviation between model and measurements.

Step	Optimised Parameters	Measure-ment	Fitted On	Absolute/ Relative	Specific Conditions
1	k_{ov} , C_{GSO}	VI	C_{cg}	Relative	$V_{GS} < 0V$
2	C_{ox}	V	C_{gg}	Relative	-
3	Repeat steps 1 and 2				

1.Note that in Table 10 parameters θ_{R1} and θ_{R2} are not included, which implies that the series-resistamce is assumed to be voltage-independent. This holdss true for modern CMOS technologies, where no use is made of LDD-structures.
2.Although parameter k_{ov} can be determined from overlap gate current, see Table 9, it is nonetheless more accurately determined from the C_{cg}-V_{GS} characteristics.

Since the reference temperature T_R has been chosen equal to room temperature, the modelled behaviour at room temperature is not affected by different values of the temperature scaling parameters. As a first-order estimation of the temperature scaling parameter values, the default values as given in Section 12.2.2 are used. Again the parameter extraction scheme is slightly different for the long-channel and for the short-channel case.

Table 12: Temperature scaling parameter extraction procedure for a long-channel n-MOSFET, where measurements have been performed at various temperature values. For p-type transistors all voltages and currents have to be multiplied by -1. The optimization is either performed on the abso-lute or relative deviation between model and measurements. Parameter I_{tst} is 2.5 μA for NMOS and 0.8 μA forPMOS.

Step	Optimised Parameters	Measure-ment	Fitted On	Absolute/ Relative	Specific Conditions
1	$S_{T;\phi_B}$	I	I_D	Relative	$I_D < W/L \cdot I_{tst}$
2	η_β, η_{sr}, η_{ph}, ν_{exp}, $S_{T;\eta_{mob}}$	I	I_D	Relative	$I_D > W/L \cdot I_{tst}$
3	η_{sat}	III	I_D	Absolute	-
4	$S_{T;a_1}$	IV	I_B	Absolute	$V_{GS} \geq 0V$

For an accurate extraction, the temperature scaling parameters for a long-channel device have to be determined first. In the long-channel case the carrier mobility parameters (i.e. η_{sr}, η_{ph}, ν_{exp} and $S_{T;\eta_{mob}}$) can be determined, and they can subsequently be fixed for the short-channel devices. In Table 12 the extraction procedure for long-channel transistors is given. In Step 1 the subthreshold temperature dependence is optimized, followed by the optimization of mobility reduction parameters in Step 2. Next the temperature dependence of velocity saturation is optimized in Step 3. In Step 4 finally the temperature dependence of impact ionization is determined.

For short-channel devices the values of the mobility reduction temperature scaling parameters (i.e. η_{sr}, η_{ph}, ν_{exp} and $S_{T;\eta_{mob}}$) of the long-channel device are copied, and next the extraction procedure asgiven in Table 13 is executed. In contrast to the long-

channel case, the extraction procedure for short-channel devices optimizes the parameter for series-resistance.

Table 13: Temperature scaling parameter extraction procedure for a short-channel n-MOSFET, where measurements have been performed at various temperature values. For p-type transistors all voltages and currents have to be multiplied by -1. The optimization is either performed on the absolute or relative deviation between model and measurements. Parameter I_{tst} is 2.5 μA for NMOS and 0.8 μA for PMOS.

Step	Optimised Parameters	Measure-ment	Fitted On	Absolute/ Relative	Specific Conditions
1	$S_{T;\phi_B}$	I	I_D	Relative	$I_D < W/L \cdot I_{tst}$
2	η_β, η_R	I	I_D	Relative	$I_D > W/L \cdot I_{tst}$
3	η_{sat}	III	I_D	Absolute	-
4	$S_{T;a_1}$	IV	I_B	Absolute	$V_{GS} \geq 0V$

12.8.4 Extraction of Geometry Scaling Parameters

In general the most important part of the geometry scaling scheme is the determination of ΔL and ΔW, see eqs. (12.112) and (12.113), since it affects the DC-, the AC- as well as the noise model. Tradi-tionally ΔW can be determined from the extrapolated zero-crossing in the gain factor β versus mask width W. In a similar way ΔL can be determined from the inverse gain factor $1/\beta$ versus mask length L. For modern MOS devices with pocket implants, however, it has been found that the above ΔL extraction method is no longer valid [47],[49]. Another, more accurate method is to measure the gate-to-bulk capacitance C_{GB} in accumulation for different channel lengths [48],[49]. In this case the extrapolated zero-crossing in the C_{GB} versus mask length L curve will give ΔL. Unfortunately for CMOS technologies in which gate current is non-negligible, capacitance measurements may be hampered by gate current [50]. In this case either gate current parameter I_{GINV} or I_{GACC} plotted as a function of channel length L may be used to extract ΔL [50].

In MM11, Level 1101, one can use either physical or binning geometry scaling rules. When using the binning rules of Section 12.5.1, the scaling parameters for one bin can be directly calculated from the minisets of the four corner devices of the bin. The binning scheme ensures that the minisets are exactly reproduced in the bin corners,

and that no humps occur in parameter values across bin borders. The exact way to calculate binning parameters from minisets is described in Appendix B.

When using the physical scaling relations of Section 12.5.1 it is possible to calculate a parameter set for a process, given the parameter set of typical transistors of this process. To accomplish this, transistors of different lengths, widths and at different temperatures have to be measured. Using these measurements the sensitivities of the parameters on length, width and temperature can be found. For the determination of a geometry-scaled parameter set a three-step procedure is recommended:

1. Determine minisets (ϕ_B, k_0, β , ...) for all measured devices, as explained in Sections 12.8.2 and 12.8.3.
2. The width and length sensitivity coefficients are optimized by fitting the appropriate geometry scaling rules to these miniset parameters.
3. Finally the width and length sensitivity coefficients are optimized by fitting the result of the scaling rules and current equations to the measured currents of all devices simultaneously.

Parameter sets have been determined for several processes using this parameter extraction strategy and taking care of not exceeding the supply voltage. For all processes good results have been obtained.